SOLID-SUPPORTED PHOSPHOLIPID BILAYERS:

SEPARATION MATRIX FOR PROTEOMICS APPLICATIONS

A Dissertation

by

ARNALDO JOEL DIAZ VAZQUEZ

Submitted to the Office of Graduate Studies of
Texas A&M University
in partial fulfillment of the requirements for the degree of

DOCTOR OF PHILOSOPHY

May 2008

Major Subject: Biochemistry

SOLID-SUPPORTED PHOSPHOLIPID BILAYERS:

SEPARATION MATRIX FOR PROTEOMICS APPLICATIONS

A Dissertation

by

ARNALDO JOEL DIAZ VAZQUEZ

Submitted to the Office of Graduate Studies of
Texas A&M University
in partial fulfillment of the requirements for the degree of

DOCTOR OF PHILOSOPHY

Approved by:

Co-Chairs of Committee,	Paul S. Cremer
	James C. Hu
Committee Members,	David H. Russell
	Gregory D. Reinhart
Head of Department,	Gregory D. Reinhart

May 2008

Major Subject: Biochemistry

ABSTRACT

Solid-Supported Phospholipid Bilayers: Separation Matrix

for Proteomics Applications. (May 2008)

Arnaldo Joel Diaz Vazquez, B.S.,

University of Puerto Rico – Rio Piedras

Co-Chairs of Advisory Committee: Dr. Paul S. Cremer
Dr. James C. Hu

This dissertation focuses on the development of biological platforms on which the function and characterization of transmembrane proteins can be performed simultaneously utilizing a biomembrane mimic consisting of a solid supported phospholipid bilayer (SLB). The study centered on the platform development, biophysical measurements of transmembrane proteins and membrane species chromatography. Membrane proteins play an essential role in various cellular and physiological processes. Their normal functions are essential to our health, and many impaired proteins have been related to serious diseases. Gaining a better understanding of membrane proteins is an essential step towards the development of more specific and competent drugs.

This research study is divided into two main parts. The first part centered on the creation of a new platform for allowing transmembrane proteins to freely move inside supported lipid bilayers with the same mobility that can be found in vesicle systems. SLBs have been extensively used as model systems to study cell membrane processes

because they maintain the same two-dimensional fluidity of lipids within the membrane found in live cells. However, one of the most significant limitations of this platform is its inability to incorporate mobile transmembrane species. Our strategy involves supporting the lipid bilayer on a double cushion, where we not only create a large space to accommodate the transmembrane portion of the protein, but also passivate the underlying substrate to reduce non-physiological protein-substrate interactions. High diffusion constants and high mobile fractions were obtained for a transmembrane protein reconstituted within this double cushion system.

The second area of this study focuses on the creation of a new method to rapidly separate membrane components using electrophoresis in SLBs. This work showed that even subtly different chemical isomers can be well-separated by a simple electrophoretic technique when cholesterol is present in the separation matrix. As a first step towards the purification of proteins, this work showed that streptavidin proteins doubly bound to a bilayer by a biotinylated lipid can be separated from streptavidin proteins which are singly bounded.

DEDICATION

Dedicated to the people who often believe in me more than

I do myself, my parents:

Maria M. Vazquez

and

Ramon L. Diaz

for their loving support in teaching me the value of an education

and

to my future wife Jessica Aud for all her loving support, patience and understanding

and

to my brother and sister, Raymi and Yiselie

and

my beautiful nieces, Alondra Nicole and Alanys Michelle

ACKNOWLEDGEMENTS

This work would not have been possible without the help and contribution of many people. First, I would like to give thanks to my advisor and mentor Dr. Paul S. Cremer for his guidance, support, expertise, and more than anything for giving me the chance of joining his group and motivating me during the process of my graduate career.

I sincerely thank Dr. James C. Hu for giving me the opportunity of joining the Department of Biochemistry & Biophysics and to participate in the Chemical/Biology Interface (CBI) Program. I want to express my appreciation to Dr. Gregory Reinhart and Dr. David H. Russell for their cooperation and for serving as my committee members. I greatly appreciate the time you have taken to guide me through my committee meetings, preliminary examination, and defense. Thanks for all the helpful advice you have given me.

I definitely owe a big thanks to Dr. Virginia Cornish for allowing me to do research at Columbia University. Dr. Cornish was instrumental in motivating me to pursue a career in science. She always has been a positive influence during my graduate career. Her guidance as a scientist and as a mentor has been exceptional.

I sincerely thank my fellow Cremer group members and friends for their support, motivation, and help during these years. Dr. Fernando Albertorio, thank you for your help, guidance and so many hours of supportive and helpful discussions. Thanks to Dr. Susan Daniel for her leadership and scientific contribution to my work. I especially would like to thank, Mrs. Stacy Sherrod, for all of her help and contribution to my

research. Her enthusiasm toward science is contagious and she has always been an example of hard-work, dedication and creativity.

I also want to thank the National Institutes of Health (NIH) for financial support. Other financial support was provided by the Defense Advanced Research Project Agency (DARPA).

Last but not least, I would like to thank my family, my lovely fiancée, and my good friends for all their love, support, and faith. Mom and Dad, thanks for your unconditional love and support. Thank you for your understanding and countless sacrifices. I love you both very much. Jessica thanks for all your help. I really appreciate your understanding, love, and patience. I can't wait to marry you. Raymi, Yiselie, Alondra, and Alanys, I miss you and love you all. Gabriela thanks for keeping my spirits up whenever things got a little out of control. Finally, thanks to all the friends I have made over the past years. Your contributions have been crucial to my career.

TABLE OF CONTENTS

CHAPTER Page

LIST OF FIGURES

FIGURE Page

FIGURE Page

FIGURE Page

FIGURE Page

LIST OF TABLES

CHAPTER I

INTRODUCTION

1.1 Purpose and Objectives

Advances in sensor technology, proteomics and drug design have led to an intense interest in developing better and more accurate techniques for the study and characterization of membrane proteins. One third of the genome of any organism encodes membrane proteins such as receptors, transporters and ion channels.[1,2] These proteins play an essential role in many cellular and physiological processes, such as cell signaling, transport of ions and nutrients, viral entry and pathogen attack. Cell signaling governs basic cellular activities and coordinates cell actions. The ability of cells to perceive and correctly respond to their microenvironment is the basis of development, tissue repair, and immunity. Errors in cellular information processing are responsible for diseases such as cancer, autoimmunity, depression, heart disease, diabetes, addictions and cystic fibrosis. Therefore, a significant effort is devoted by scientists around the world to understand these proteins, i.e. determining their sequence, structure, and function.

Membrane proteins are notoriously difficult to prepare in pure, correctly-folded form in sufficient quantity for drug discovery purpose. Because they make up 60 percent

---

This dissertation follows the style and format of the *Journal of the American Chemical Society.*

of all drug targets,[3] researchers are working to overcome the challenges. Current methods to separate and purify membrane proteins require expression of the protein within a host cell, lysis of the membrane, solubilizing the proteins with a detergent (denaturing them, causing loss of structure and function), and their separation by gel electrophoresis techniques. After this experimental procedure, the yield of transmembrane proteins is small; these constraints make it difficult to simultaneously study the function and determine the sequence and structure of the macromolecules. Therefore, improvements within this field will be extremely helpful for biotechnological industry and biomedical research.

This dissertation focuses on the development of a system in which the function and characterization of transmembrane proteins can be done simultaneously, utilizing a biomembrane mimic consisting of a solid supported phospholipid bilayer (SLB) lab-on-a-chip. The study focuses on the platform development, biophysical measurements of transmembrane proteins and membrane species chromatography. Supported phospholipid membranes retain two-dimensional lateral fluidity and provide an excellent environment for membrane proteins. These key parameters made this membrane supported platform an ideal system for applications in biosensors and lab-on-a-chip devices. My work is divided into two areas. The first area is centered in the creation of a new platform for allowing transmembrane proteins to freely move inside supported lipid bilayers with the same mobility that can be found in vesicle systems. The second area focuses on the creation of a new method to rapidly separate membrane components using electrophoresis in a solid supported bilayer.

The first chapter of this dissertation emphasizes the purposes and objectives of this dissertation, as well as background information in the area of study. An overview of the analytical techniques and experimental procedures employed throughout this study is presented in Chapter II. A double cushion system which affords two-dimensional lateral mobility for a transmembrane protein is described in Chapter III. Chapter IV focuses on the development of a simple on chip supported bilayer separation matrix for use in separating membrane-bound species. Chapter IV also includes the imaging of the separated species by Mass Spectrometry. In Chapter V we move one step further and expand supported bilayer electrophoresis for the movement of peripheral proteins. Chapter VI focused on the biopreservation of supported lipid bilayers using trehalose. Finally, Chapter VII contains a compilation of conclusions and suggestions for future work in the field.

1.2 The Cell Membrane

Structure and Properties of the Cell Membranes

The biological membrane plays a significant role in almost all cellular processes. The membrane surrounding the living cell serves several functions, such as control of solute permeability and recognition events.[4,5] Membranes regulate the flow of ions, water and other molecules entering and leaving the cell. They contain biomolecules that aid in directing the flow of information between cells, either by recognizing signal molecules received from other cells or by sending chemical or electrical impulses to other cells via signal transduction pathways.

In 1972, Singer and Nicolson, presented the fluid mosaic model to explain the arrangement of biological species in the cell membrane.[6] The model states that the membrane consists of a phospholipid bilayer with proteins of various lengths and sizes interspersed with cholesterol among the phospholipid. The struture is highly fluidic and the lipids and proteins are free to move in the plane of the membrane. Figure 1.1 shows a diagrammatic representation of the general structure of the biological membrane.

The bilayer consists of a thin layer of amphipathic lipids which spontaneously self-arrange so that the hydrophobic tails are protected from the surrounding aqueous environment, causing the hydrophilic head groups to orient toward the cytosolic and the extracellular medium.[5] The forces that hold these structures together are weak Van der Waals, hydrophobic, hydrogen-bonding and electrostatic interactions. There are three major types of lipids found in bilogical membranes: phospholipids, glycolipids and cholesterol. Phospholipid molecules are the major structural components of most membranes, including phosphatidylcholine (PC), phosphatidylethanolamine (PE), phosphatidylserine (PS), phosphatidylinositol (PI), and cardiolipin. These molecules, also called glycerophospholipids, consist of a phosphate-containing head group with saturated or unsaturated hydrocarbon chains connected to a glycerol via ester bonds. The length and degree of unsaturation of fatty acids chains have a profound effect on the membrane fluidity. Glycosphingolipids, another class of lipids in the membrane, which include cerebrosides and gangliosides, differs from phospholipids in that glycolipids have a sugar molecule, such as glucose or galactose, instead of the phosphate-containing

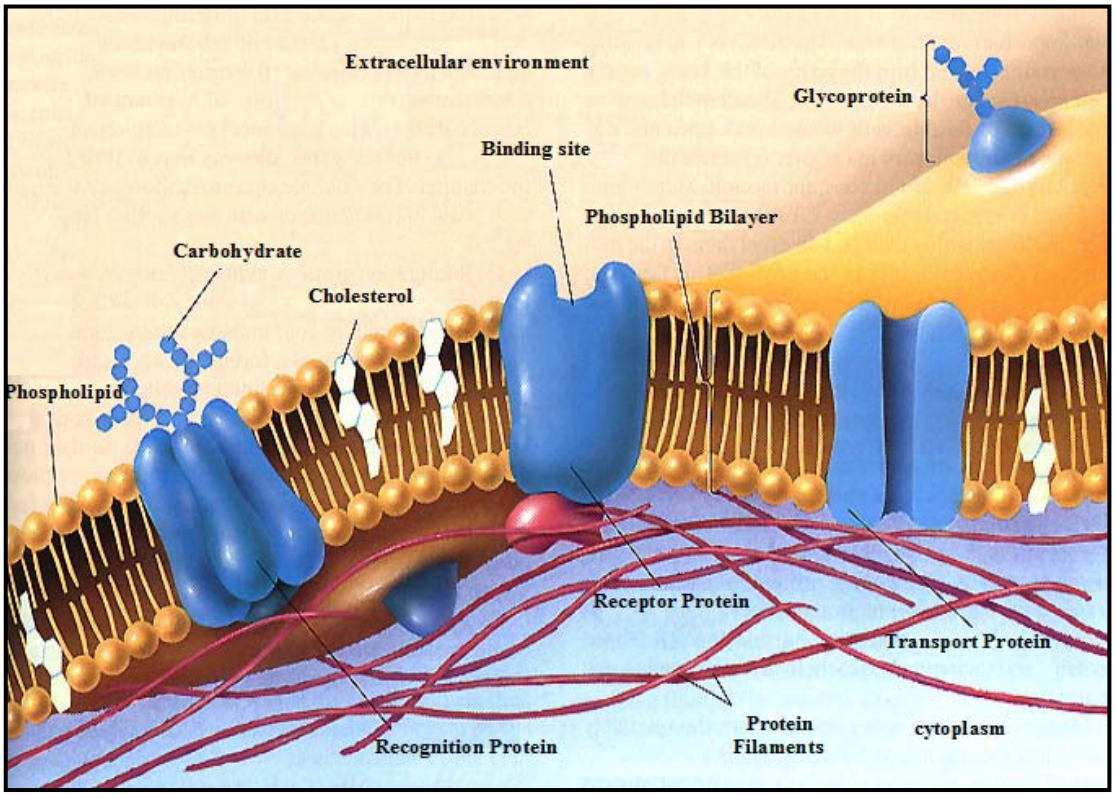

Figure 1.1 A schematic picture of the cell membrane composed of a lipid bilayer and integral proteins.[7]

head groups. These kinds of lipids are found only on the outer surface of the membrane with their sugar moieties exposed to the extracellular environment.

Cholesterol is a small molecule non-uniformly distributed throughout the cell membranes of eukaryotic organisms.[8] It has a structure significantly different from the phospholipids and glycolipids. Cholesterol contains a four-ring steroid structure together with a short hydrocarbon side-chain and a hydroxyl group. It is known that cholesterol modifies the structure and dynamic properties of the membrane by changing the packing properties within the bilayer. Increasing amounts of cholesterol lead to a decrease in the fluidity and permeability of the membrane. The interaction between cholesterol and lipids are thought to be essential for the formation of rafts in the cell membrane. It has also been shown that cholesterol interacts more strongly with saturated lipids than with the highly unsaturated lipids.

Bilayer fluidity is affected by different factors such as temperature, fatty acid composition and cholesterol content. At low temperature, the hydrocarbon tails of the lipids can pack closely together to form an ordered arrangement know as the gel state. As the temperature is increased, the lipid molecules vibrate more rapidly causing the bilayer to melt into a more disordered arrangement, which is more fluidic. The temperature at which the lipid bilayer melts is called the phase transition temperature; for most biological membranes this is in the range 10-40 °C.

Membrane Proteins

While the lipid bilayer determines the basic structure of biological membranes, the majority of the cellular and physiological processes are carried out by membrane proteins. About 25-30% of all proteins are membrane proteins.[1,2,9] Membrane proteins are classified based on their interaction with the cell membrane. Peripheral membrane proteins are those proteins that temporarily adhering to the biological membrane through electrostatic interactions and hydrogen bonding with other membrane proteins or lipids head groups. Peripheral proteins can be easily removed from the membrane surface by mild treatments such as changes in pH or ionic strength.[10] Transmembrane proteins refer to those proteins that span the whole biological membrane. The transmembrane regions of the proteins are either beta-barrels or alpha-helical. These proteins are key players in numerous biological processes, such as cell signaling and the transport of ions and nutrients. They are more difficult to isolate than peripheral proteins, as they are strongly bounded to the membrane by hydrophobic interaction between the membrane proteins and the lipid bilayer. This strong interaction can only be disrupted by the use of detergents, organic solvents, or denaturant. Other proteins are associated to the lipid membrane via a covalent linkage between the protein and the lipid head groups. Figure 1.2 shows the different types of membrane proteins.[11]

The first evidence for the existence of integral membrane proteins was obtained from freeze-fracture techniques. In this procedure, developed back in the 60's by Daniel Branton and coworkers,[12] membranes are rapidly frozen in liquid nitrogen before being fractured with a cold microtome knife. The bilayer comes apart into its two monolayers,

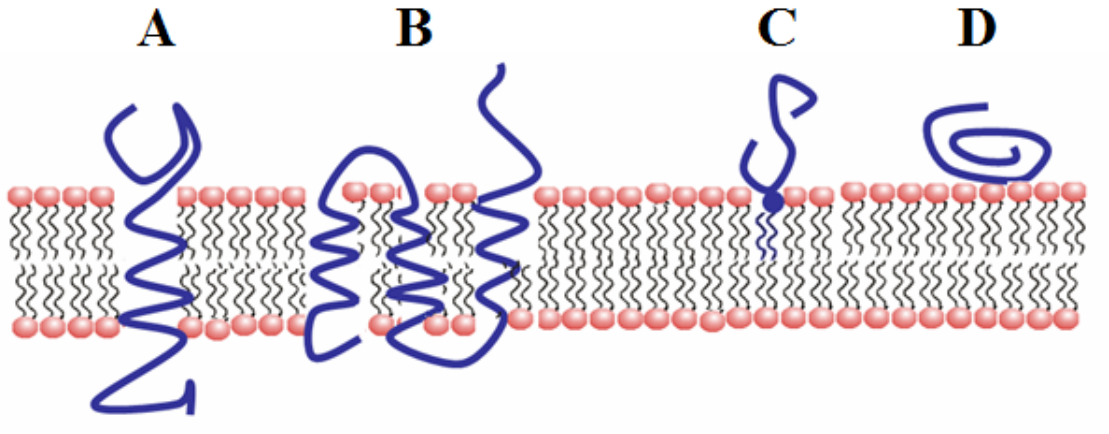

Figure 1.2 Schematic representation of the different types of membrane proteins. A) Single-pass transmembrane protein ; B) Multiple-pass transmembrane protein; C) Lipid-linked membrane protein; D) Peripheral proteins.

which can be examined by electron microscopy.

Membrane proteins act as receptors, transporters, channels, converters, and are responsible for key functions such as development, cell-cell interactions, energy conversion, nerve transmission, muscle contraction, signaling, and apoptosis. Mutations or changes in membrane proteins cause a vast array of human diseases such as cystic fibrosis, diabetes, Alzheimer's, hypertension, and heart failure. Much signaling occurs across the cell membrane via G-protein-coupled receptors (GPCRs). GPCRs are the largest group of membrane receptors on a cell surface and play important roles in many signal transduction pathways, such as those found in the photoreceptors that trigger the visual pathway.[13] GPCRs account for about 3-4% of the human genome.[13,14] They possess a common structural motif of seven α-helical membrane-spanning domains.[15] Mutations in these protein receptors are implicated in a wide range of human diseases such as cancer, neurological, cardiovascular, degenerative, metabolic, and inflammatory diseases.[16] Despite the fact that this group of proteins accounts for over 50% of current drug targets there is only very little structural information on GPCRs.[17,18] In 2000, the first 3D structure for a single GPCR was published.[14]

Ion and water channels embody another group of significant membrane proteins.[19] Potassium channels represent the largest and most diverse group of ion channels and are involved in a multitude of physiological functions. In 1998, MacKinnon and coworkers published the first potassium channel structure.[20] These tetrameric integral membrane proteins are involved in numerous fundamental biological processes, including signal transduction, maintenance of cellular osmotic balance, and

electrical signaling in the nervous system. Mutations in ion channels are associated with diverse human disorders. Aquaporins are membrane water channels that play critical roles in controlling the water content of cells.[21] Movement of water across the cell membrane needs to be regulated in order to maintain the internal pressure of the cell. This group of proteins, discovered by Peter Agre in the early nineties,[21] facilitates the movement of water molecules into and out of cells across cell membranes, preventing the cell from swelling or shrinking. Aquaporins are involved in numerous human disorders such as abnormalities of kidney function and loss of vision.[22]

Although membrane proteins represent the most important drug targets,[23] very limited structural information is currently available on membrane proteins, their mechanisms of action, and the roles they play in disease. Only a small percent of the structures of proteins available belong to the group of membrane proteins.[24] The 3D-structures of the proteins are essential for understanding their biological functions and for the development of new drugs. The low success in the crystallization of membrane proteins can be accredited to the following problems;[2,18] (1) it is hard to purify membrane proteins in sufficient amounts; (2) it is difficult to find an effective overexpression system; and (3) membrane proteins tend to denature during the purification procedures.

Current methods to purify proteins require expression of the protein of interest within a bacterial or mammalian host cell. The first step of a purification process involves lysis of the cell, which can be done using chemicals and enzymes, sonication or a French Press. Centrifugation is used to separate soluble proteins from cell membranes

and other cellular components. The membrane proteins can be released from the membrane by disruption of the cell membranes with ionic or non-ionic detergents. Non-ionic detergents, such as Triton-X-100 and dodecyl-β-D-maltoside, are used most commonly for extraction and purification of membrane proteins. After solubilization, the proteins are commonly purified by different chromatographic techniques. These techniques separate mixtures of proteins on the basis of their charge, their degree of hydrophobicity, their binding affinity for certain molecules, or their size. Typically, affinity chromatography is employed for the purification of proteins. In this chromatographic technique, proteins are separated according to their ability to bind to a specific ligand that is connected to a solid phase.[10] Proteins that do not bind the ligand are washed through the column; then the protein of interest is eluted from the column. Other purification techniques such as ion exchange chromatography, gel filtration chromatography, and size exclusion chromatography can also be employed for the purification of proteins.[10] Finally, the purity of the protein of interest is judged by sodium dodecyl sulfate polyacrylamide gel electrophoresis (SDS-PAGE). In SDS-PAGE, proteins are separated based on their size.[10] Another way to separate a mixture of proteins is by using two-dimensional gel electrophoresis.[25] In 2-D electrophoresis proteins are separated not only by their size but also by their charge. Figure 1.3 shows a typical purification procedure used to purify membrane proteins.

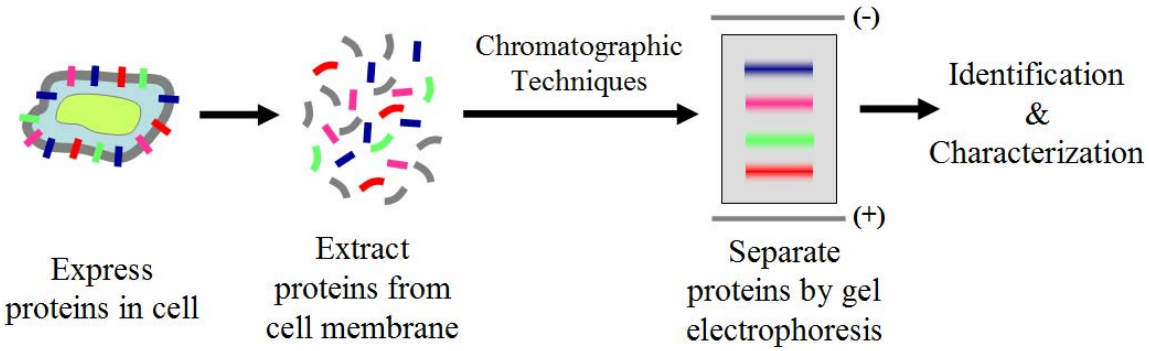

Figure 1.3 Cartoon representation of a typical procedure for the purification of membrane proteins.

1.3 Solid Supported Phospholipid Bilayers

Supported lipid bilayers (SLBs) have been widely employed as model systems for mimicking native cellular structures. Pioneered by McConnell and coworkers, [26-28] this system has been used in fundamental and applied studies of lipid assembly,[29,30] membrane structure,[31,32] dynamics,[33] multivalent ligand-receptor interactions,[34,35] electrochemical properties of membranes,[36] development of membrane-based biosensors,[37] and microscopic separation devices.[38] Supported bilayers consist of a continuous fluid membrane of lipids that is held near a surface, typically glass or SiO_2, as shown in Figure 1.4. The membrane is maintained by a balance of van der Waals, electrostatic, hydrophobic, and steric interactions.[39-41] A thin layer of water (Figure 1.4) is trapped between the bilayer and the underlying solid support.[42-45] This water layer helps to maintain the lateral mobility of lipids in both leaflets of the bilayer, preserving an important physical property of native biological membranes. This lateral fluidity makes these platforms ideal for developing biosensors, because they can readily mimic the same two-dimensional rearrangements that take place on cell surfaces during ligand-receptor recognition events.[41,46-48]

Various methodologies can be employed to form solid supported lipid bilayers.[41,49-52] They may be readily formed by either Langmuir-Shafer methods[53] or through the fusion of small unilamellar vesicles (SUVs) to a planar solid substrate.[26,28,29] The Langmuir-Shafer method has been used for the formation of hybrid-lipid bilayers,[53] cushioned membranes,[54,55] and for the incorporation of membrane species within the solid-supported phospholipid membrane.[27,54] This methodology involves the transfer of a

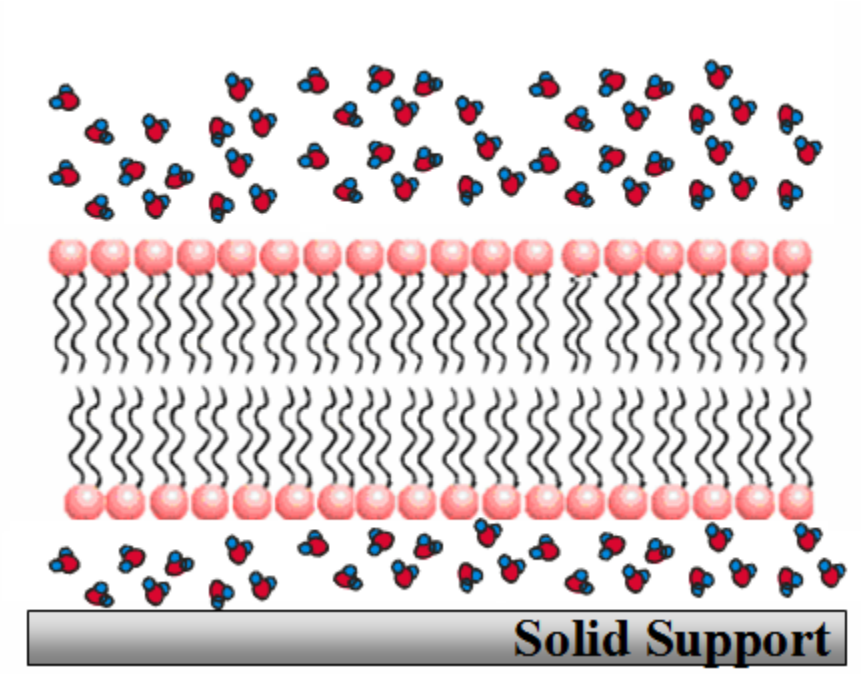

Figure 1.4 Schematic diagram of a supported lipid bilayer on a planar borosilicate glass substrate. The membrane is separated from the underlying inorganic support by ~ 1 nm thick layer of water. This water layer acts as a lubricant to maintain the fluidity of the lipids in the bilayer.

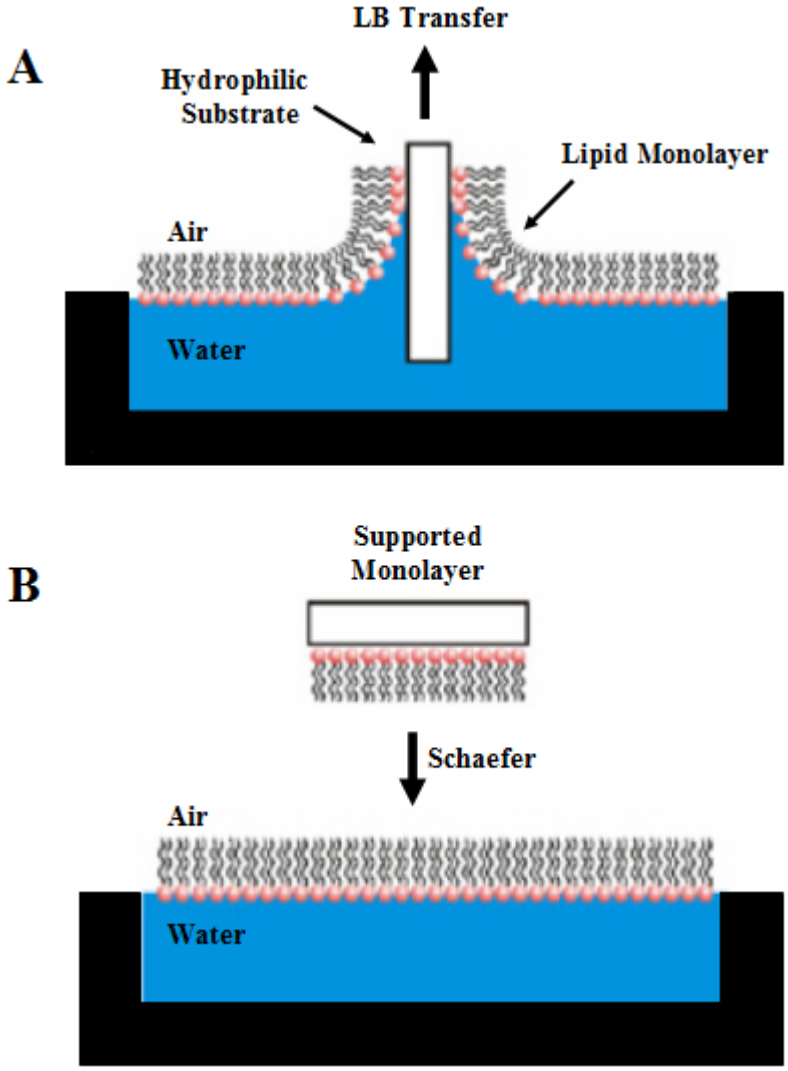

Figure 1.5 The assembly of a solid supported lipid bilayer by Langmuir-Blodget (A) followed by the Schaffer technique (B).

lower leaflet of lipids from the air-water interface by pulling a hydrophilic substrate through a lipid monolayer, as shown in Figure 1.5.[27,56] The hydrophobic tails of the lipids will orient themselves toward the air, while the polar head groups orient towards the hydrophilic substrate. The upper leaflet of the bilayer can be formed by horizontally dipping the substrate through another lipid monolayer by a Shaefer technique or via the fusion of vesicle.

The vesicle fusion method involves the spontaneous adsorption and fusion of small unilamellar vesicles from an aqueous suspension with an appropriate substrate. The process of vesicle fusion has been used to form supported bilayers on substrates, such as borosilicate glass,[27,41] oxidized silicon,[27] titanium dioxide,[57] mica,[58-60] self-assembled monolayers, oxide PDMS, polymers, and quartz. Figure 1.6 depicts a model for the steps involved in the process of bilayer formation. In this model, small unilamellar vesicles, having a diameter of 50 – 100 nm, will absorb, rupture, and ultimately fuse together to form a continuous phospholipid bilayer on a solid substrate. The process of vesicle fusion depends on a series of key parameters. The size of the vesicles, concentration and charge will affect the vesicle curvature and their interaction with the substrate. Surface charge, roughness and hydrophilicity also play important role in the assembly of solid supported lipid membranes.

Supported lipid bilayers offer distinct advantages over other systems, such as freestanding black lipid membranes and spherical lipid vesicles. Their planar geometry stabilized the film's. Also, they are easy to incorporate into microfluidics devices and simple to analyze by many surface specific techniques, such as atomic force microscopy

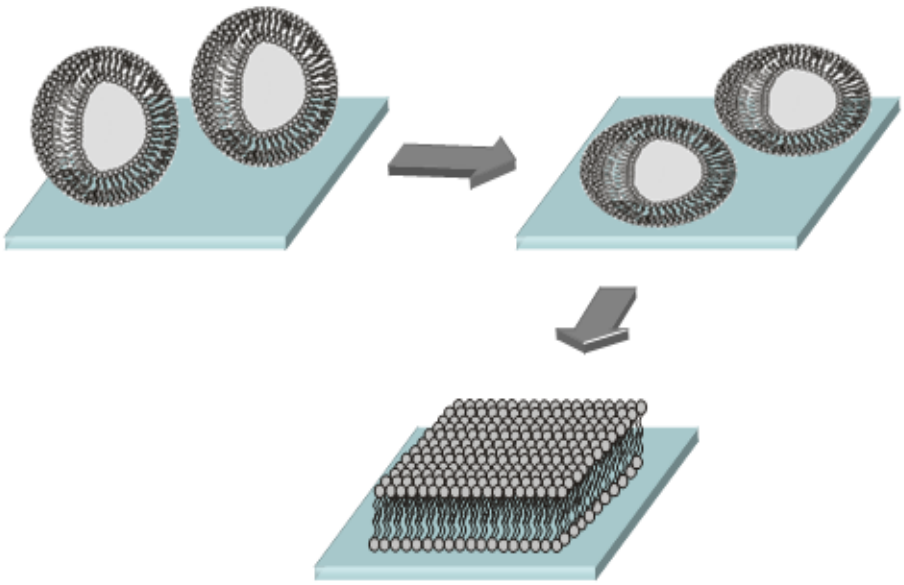

Figure 1.6 Spontaneous formation of a solid-supported lipid bilayer via vesicle fusion to a planar borosilicate substrate.

(AFM),[61-65] total internal reflection fluorescence (TIRFM),[66,67] vibrational sum frequency spectroscopy (SFG),[40] and surface plasmon resonance (SPR)[68,69] can be employed to monitor these solid -supported lipid bilayers.

While this system offers greater stability and robustness, the major disadvantage is the successful incorporation of mobile transmembrane proteins within the solid supported lipid bilayer.[26,70] Many interfacial biochemical reactions on cell membranes depend on the lateral mobility or fluidity of the membrane and its constituents. To maintain these properties, the interaction between the membrane and the bare solid surface should be minimal. However, the lipid membranes that are directly supported on a substrate such as borosilicate, are only separated from the substrate by a thin (~ 1 nm) layer of water. This water layer does not provide sufficient spacing between the membrane and the substrate. (Figure 1.5). Thus, exposed functional extracellular domains of an integral membrane protein can interact directly with the underlying inorganic substrate (Figure 1.7), causing denaturation, loss of function, and inhibition of lateral mobility. Due to this, such systems cannot be used to develop biological sensors that can monitor change in protein interactions in response to extracellular stimulus.

1.4. Polymer Cushioned Phospholipid Bilayers

Although solid supported phosphoslipid membranes are excellent biological platforms for the investigation of many cellular processes, such as multivalent ligand-receptor binding, lipid micro-domain formation, membrane fusion, and pathogen attack, they have difficulty mimicking an appropriate environment for transmembrane proteins.

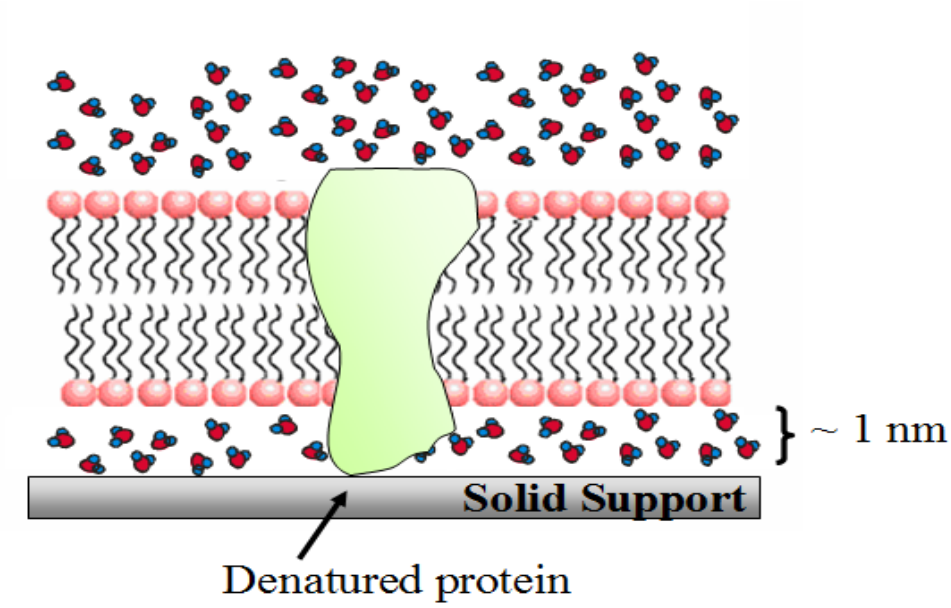

Figure 1.7 Exposed domains of transmembrane proteins can become immobilized and denatured on the underlying inorganic solid support.

Phospholipid membranes that are directly supported on a substrate, such as glass, are only separated from the substrate by a thin (~ 1 nm) layer of water.[27,43] This membrane-substrate distance is usually not sufficient to avoid direct contact between transmembrane proteins incorporated in the membrane and the underlying solid surface. This problem is significant because transmembrane proteins can interact strongly with the underlying substrate and can even become immobilized.

Efforts to overcome this problem have involved the use of soft polymeric materials of typically less than 100 nm in thickness to separate the phospholipid membrane from the bare substrate.[55,70-72] The polymer film acts as a support, similar to the cytoskeleton found in actual mammalian cell membranes. The addition of a polymer cushion should significantly reduce the frictional coupling between the membrane incorporated proteins and the solid support, avoiding the risk of protein denaturation. The presence of the polymer cushion still allows for investigation by an array of surface science techniques. Another potential advantage of polymeric platforms is the ability to avoid nonspecific adsorption of aqueous proteins from solution. This kind of nonspecific adsorption typically occurs at defect sites in a solid supported membrane lacking polymer layers.

An important condition when choosing a successful polymer cushion is that the supported lipid membrane must be thermodynamically and mechanically stable. Also, the selected polymer should be very hydrophilic and should not engage in extensive physical interactions with the membrane and the underlying solid support. Different types of polymer cushions have been explored for supporting phospholipid bilayers.

These included chitosan, polyelectrolytes,[73-76] cellulose,[77] dextran,[78] and lipopolymers tethers.[54,60,79-83] Also, some research groups have employed nanoporous materials[84,85] as a support for the lipid membrane.

One approach to separate the lipid membranes from the solid substrate is to use hydrated polymers as cushions (Figure 1.8B). In 2003, Sackmann, Tanaka, and coworkers used ultrathin layers of cellulose as a cushion for membranes with incorporated, large transmembrane proteins, such as integrin receptors. Around 25 % of the integrin receptors on the cellulose cushion retained their lateral mobility and functionality. Integrins receptors incorporated in membranes, supported on bare glass substrates were essentially immobilized. Another strategy used to overcome this problem is to incorporate lipopolymers within the lipid bilayer (Figure 1.8C). Lipopolymers consist of a soft hydrophilic polymer layer, presenting lipid like molecules at their surface which insert into a phospholipid membrane and tether it to the polymer spacer. Typically, the lipopolymer is chemically grafted to the underlying substrate via photoreactive coupling, epoxy group linkage, silane bonding, or sulfur-metal bond formation. Tamm and coworkers designed a tethered polymer-supported lipid bilayer, in which PEG-conjugated phospholipids were covalently bonded to the silicate substrates.[54] These lipopolymers cushions support lateral mobility of two membrane's proteins, cytochrome b5 and annexin V, that are not free to move on a membrane supported on a bare glass substrate. Once again, only a small percent of the proteins (~20%) retain their lateral mobility.

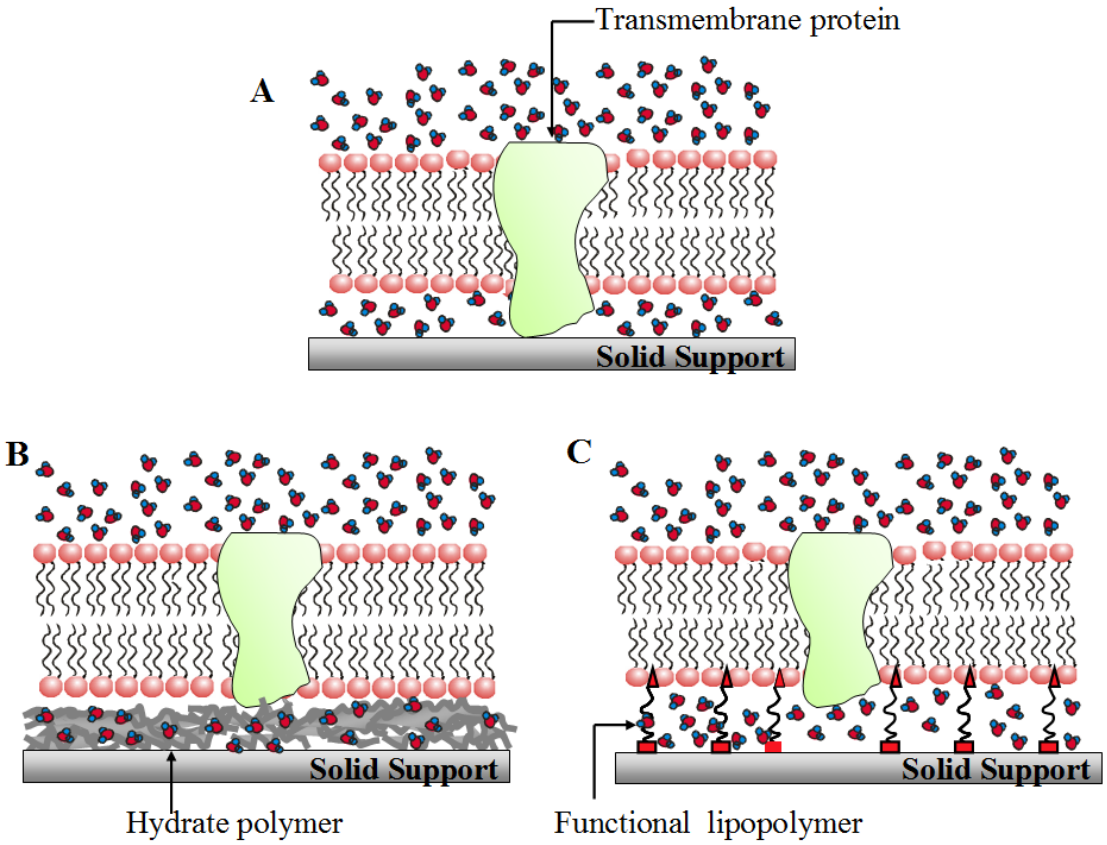

Figure 1.8 Methods for preparing supported lipid membrane. a) membrane supported on solid substrate; b) membranes that are supported using a polymer cushion; c) membranes that are supported using lipopolymer tethers.

1.5 Summary

Membrane proteins are the targets of a large number of today's pharmacological and toxicological drugs and are responsible, in part, for their uptake, metabolism, and clearance. Despite of their importance, the structure and function of membrane proteins are not well understood, and only a small number of membrane proteins have been studied in detail. Current methods employed for the purification of membrane proteins are often laborious, and a high amount of functional protein is not easy to obtain. Due to the transmembrane protein topology, detergents are required during the purification procedures in order to maintain the correct folding of the protein. Detergents have a negative impact on the yields and stability of the proteins and often interfere with the crystallization process.

The main goal of the study reported herein is to develop novel biological platforms that can be used in performing biophysical studies of transmembrane proteins and in the purification of membrane species. This will open the door towards the study of transmembrane proteins, the separation and "on-chip" purification for subsequence proteomic analysis by, for example, mass spectrometry.

CHAPTER II

EXPERIMENTAL

2.1 Synopsis

This chapter provides a general overview of the main analytical and surface analysis techniques used in this research project. The techniques presented here were used to obtain physical, chemical and morphological data needed to obtain a better understating of our model system.

Fluorescence recovery after photobleaching (FRAP)[86] has been employed to measure the two-dimensional lateral fluidity of different membrane components, such as fluorescently labeled lipids and proteins. Supported lipid bilayer electrophoresis,[87] a new method for the purification and characterization of membrane species, will be introduced.

Methods to dry the supported bilayer and techniques, such as site specific labeling of proteins, soft lithography for the preparation of microfluidic devices and thin layer chromatography, will be explained.

2.2 Conjugation of Fluorescently Labeled Proteins

Specific dye labeling of proteins, such as streptavidin and IgG, was accomplished by incubating the proteins with an amine reactive dye, such as Alexa Fluor-594. Alexa Fluor dyes are generally brighter and less pH-sensitive than common dyes (e.g. fluorescein, rhodamine) of equivalent excitation and emission. Also, the Alexa dyes have high quantum efficiency, chemical and thermal stability, and high solubility in aqueous solutions.

Figure 2.1 shows the chemical structure of Alexa Fluor 594. The Alexa Fluor 594 reactive dye has a succinimidyl ester moiety that reacts efficiently with primary amines of proteins to form stable dye–protein conjugates. Succinimidyl esters react efficiently at the pH 7.5–8.5. The labeling of proteins such as streptavidin and IgG has been performed according to established procedures. Size exclusion chromatography (SEC) was used to separate the labeled species from any unreacted dye present. Measurements in a UV-absorption were done to calculate the concentration of the protein and the degree of labeling. Alexa Fluor 594 dye–labeled proteins have an absorption and fluorescence emission maximum of approximately 590 nm and 617 nm, respectively.

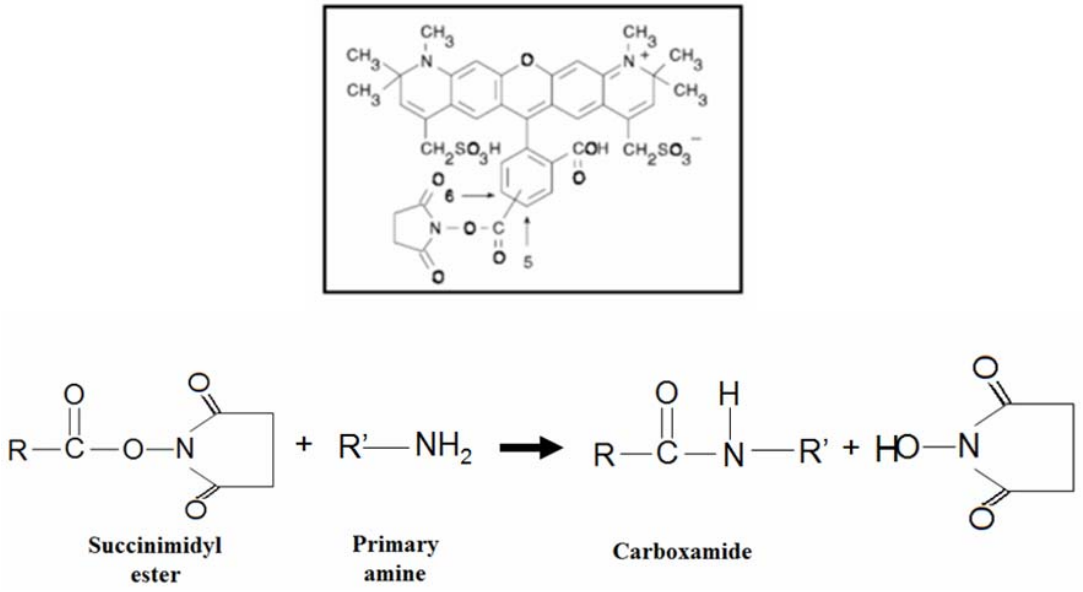

Figure 2.1 (Top) Chemical structure of Alexa Fluor 594 carboxylic acid, succinimidyl ester (MW ~820).[88] (Bottom) The Alexa Fluor 594 reactive dye has a succinimidyl ester moiety that reacts efficiently with the primary amines of the proteins and thus allows for the labeling of biomolecules.

2.3 Preparation of Microfluidic Devices by Soft Lithography

Soft lithopgraphy, a microfabrication process developed by George Whitesides and coworkers,[89-91] refers to a set of methods for fabricating or replicating structures using elastomeric stamps, molds, and conformable photomasks. This methodology has some advantages over other forms of lithography, such as photolithography and electron beam lithography. It is a convenient, effiencient, and low-cost method for carrying out micro- and nanofabrication.[92] This technique has been widely applied in the areas of biotechnology and plastic electronics.

Figure 2.2 shows a schematic representation of the general procedure of the soft lithography procedure used to prepare microfluidic devices.[93,94] In the first step a desired structure or pattern is transferred from a photomask to a photoresist polymer coated glass slide by exposing the photoresist coated glass to UV radiation. S-1813, a low viscosity positive photoresist is used to coat the microscope glass slides. Next, the exposed slides are developed by chemical etching according to established procedures.[90] Remaining areas of undesired photoresist are removed with acetone. At this step, a profilometer is used to characterize the quality of the product. In the last step, the device is created by pouring a degassed resin, such as poly(dimethylsiloxane) PDMS, on the top of the etched surface. After the curing process is done, a negative image of the photomaster is transferred to the PDMS stamp. Figure 2.3 shows a picture of a 7-channel PDMS microfludic device.

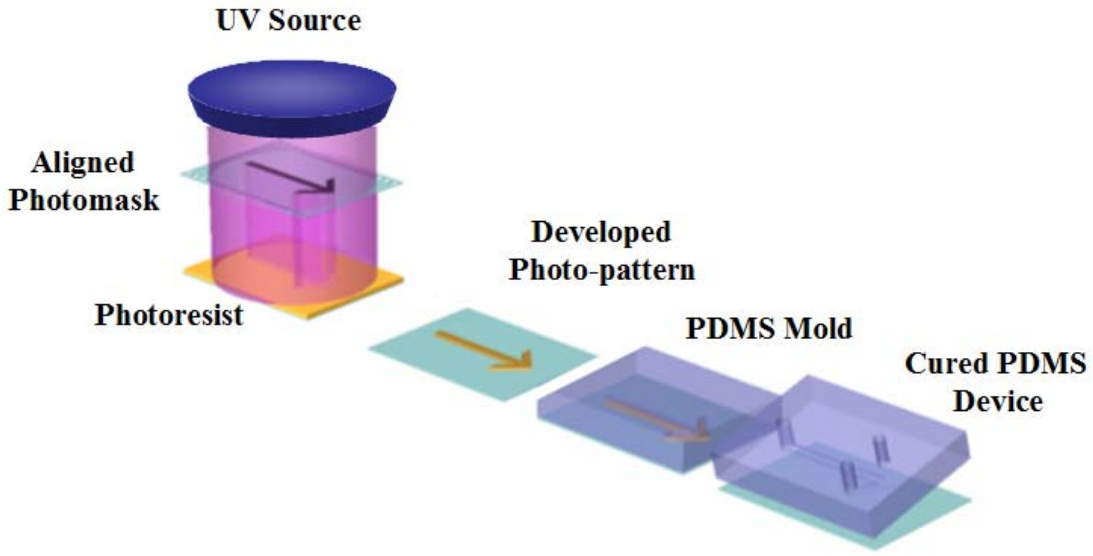

Figure 2.2 Schematic representation of the soft lithography procedure used to prepare microfluidic devices.[95]

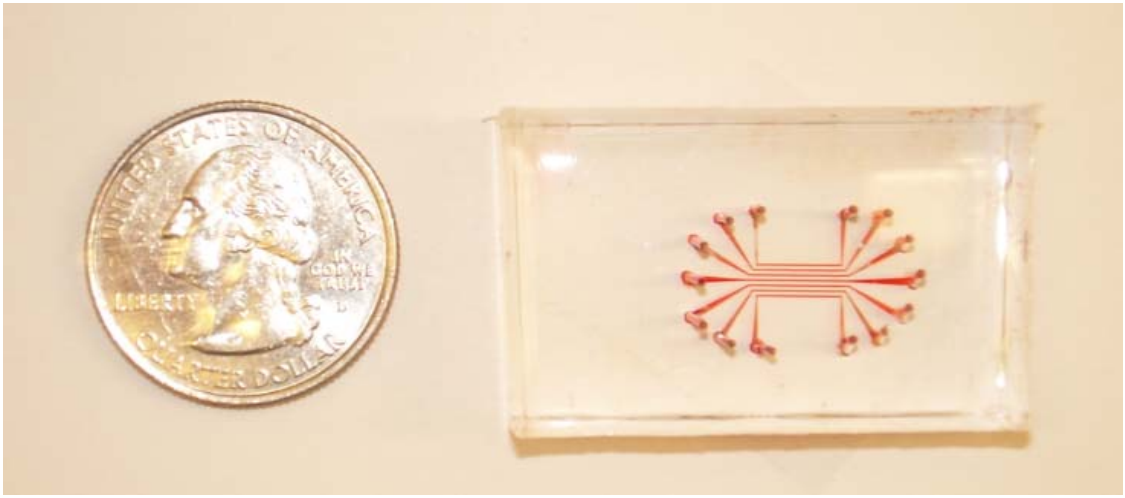

Figure 2.3 Photograph of a 7-channel microfluidic device. A red dye was used for visualization purposes.

2.4 Fluorescence Recovery after Photobleaching (FRAP)

The technique of fluorescence recovery after photobleaching (FRAP) has long been recognized as a powerful tool for investigating the two-dimensional lateral mobility of fluorescent particles, for example, the motion of fluorescently labeled lipids and proteins within membranes.[86,96] Information obtained from FRAP experiments includes: 1) identification of transport process type; 2) determination of the diffusion constant; and 3) the fraction of total fluorophores, which is mobile.

A schematic representation of the technique is shown in Figure 2.4. First, a specific region of the sample containing mobile fluorescent molecules is photobleached by a high-intensity focused laser beam. This causes irreversible photochemical bleaching of the fluorophores in that region. The exchange of bleached with unbleached molecules leads to a recovery of the initial fluorescent intensity. The measured data from a FRAP experiment is the time-dependent recovery of the fluorescence intensity inside the bleach spot. Figure 2.5 shows a graphical representation of this phenomenon.

The fluorescence intensity before and throughout the experiment are normalized using the following equation:

$$y = \frac{F_o - F_t}{F_i - F_0} \tag{2.1}$$

where y is the normalized fluorescence intensity, F_i is the fluorescence intensity before bleaching, F_o is the intensity of the photobleached region at times equal to 0, and F_t is the intensity of the bleached region as a function of time. An assumption in our FRAP experiments is that the fluorescently labeled species is uniformly distributed within an

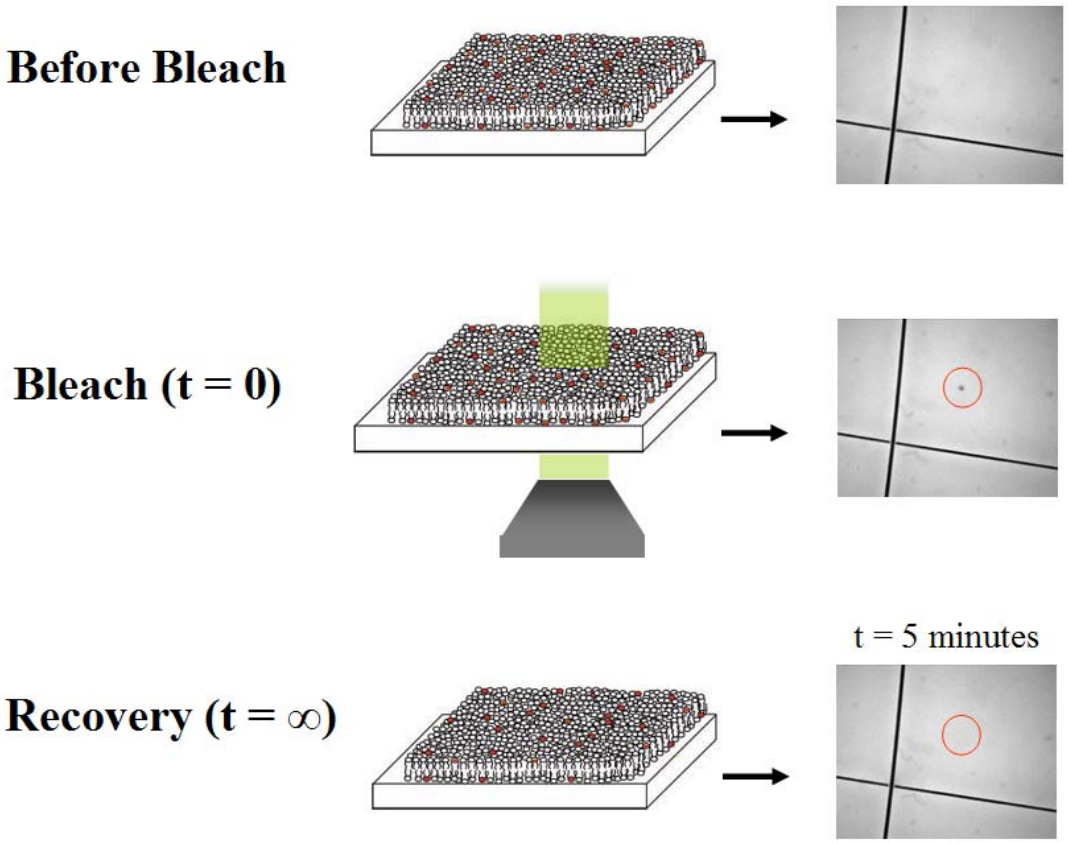

Figure 2.4 Physical processes involved in a fluorescence recovery after photobleaching experiment.

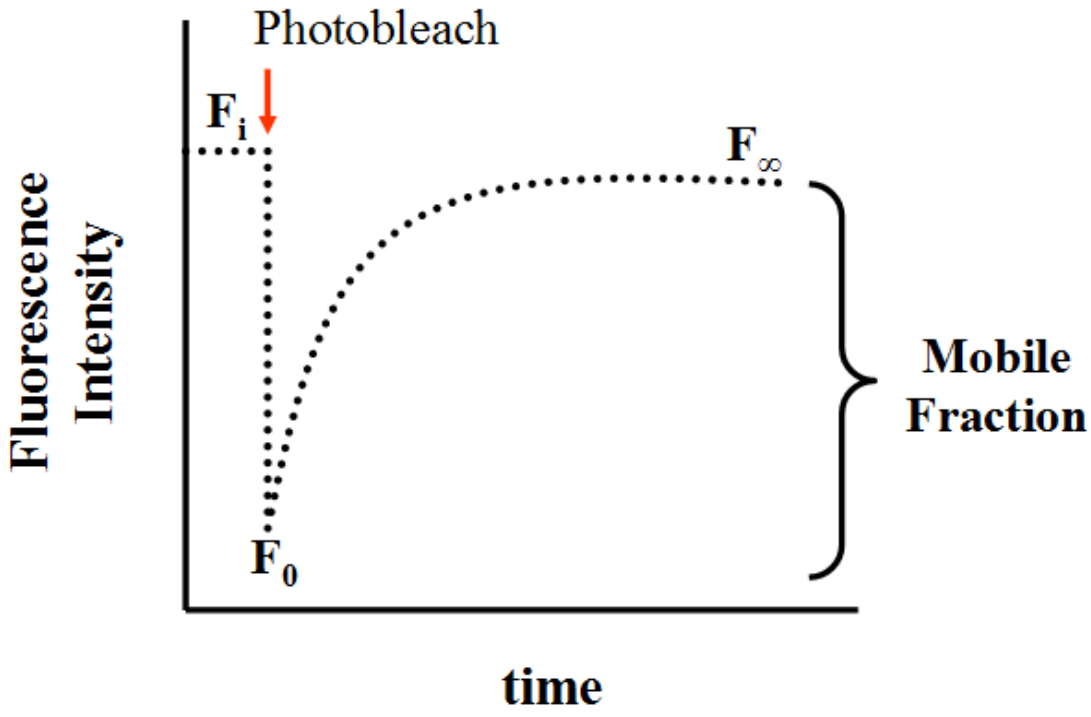

Figure 2.5 A FRAP curve showing the physical processes involved in a fluorescence recovery after photobleaching experiment.

infinite two-dimensional plane and that we are only measuring the two-dimensional diffusion of that species.[86] Applying first order kinetics allows us to fit the FRAP curve to a single exponential rise to maximum equation as follows:

$$y = a(1 - e^{-kt}) \qquad (2.2)$$

where *a* is the mobile fraction of the species and k is a constant. The time at half recovery, denoted as $t_{1/2}$ may be calculated by $t_{1/2} = \ln(2/k)$ since the process follows first order kinetics.

To calculate the lateral diffusion we will employ the following equation[86]:

$$D = \frac{w^2}{4\tau_{1/2}}\gamma_D$$

where w is the full width at half-maximum of the Gaussian profile of the focused beam, $t_{1/2}$ is the half time of fluorescence recovery, and γ_D is a correction factor that depends on the bleach time and the geometry of the laser beam and varies from 1.1 to 1.45.

It should be noted that the FRAP experiment depends on the control of various parameters. The laser beam is typically Gaussian and circular; however, variants of this technique may employ an elliptical beam.[97] The laser power and bleach time must remain constant in order to insure consistent results. For rapidly-diffusing molecules the bleach time must be short and post-bleach images recorded rapidly. Other factors that affect the diffusion measurements by FRAP include temperature and photobleaching of the sample during data acquisition. This may be controlled by adjusting the image acquisition time intervals during the time-laps imaging. The fluorophores that are used

as fluorescent markers should be bright and stable under low intensity illumination. This is important during image acquisition in the pre- and postbleach phase. Also, the fluorophores should bleach quickly and irreversibly under high intensity illumination during the bleach phase.

The fluorescence recovery after photobleaching (FRAP) curves used for this study were obtained by irradiating our samples with a 2.5 W mixed gas Ar^+/Kr^+ laser beam (Stabilite 2018, Spectra Physics). 100 mW of power was directed onto the sample for a time period of approximately one second. The beam, which was sent through a 10X objective, had a full width of ~ 13 μm at the sample plane. The recovery of the photobleached spot was followed as a function of time using time-lapse imaging under a fluorescence microscope (Nikon Eclipse TE2000U) equipped with a Sensys CCD camera (Photomatrics, Roper Scientific) and employing MetaMorph software (Universal Imaging). The fluorescence inverted microscopy system used for making FRAP measurements is shown in Figure 2.6.

Figure 2.7 shows a typical FRAP curve for a phospholipid bilayer supported on a hydrophilic glass substrate. The bilayer is composed of 99.9 mol % phosphatidylcholine lipids and 0.1 mol % Texas Red DHPE as fluorescent probe. A diffusion constant of 4.3 (±0.2) x 10^{-8} cm^2/s with 97% recovery was obtained for labeled phospholipids within the bilayer.

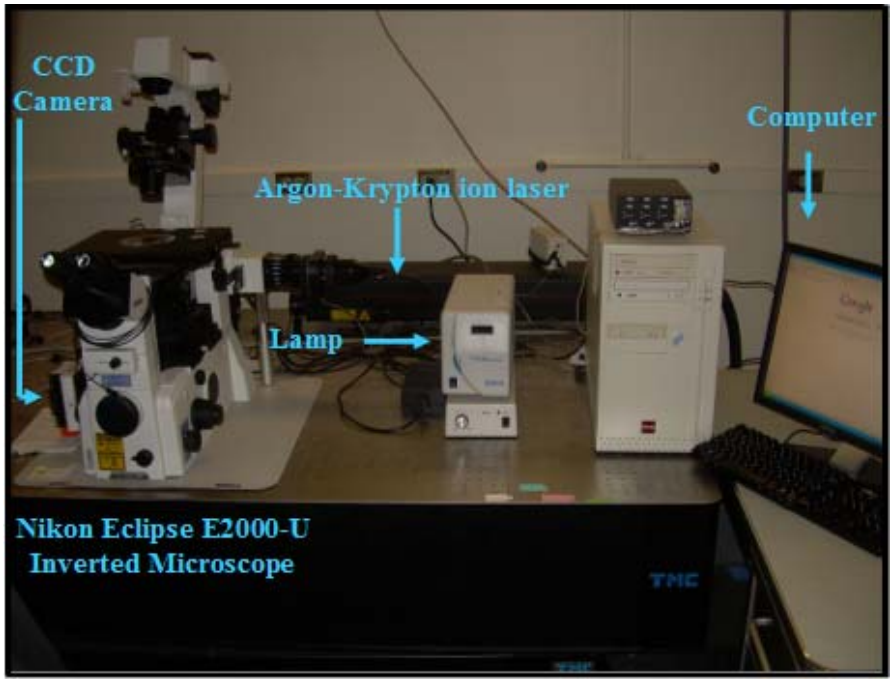

Figure 2.6 Inverted fluorescence microscope system used to obtain fluorescence recovery after photobleaching data.

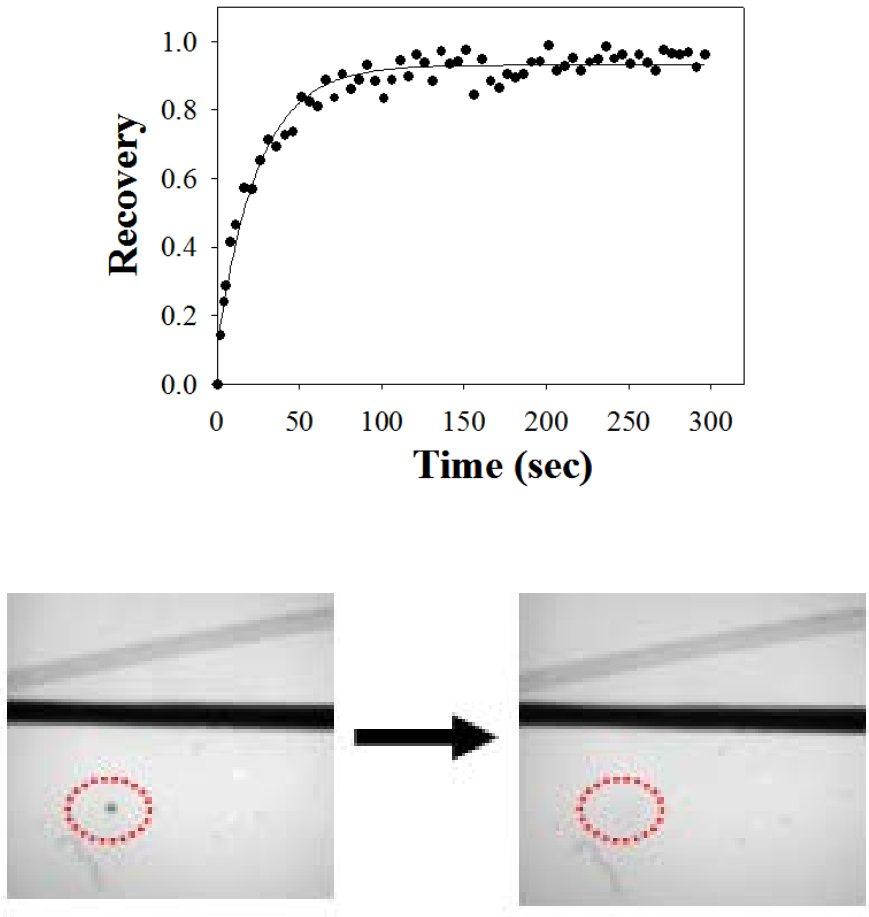

Figure 2.7 (Top) Fluorescence recovery after photobleaching for a membrane containing 99.9 mol % POPC bilayer with 0.1 mol% Texas Red DHPE as a fluorescent probe. The mobile fraction of the dye moiety in the bilayers is 0.97. (Bottom) Fluorescence micrographs of the same membrane showing the laser bleach spot both before and after recovery. The black lines in the images are scratches that were intentionally made with metal tweezers for estimation of the background contribution to the measured fluorescence intensity.

2.5 Supported Lipid Bilayer Electrophoresis

Charged species within a supported phospholipid membrane have been manipulated or separated by applying electric fields. Boxer and coworkers explored the use of electric fields to induce the motion of glycan-phosphatidyl inositol (GPI) tethered proteins in supported bilayers. Others charged species, such as lipids and adsorbed DNA molecules, have been manipulated in this manner.

Recently, we have developed a method that can be used to separate charged species using electrophoresis in a solid supported phospholipid bilayer. Figure 2.8 shows a schematic representation of the electrophoresis device. The device consists of a planar phospholipid bilayer supported on a hydrophilic substrate, such as glass (Fig. 2.9). On one side of the bilayer, liposomes containing fluorescently-conjugated phosphatidylethanolamine lipids (two isomers of Texas Red dye and a green dye, BODIPY) were spliced. Then an electric field was applied across the supported membrane laterally. The electric field induced an electrophoretic movement of the charged species within the supported membrane. Species separated based on their charge, size, and interaction with the surrounding bilayer medium. The device functions much like a chromatographic separation, except here our separation medium is the bilayer itself, which preserves the native environment of the species within it, avoiding denaturation due to exposure of the species to external factors. This is an advantage over conventional membrane protein purification techniques, such as gel electrophoresis.

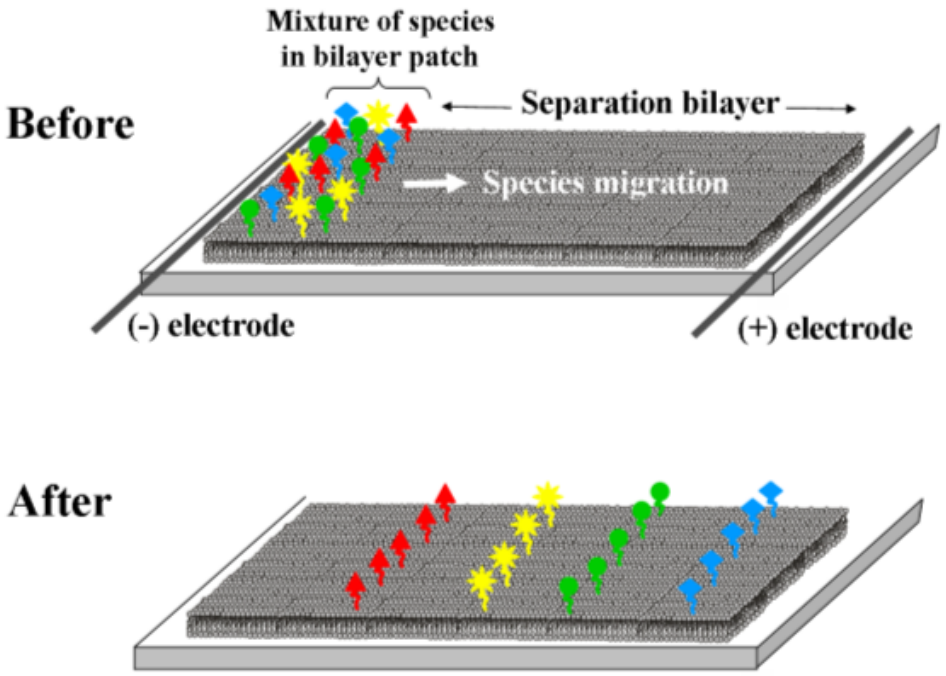

Figure 2.8 Three-dimensional schematic representation of solid-supported bilayer electrophoresis for the purification of membrane species. The top panel shows the solid-supported bilayer with the left most side containing a mixture of species to be separated. Two platinum electrodes are placed along the edge of the bilayer and a potential applied across them. After a certain amount of time, the species separate into well-defined bands, as shown in the lower panel.

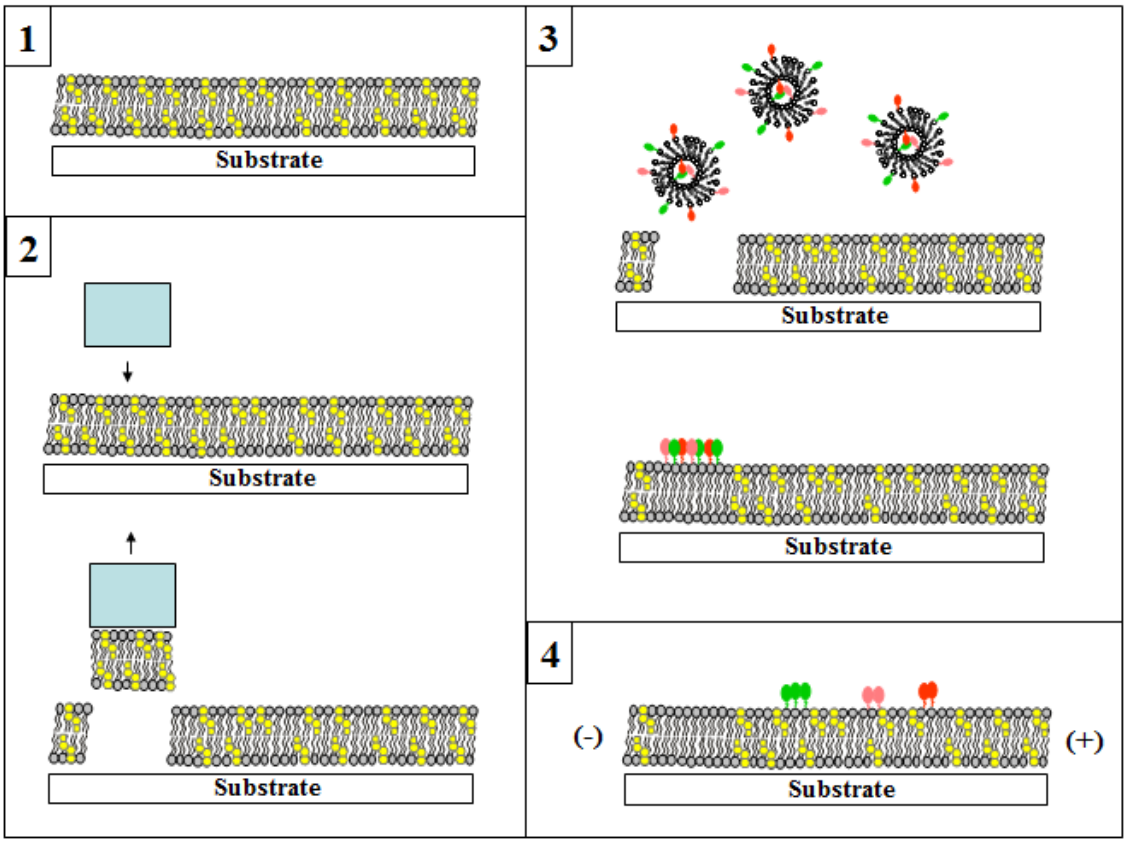

Figure 2.9 Procedure to form bilayer and separate a mixture of dye labeled lipids by electrophoresis. (1) First form a bilayer containing 25 mol% cholesterol (yellow) in POPC lipids (gray) via vesicle fusion. (2) Gently press the edge of a glass coverslip slide coated with Teflon tape into the bilayer and plow out a thin line of the bilayer. The resulting region will be devoid of any bilayer. (3) Add vesicles containing the mixture of fluorophores to be separated to the bulk aqueous phase above the supported bilayer. These vesicles will fuse in the bare region. (4) Apply a potential laterally across the bilayer and observe the resulting separation of fluorescent lipids, as indicated by the colored arrows corresponding to each type of lipid.

2.6 Thin Layer Chromatography (TLC)

Thin Layer Chromatography, introduced in 1938 by Izmailov and Shraiber, is a chromatographic technique commonly used to separate mixtures of substances into their components. This chromatography technique consists of a stationary phase and a mobile phase. The stationary phase is made of a thin layer of absorbent material, usually silica gel, aluminum oxide, or cellulose coated onto a piece of glass, metal, or rigid plastic. The mobile phase is an organic solvent or mixture of organic solvents. The mobile phase moves up through the stationary phase via capillary action. As the mobile phase travels up the plate, the different components of the mixtures travel at different rates and the mixture is separated into the different components. TLC takes advantage of the different affinity of the analyte with the mobile and the stationary phases to achieve separation of the mixture.

Herein, TLC was used to determine and purify the different isomers of Texas Red-DHPE. Several small spots of Texas Red DHPE in chloroform were spotted on a TLC plate and eluted with 100% ethanol (Figure 2.10). Texas Red labeled phospholipids were recovered from the TLC plate by carefully scraping the separated bands with a razor blade and resuspending in ethanol to extract the lipids from the silica beads. The mixture was centrifuged at 13,500 RPM (5415, Eppendorf) for 5 minutes and the supernatant was collected. This procedure was repeated until no Texas Red phospholipids were detected in the pellet. In order to remove the ethanol, the samples were dried with nitrogen, followed by desiccation under vacuum for 1 hour.

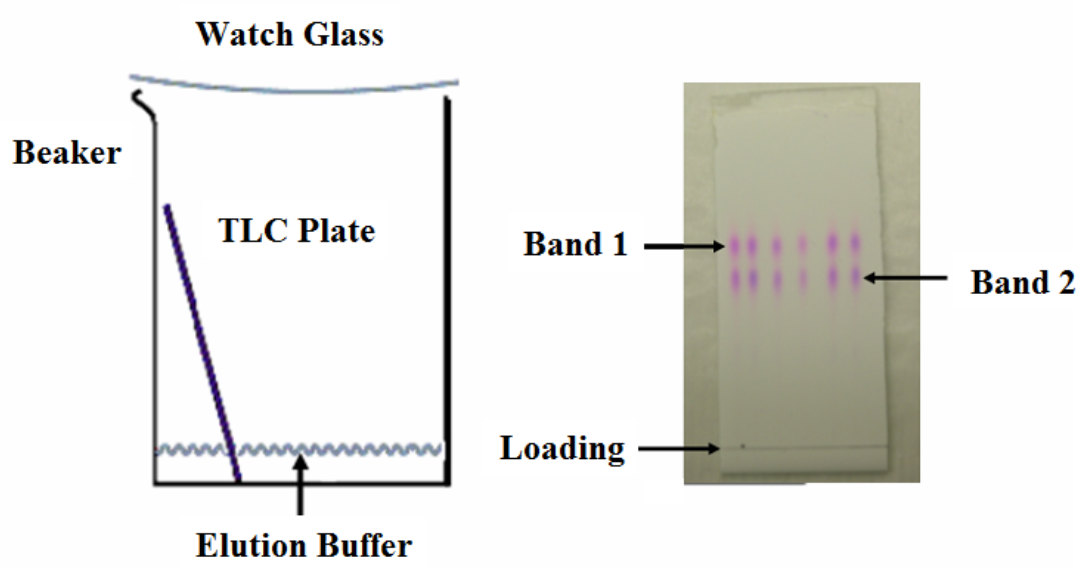

Figure 2.10 (Right) Schematic representation of a TLC experiment. (Left) Image of a TLC plate after Texas Red DHPE separation. Six individual spots of Texas Red DHPE were placed at the bottom of the plate (horizontal loading line) and eluted with ethanol for approximately 20 minutes.

CHAPTER III

DOUBLE CUSHIONS ENABLE THE FORMATION OF FLUID TRANSMEMBRANE PROTEINS IN SUPPORTED LIPID MEMBRANES

3.1 Synopsis

Supported lipid bilayers (SLBs) have been widely used as model systems to study cell membrane processes because they preserve the same two-dimensional membrane fluidity found in living cells. One of the most significant limitations of this platform, however, is its inability to incorporate mobile transmembrane species. It is often postulated that transmembrane proteins reconstituted in SLBs lose their mobility because of direct interactions between the protein and the underlying substrate. Herein, we demonstrate a high mobile fraction for a transmembrane protein, annexin V. Our strategy involves supporting the lipid bilayer on a double cushion, where we not only create a large space to accommodate the transmembrane portion of the macromolecule, but also passivate the underlying substrate to reduce non-specific protein-substrate interactions. The thickness of the confined water layer can be tuned by fusing vesicles containing polyethyleneglycol (PEG)-conjugated lipids of various molecular weights to a glass substrate that has first been passivated with a sacrificial layer of bovine serum albumin (BSA). The two-dimensional fluidity of these systems was characterized by fluorescence recovery after photobleaching (FRAP) measurements. Uniform and mobile phospholipid bilayers with lipid diffusion coefficients around 3×10^{-8} cm^2/sec and percent mobile fractions over 95 % were obtained. Moreover, we obtained annexin V

diffusion constants around 3 x 10^{-8} cm^2/sec with mobile fractions up to 75%. This represents a significant improvement over bilayer platforms fabricated directly on glass or using single cushion strategies.

3.2 Introduction

Supported lipid bilayers (SLBs), pioneered by McConnell et al.,[26-28] have successfully reproduced many aspects of cell membrane behavior. They possess the same two-dimensional fluidity and have been employed to investigate lipid assembly, [29,30] membrane structure,[31,32] dynamics,[33] and multivalent ligand-receptor binding.[34,35] They have even been used in the development of biosensors platforms[37] and separation devices.[98] Despite this, the incorporation of transmembrane proteins into SLBs has not yet been satisfactorily achieved. The problem lies in the limited space between the bottom leaflet of the bilayer and the underlying solid support. This distance, which is typically only on the order of one nanometer, is not usually sufficient to accommodate species that protrude extensively beyond the lower leaflet of the bilayer. Several research groups have explored methods to increase this spacing. Most strategies involve the placement of a polymer cushion between the membrane and support.[54,60,71,73-83,99-103] To date, however, these experiments generally report that proteins which protrude extensively beyond the lower leaflet have a 25% mobile fraction or less. In other words, more than three quarters of the protein molecules are immobilized by the underlying support and perhaps partially denatured.

SLBs have a complex series of interactions with underlying planar glass

supports. These include van der Waals, electrostatic, hydrophobic, and steric interactions.[39-41] Such forces act together to leave a thin layer of hydration water trapped between the bilayer and the substrate.[42-45] This water layer helps to maintain the lateral mobility of lipids in both leaflets of the bilayer. It would be important to extend this same principle to membrane proteins. To this end, soft, hydrophilic polymeric materials have been a popular choice for cushion materials because they readily imbibe large amounts of water.[55,70,71,104] Ideally, the polymer film should act like the cytoskeleton found in mammalian cell membranes. Such an approach, in principle, should significantly reduce frictional coupling and avoid protein denaturation. Methods for the preparation of polymer supports include the chemical grafting of polymers, such as cellulose or dextran directly onto the solid surface followed by the subsequent deposition of lipid bilayers.[77,78] A slightly different approach involves the reconstitution of lipopolymers that also provide a spacer between the underlying substrate and the phospholipid bilayer.[54,60,71,79-83,101-103,105] The difference in this case is that alkyl side chains emanating from the lipopolymer directly intercalate into a nascently transferred lipid film.

Despite extensive work on cushion designs, only a few studies describe the use of these systems to study the lateral mobility of transmembrane proteins.[54,99,106,107] Tamm and coworkers[54] designed a PEG-conjugated phospholipid membrane that could be covalently bonded to silicate substrates. Lateral diffusion of cytochrome b_5 and annexin V were measured by FRAP in this system. Although lateral diffusion coefficients were obtained, only 25% of the cytochrome b_5 displayed a diffusion

constant value that was on the same order of magnitude as the lipids. The rest of the cytochrome b_5 molecules diffused several orders of magnitude more slowly or not at all, due presumably to interactions between the proteins and the underlying polymer network. Similar results were obtained for annexin V. Another protein mobility study was performed by Tanaka, Sackmann, and coworkers.[99] In this case human, platelet integrin $\alpha_{IIb}\beta_3$ was investigated in a supported bilayer system that rested on a cellulose cushion. Again, only about one quarter of the proteins were mobile in the presence of the cushion and none were mobile without it. In a third example, Smith, Wirth, and coworkers[107] studied the mobility of the human delta-opioid receptor on acrylamide cushions of various thicknesses. In this case, however, only data for an individually mobile protein molecule were reported rather than the mobile fraction for a population of membrane embedded proteins. Finally, Brozik and coworkers used nanoporous microbeads rather than a polymer cushion strategy to support lipid membranes with bacteriorhodopsin.[85] High protein mobile factions were obtained (~78%) with D = 3.8 x 10^{-10} cm^2/sec for proteins in the pores of the bead. It would be important, if the same type of mobility can be extended to systems with planar geometry.

In the work described herein, we investigate the two-dimensional fluidity of a transmembrane protein, annexin V, reconstituted into a double cushion planar supported

membrane system. Annexin V is a multi-helical intracellular protein that binds to negatively charged phospholipids in a Ca^{2+}-dependent manner.[108] The function of this protein has been ascribed to different membrane-associated events including vesicular trafficking, membrane fusion, and ion channel formation.[109] It has been reported that annexin V forms ion channels in phospholipid bilayers at mildly acidic pH values.[110-112]

Figure 3.1 illustrates our strategy for achieving high mobile fractions of annexin V. A first cushion layer is formed by uniformly adsorbing BSA onto a planar glass support. This protein monolayer passivates the substrate and thereby helps prevent strong interactions with the underlying oxide surface. The second layer of the cushion is formed when lipid vesicles containing (poly)ethyleneglycol-conjugated lipids are fused on top of the first layer. The spacing between the BSA film and the lower leaflet of the bilayer can be modulated by changing the number density and molecular weight of the PEG lipopolymer incorporated into the lipid bilayer. The best results were achieved when a 0.1 mg/ml BSA solution was incubated over the surface for 20 minutes and the lipid bilayer consisted of 0.5 mol% PEG^{5000}. In that case, the mobile fraction of annexin V was ~ 75% with a diffusion constant of 3×10^{-8} cm^2/sec.

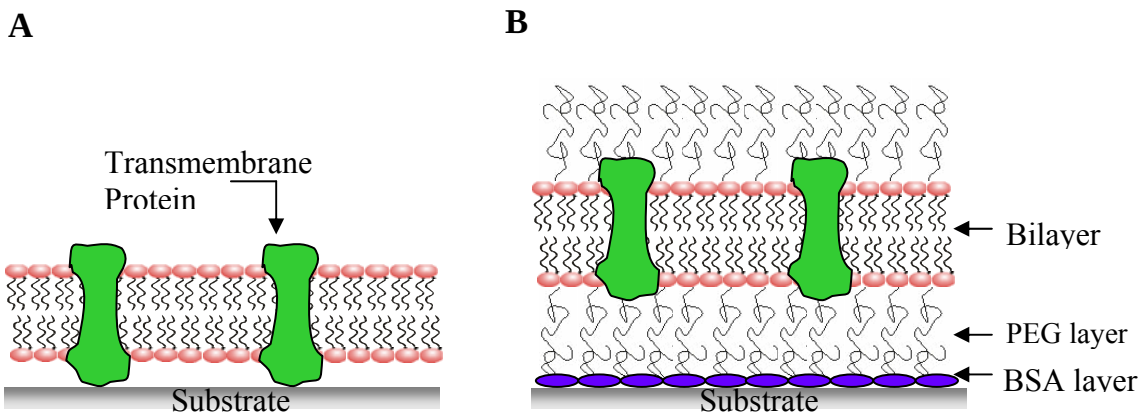

Figure 3.1 Schematic diagram of the supported bilayer systems used in this work. (A) A bilayer supported directly on a bare glass substrate. Membrane proteins, which protrude beyond the lower leaflet of the bilayer, become immobilized by direct interactions with the underlying glass surface. (B) The double cushion system creates more space between the bilayer and support and also mitigates interaction with the substrate.

3.3 Experimental

Materials

1-Palmitoyl-2-oleoyl-*sn*-glycero-3-phosphocholine (POPC), bovine brain L-α-phosphatidylserine (brain-PS), and 1,2-dioleoyl-*sn*-glycero-3-phosphoethanolamine-*N*-[methoxy(poly(ethylene glycol))] (PEG-PE) were purchased from Avanti Polar Lipids (Alabaster, AL) with PEG molecular weights of 550, 2000 and 5000. *N*-(Texas Red sulfonyl)-1,2-dihexadecanoyl-*sn*-glycero-3-phosphoethanolamine (Texas Red DHPE) was obtained from Molecular Probes (Eugene, OR). Bovine serum albumin (BSA) was purchased from Sigma Aldrich (St. Louis, MO). Phycoerythrin-labeled recombinant human annexin V with a molecular weight of 35,800 Da, was obtained from Alexis Biochemicals (San Diego, CA).

Purified water from a NANOpure Ultrapure Water System (Barnstead, Dubuque, IA) was used to prepare all buffer solutions. The water had a minimum resistivity of 18 MΩ·cm. Phosphate-buffered saline (PBS) was prepared using 10 mM sodium phosphate with the addition of 150 mM NaCl (Sigma-Aldrich). The pH was adjusted to 7.4 by the dropwise addition of NaOH (EMD, Germany). Tris(hydroxymethyl)aminomethane was used to prepare 10 mM Tris (Fluka-BioChemika) buffer with 8 mM $CaCl_2$ (Acros Organic), and 100 mM sodium chloride (Sigma-Aldrich). Polydimethylsiloxane (PDMS) was used to fabricate well structures. The polymer and cross-linker were purchased from Dow Corning (Sylgard Silicone Elastomer-184, Krayden Inc.).

Small Unilamellar Vesicles

Small unilamellar vesicles (SUVs) were prepared as previously reported.[29,113,114] Briefly, the desired amount of POPC, PEG-PE lipopolymer, and PS were mixed in appropriate proportions from stock solutions in chloroform and allowed to dry under a stream of nitrogen followed by desiccation under vacuum for 4 hours. In some cases 0.1 mol% Texas Red DHPE was used as a fluorescent probe. After evaporation of the solvent, the lipids were reconstituted in Tris buffer and subjected to ten freeze-thaw cycles by alternating between immersion in liquid nitrogen and a 30 ºC water bath. The solution was then extruded five times through a polycarbonate filter (50 nm pore size) to produce vesicles of uniform size. Small unilamellar vesicles prepared by this method were 80 ± 10 nm in diameter as determined by dynamic light scattering using a 90Plus Particle Size Analyzer from Brookhaven Instrument Corp.

Supported Lipid Membranes

Supported lipid bilayers were prepared by the adsorption and fusion of SUVs onto clean planar borosilicate coverslips (VWR International).[26,46,115,116] Polymer-conjugated bilayers were prepared by the same vesicle fusion method, but using the desired amount of PEG-PE as previously reported.[113,117] Coverslips were cleaned with 7X detergent solution (MP Biomedicals, Solon, OH)[66] and annealed in a kiln at 550 °C for five hours to yield flat surfaces with room mean square roughness (RMS) values on the order of ~0.13 nm over a 1 μm^2 area as determined by atomic force microscopy. Vesicle fusion was performed via the introduction of a 100 μL SUV solution onto the

clean glass. The solution was confined to a circular area (~8 mm in diameter) in the center of the surface by a thin hydrophobic PDMS microwell.[113] After a 10 min incubation period, the bilayer was extensively rinsed with buffer to remove excess vesicles.

Lipid bilayers supported on a protein film were prepared by fusing vesicles in a manner similar to the one described above. In this case, however, a 100 μL BSA solution in Tris was introduced to the microwell first, incubated for a period of 20 minutes, followed by thorough rinsing with buffer. Solutions of BSA were prepared at concentrations ranging from 0.001 mg/ml to 0.5 mg/ml. Prior to use, the protein solutions were centrifuged at 13,500 RPM for 20 minutes (5415, Eppendorf) to remove any aggregates from the bulk solution.

Reconstitution of Annexin V

Each supported bilayer was incubated for 20 minutes with Tris buffer containing 8 mM $CaCl_2$ before the introduction of protein solution. It should be noted that the divalent metal ion is required for annexin V incorporation into the membrane.[54,108] At this point, a solution of phycoerythrin-labeled annexin V (0.1 mg/ml) in Tris buffer was introduced into the bulk solution above the surface and incubated for 30 minutes. The bilayers were extensively washed with a buffer solution containing EDTA (10 mM Tris, pH 6.0, 100 mM NaCl, and 5 mM EDTA) to remove any excess protein bound to the upper leaflet. It has been previously shown that annexin V molecules, which are not fully inserted into the bilayer, can be easily removed from the interface by exposing the

system to 5 mM EDTA.[118,119] We, therefore, exposed our system to the same conditions to remove all partially bound annexin V molecules from the interface before performing FRAP experiments. In a final step, fresh Tris was flowed over the bilayer at pH 6.0 and FRAP experiments were performed. Under these conditions, the annexin V should be fully inserted into the membrane.[110-112] By contrast, working at somewhat higher pH does not lead to protein insertion.[120]

Fluorescence Recovery after Photobleaching

FRAP[86,96] experiments were carried out with a 2.5 W mixed gas argon/krypton ion laser (Stabilite 2018, Spectra Physics). Samples were irradiated at 568.2 nm with 100 mW of power for 1 second. A 13 μm full width at half-maximum bleach spot was made by focusing the light onto the bilayer through a 10× objective. The fluorescence recovery was measured using MetaMorph Software (Universal Imaging). The fluorescence intensity of a bleached spot was determined as a function of time after background subtraction and intensity normalization. All fluorescence recovery curves were fit to a single exponential equation to obtain the mobile fraction of labeled lipids and proteins and the half-time of recovery, $t_{1/2}$. The equation employed to calculate the lateral diffusion constant of dye-labeled lipids and proteins was as follows:[86]

$$D = (w^2/ 4t_{1/2}) \gamma_D \quad (3.1)$$

where w is the full width at half-maximum of the Gaussian profile of the focused beam and γ_D is a correction factor that depends on the bleach time and the geometry of the laser beam.[86] The value of γ_D was 1.1.

3.4 Results

Protein Supported Lipid Membranes

In a first set of experiments, BSA was coated onto clean glass coverslips from a Tris buffer solution at concentration of 0.1 mg/ml. After rinsing, POPC vesicles were introduced above the protein film in Tris buffer at a concentration of 1 mg/mL. The vesicles contained 0.1 mol% Texas Red DHPE for visualization under an epifluorescence microscope. The inset images in Figure 3.2 show fluorescence micrographs of this bilayer immediately after photobleaching and again 300 sec later. The FRAP curve denotes the fluorescence intensity in the bleached spot as a function of time. As can be seen, relatively complete recovery was observed with a diffusion constant of 4.0 ($\pm$0.3) $\times$ 10^{-8} cm^2/sec. Moreover, the sample recovered roughly 97% of its initial fluorescence at $t = \infty$.

These experiments were repeated at a total of 7 different BSA concentrations ranging from 0.01 to 0.5 mg/ml. The diffusion constant values for Texas Red DHPE in the POPC membranes are plotted in Figure 3.3. As can be seen, these values remained unchanged between 0.01 and 0.1 mg/ml BSA. Recovery was nearly complete in each case (0.97 $\pm$ 0.01). At 0.2 mg/ml, the diffusion slowed dramatically and the mobile fraction of Texas Red DHPE was 0.60. Long-range diffusion was completely arrested when the BSA concentration was 0.3 mg/ml or higher.

Analogous experiments were performed with membranes containing 79.9 mol% POPC, 20 mol% brain-PS and 0.1 mol% Texas Red DHPE. In that case, however, the results were quite different. Indeed, no fluorescence recovery was observed for these

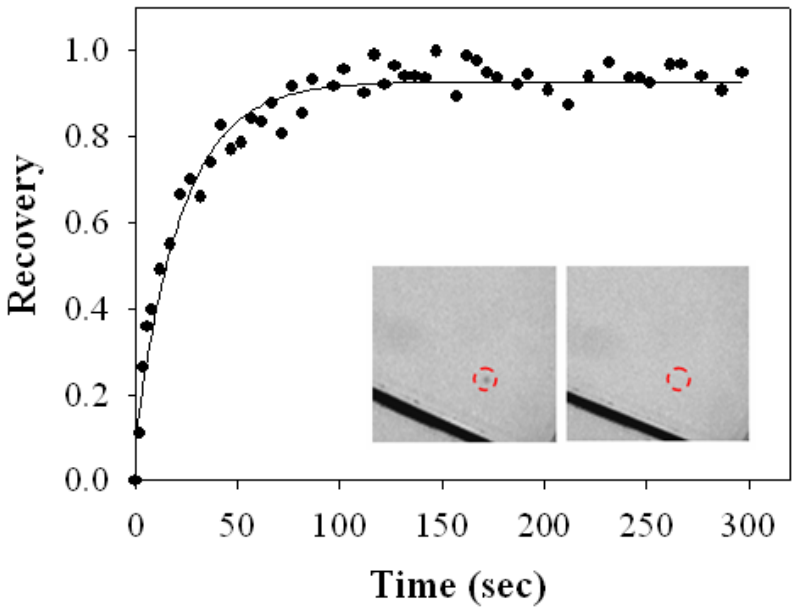

Figure 3.2 FRAP curve from a BSA supported POPC bilayer with 0.1 mol% Texas Red DHPE. The BSA was introduced at 0.1 mg/ml. The black lines in the inset fluorescence images are scratches that were intentionally made with pair of metal tweezers for estimation of the background contribution to the measured fluorescence intensity. The dashed red circles highlight the position of the beach spot. The inset images, which are 230 μm x 230 μm, were captured immediately after photobleaching and again 300 sec later.

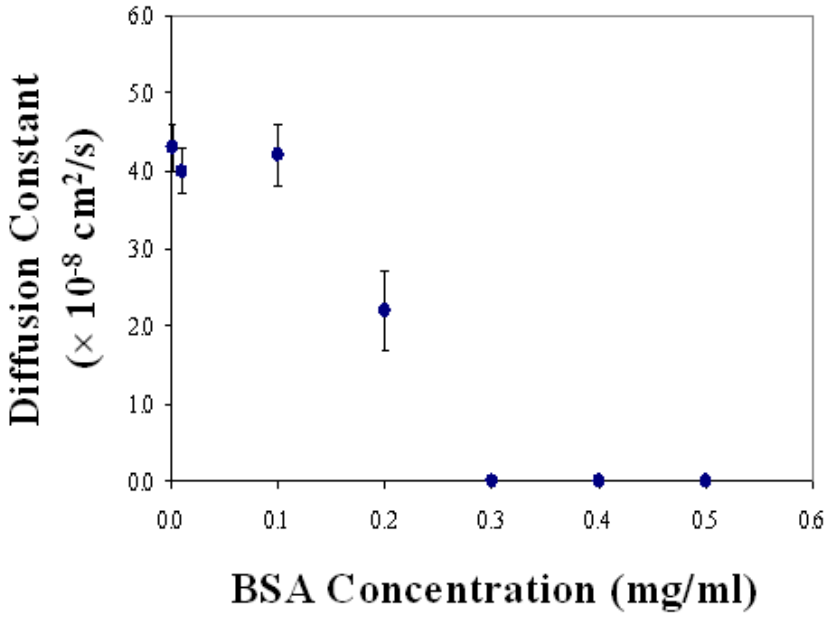

Figure 3.3 Diffusion of Texas Red-labeled lipids in POPC bilayers as a function of the BSA incubation concentration.

membranes introduced above BSA films formed from 0.1 mg/mL solutions. It has been reported in the literature that the addition of Ca^{2+} into the buffer can sometimes aid bilayer formation when PS lipids are present.[57] We therefore repeated these experiments in the presence of 8 mM Ca^{2+} under otherwise identical conditions. Again, the Texas Red DHPE probes were found to be completely immobile. A final control was performed in the in the presence of PS lipids without the BSA cushion. In this case the bilayer was mobile with D = 3.5 (± 0.1) × 10^{-8} cm^2/s and a 0.90 mobile fraction.

Polymer Supported Lipid Membranes without BSA

Polymer supported lipid bilayers were prepared as previously reported.[113] The lipopolymer was added to POPC vesicles containing 20 mol% brain-PS and 0.1 mol% Texas Red DHPE. PEG-PE lipids with three different molecular weights and concentrations were employed: 7 mol% for PEG^{550}-PE, 1.4 mol % for PEG^{2000}-PE, and 0.5 mol % for PEG^{5000}-PE, respectively. These particular values were chosen to correspond to the onset of the mushroom-to-brush transition as calculated by Marsh and coworkers.[121] All experiments were performed on clean glass coverslips without the introduction of BSA. Fluorescence imaging experiments confirmed the supported membranes were homogeneous down to the diffraction limit. FRAP measurements were also made and the values for the diffusion constant and mobile fraction are provided in Table 3.1. As can been seen, these values were consistent with high quality supported bilayers in each case. It should distinguished that the PEG moiety is not chemically grafted to the surface and that the lipopolymer remains mobile on the surface under these

Table 3.1 Lateral mobility of Texas Red-labeled lipids in glass-supported lipid bilayers containing PEG-PE.

Type of Support	**Diffusion Coefficient ($\times 10^{-8}$ cm^2/s)**	**Mobile Fraction (%)**
PEG 550	3.5 ± 0.1	95.8 ± 3.6
PEG 2000	3.6 ± 0.2	93.3 ± 3.4
PEG 5000	3.8 ± 0.4	93.5 ± 3.1

conditions.[113] Finally, it should be pointed out that the experiments associated with Table 3.1 were performed in the absence of Ca^{2+}. Control experiments were done in the presence of 8 mM $CaCl_2$ and these gave identical results to those shown in the table within experimental error.

Double Cushion System

Novel double cushion systems were investigated whereby PEGylated membranes were fused to substrates coated with BSA. To construct these systems, 0.1 mg/ml BSA was introduced above the planar glass substrates and allowed to incubate for 20 min. This concentration was chosen because it represents the highest protein concentration at which full mobility of the lipids was still observed in Figure 3.3. After extensively rinsing, POPC vesicles with 20 mol% brain-PS, 0.1 mol% Texas Red DHPE, and 7 mol% PEG^{550}-PE were fused to a protein-coated coverslip. The lateral diffusion coefficient of Texas Red DHPE was $3.2 \pm (0.3) \times 10^{-8}$ cm^2/sec with a mobile fraction of 94%. This result is quite significant because it indicates the presence of the PEG cushion mitigates the interactions between the BSA and the negatively charged brain PS to a sufficient extent to allow long range bilayer fluidity. Control experiments revealed that the addition of 8 mM $CaCl_2$ to the buffer had not influence on either the diffusion constant or the mobile fraction.

These experiments were repeated with PEG^{2000} and PEG^{5000} at their respective mushroom-to-brush concentrations and the results are provided in Table 3.2. As can be seen, both the diffusion constant and mobile fraction remained quite high for all PEG chain lengths employed.

Table 3.2 Lateral mobility of Texas Red-labeled lipids supported in the double cushion system.

Double Cushion System	**Diffusion Coefficient ($\times 10^{-8}$ cm^2/s)**	**Mobile Fraction (%)**
PEG 550 – BSA	3.2 ± 0.3	94.0 ± 4.6
PEG 2000 - BSA	3.2 ± 0.4	95.3 ± 3.1
PEG 5000 – BSA	3.0 ± 0.4	93.0 ± 1.7

Reconstitution and Lateral Diffusion of Annexin V

In a next set of experiments, the lateral diffusion of annexin V was investigated in lipid bilayers containing 20 mol% PS, 79.9 mol% POPC, and 0.1 mol% Texas Red DHPE on bare glass substrates. After a bilayer was formed, 0.1 mg/ml phycoerythrin-labeled annexin V was introduced above the interface in Tris buffer with 8 mM $CaCl_2$ and incubated for 30 minutes. Unbound protein molecules were rinsed away with EDTA and fresh buffer was added back to the system. Finally, diffusion constant and mobile fraction measurements of the biomacromolecules were made by FRAP (Table 3.3). As can be seen, three quarters of the protein molecules were immobile and the diffusion constant of the protein was significantly slower than that for Texas Red DHPE.

Identical measurements were repeated in membranes containing PEG^{2000} lipopolymer. The effect of polymer density on the lateral diffusion of phycoerythrin-labeled annexin V was quantified by varying the mol% of PEG^{2000}-PE moieties within the membrane. The mole fractions of PEG^{2000}-PE used in these experiments were 0.5%, 1.4%, and 5%. At low PEG density (0.5 mol % PEG^{2000}-PE), the PEG moiety exists in a mushroom conformation. At higher polymer density (5 mol % PEG^{2000}-PE), the PEG moiety should be well into the brush transition. The values for the diffusion constant and mobile fraction of annexin V as a function of lipopolymer density are provided in Table 3.3. As can be seen, the highest diffusion constant and mobile fraction values were found at the onset of the mushroom-to-brush transition. The decrease in mobility above and below this value makes sense. Indeed, an isolated mushroom conformation for PEG^{2000} won't be able to prevent direct indirections between annexin V and the substrate

Table 3.3 Effect of PEG^{2000} mole density on the two-dimensional lateral mobility of fluorescently labeled annexin V.

PEG^{2000}-PE Concentration	**Diffusion Coefficient ($\times 10^{-8}$ cm^2/s)**	**Mobile Fraction (%)**
0 mol%	0.3 ± 0.1	26.3 ± 3.2
0.5 mol%	1.3 ± 0.2	28.9 ± 4.8
1.4 mol%	2.0 ± 0.2	35.8 ± 3.2
5 mol%	1.0 ± 0.3	19.9 ± 2.9

at many locations on the surface. On the other hand, concentrations of PEG well into the brush transition are known to lead to lipopolymer immobilization,[113] which almost certainly affects the mobility of the membrane protein. An intermediate lipopolymer concentration avoids both of these problems.

To investigate the influence of the polymer chain length on the lateral diffusion of phycoerythrin-labeled annexin V, lipopolymers were incorporated into POPC bilayers at different molecular weights (PEG^{550}, PEG^{2000}, and PEG^{5000}) at the onset of the mushroom-to-brush transition. Increasing the length of the polymer chain increases the membrane-substrate distance.[122] This should decrease the interactions between the inserted membrane protein and the underlying substrate. Indeed, higher diffusion coefficients were obtained for annexin V reconstituted into membranes with longer polymer chains (Table 3.4). Nevertheless, the majority of the protein molecules were immobile in all cases.

Finally, the two-dimensional fluidity of annexin V was measured in double cushioned systems. Figure 3.4 shows fluorescence micrographs and the corresponding FRAP recovery curve for phycoerythrin-labeled annexin V reconstituted into the PEG-PE^{5000}/BSA system. The fluorescence recovery of the photobleached spot was remarkably high (~ 74%) and the diffusion coefficient value of the protein, $2.9 \pm (0.4) \times 10^{-8}$ cm^2/sec, was nearly as high as that for the Texas Red-conjugated lipid probes. The mobile fraction was strongly dependent on the length of the polymer chain length. Moreover, the diffusion constant also decreased with decreasing chain length. Both the

Table 3.4 Effect of polymer length (PEG^{550}, PEG^{2000}, PEG^{5000}) on the two-dimensional lateral mobility of fluorescently labeled annexin V.

Type of Support	**Diffusion Coefficient ($\times 10^{-8}$ cm^2/s)**	**Mobile Fraction (%)**
Glass	0.3 ± 0.1	26.3 ± 3.2
7 mol% PEG 550	0.4 ± 0.1	27.7 ± 3.4
1.4 mol% PEG 2000	2.0 ± 0.2	35.8 ± 3.2
0.5 mol% PEG 5000	3.5 ± 0.4	24.6 ± 1.7

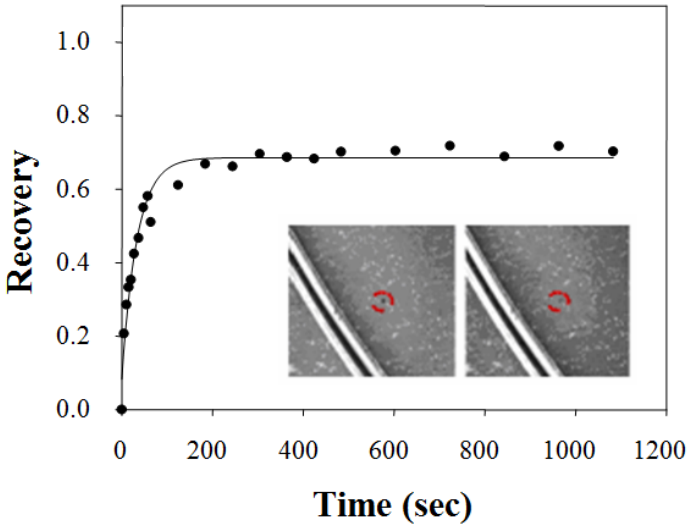

Figure 3.4 Employment of a double-cushion system for maintaining the two-dimensional lateral mobility of annexin V. Phycoerythrin-labeled annexin V was added to the bilayer and incubated for 30 min. Excess protein was rinsed away with EDTA before FRAP measurement were made. The black lines in the inset images are scratches that were intentionally made with a pair of metal tweezers for estimating the background contribution to the measured fluorescence intensity. The dashed red circles show the position of the bleach spot. The inset images, which are 300 μm x 300 μm, were captured immediately after photobleaching and again 1200 sec later.

diffusion constant and mobile fraction values obtained for annexin V are provided in Table 3.5.

3.5 Discussion

It has been reported that spacer length and density play an important role in the structure and function of supported membranes.[102,122,123] Wagner et al. reported the formation of uniform and mobile bilayers on PEG coated substrates made with silane-functionalized PEG^{2000} tethers,[54] whereby the polymer concentration was maintained slightly below the mushroom-to-brush transition. It was observed that a decrease in the mobile fraction of fluorescently labeled lipids was directly related to increasing the polymer density within the supported membrane. In 2004, Purrucker and Tanaka reported that the spacer length could strongly influence the distribution, function and lateral diffusion of transmembrane proteins.[102] They observed a homogenous distribution of labeled integrin $\alpha_{IIb}\beta_3$ when using longer polymer spacers. Such results suggest that the membrane-substrate distance is a very significant variable for successfully incorporating transmembrane proteins into supported bilayers. Finally, Kunding and Stamou reported that membrane-substrate distance in the presence of a PEG cushion could be varied by modulating the ionic strength of the solution.[122]

Herein, rapid diffusion of annexin V with a high protein mobile fraction was achieved with a double cushion system. The key difference between this platform and previous designs is the fact that a sacrificial protein layer was present between the polymer-cushioned membrane and the underlying substrate. BSA monolayers have been

Table 3.5 Lateral mobility of fluorescently labeled annexin V in the double cushion system.

Double Cushion System	**Diffusion Coefficient ($\times 10^{-8}$ cm^2/s)**	**Mobile Fraction (%)**
PEG 550 – BSA	0.5 ± 0.1	33.1 ± 6.2
PEG 2000 - BSA	2.0 ± 0.4	52.2 ± 4.7
PEG 5000 – BSA	2.9 ± 0.4	73.5 ± 2.4

previously shown to resist the adsorption of additional proteins on glass substrates[124] and are almost certainly providing a passivating layer in the present system. Evidence for this statement comes from Tables 3.4 & 3.5. Indeed, three-quarters of the annexin V molecules were immobile in the PEG^{5000}-PE system in the absence of the BSA monolayer. Such a result is consistent with the notion that the transmembrane protein molecules diffuse around on the surface until they encounter a high energy site on the glass substrate, which leads to immobilization. Once the majority of high energy sites have been passivated, however, the rest of the annexin V molecules remain mobile over periods of time sufficiently long to perform fluorescence recovery experiments.

It should be noted that the presence of the BSA film alone does not appear to be sufficient to produce a system with a high fraction of mobile protein molecules. Indeed, reducing the thickness of the PEG layer also reduces the mobile protein fraction (Table 3.5). It is curious to note that the mobile fraction increases essentially monotonically with increasing PEG length at the onset of the mushroom to brush transition. This is consistent with the notion that a minimum spacer length is required in order for protein molecules to diffuse freely.

Finally, it should be noted that the concentration of BSA incubated above the interface was key to forming high quality supported bilayers (Figure 3.3). Previous investigations have shown that relatively smooth BSA monolayers are formed with extensive spreading of protein molecules under circumstances where the BSA concentration in the bulk solution is relatively low (Figure 3.5).[124] On the other hand, high bulk protein concentrations led to more rapid BSA adsorption and higher surface

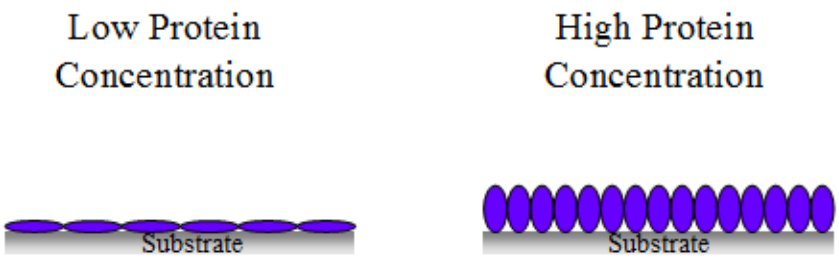

Figure 3.5 BSA coated glass coverslips. (Left) At low protein concentration, BSA forms a flat protein monolayer. (Right) At high protein concentration, a higher density of protein adsorbs more rapidly which prevents the BSA molecules from spreading.

densities. Consequently, there was much less protein spreading. The adsorption and relaxation kinetics of BSA molecules at the solid-liquid interface should play an important role in their function as cushions. It is probably the case that rougher surfaces, created with higher BSA concentrations, are not as conducive to the fusion of phospholipid vesicles. Indeed, previous studies have shown that vesicle fusion relies on relatively low substrate roughness.[41,72]

3.6 Summary and Conclusions

In conclusion, transmembrane protein mobility was maintain within our double cushion bilayer platform. With this novel system transmembrane protein diffusion values similar to the diffusion of fluorescently labeled lipids were obtained. In this study commercially available PEG-PE lipopolymers of molecular weights up to 5,000 were used. A mobile fraction of ~ 70 % was obtained with the PEG-PE 5,000. We suspect that increasing the PEG spacer to an even larger size would result in even higher mobile fractions.

CHAPTER IV

ELECTROPHORESIS IN SUPPORTED LIPID BILAYERS: SEPARATION, CHARACTERIZATION, AND IMAGING OF MEMBRANE BOUND SPECIES*

4.1 Synopsis

It is well-known that the purification of membrane species is a difficult process. The processing conditions are often harsh, which can result in alteration of native structures. We have developed a new method to rapidly separate membrane bound species without exposing the molecules to harsh environments. In this method we employ a solid supported bilayers made of POPC doped with cholesterol as a separation medium to laterally separate membrane species within the membrane. Cholesterol was used to reduce the diffusion of lipids within the bilayer and, therefore, substantially reduce mixing of the dye-conjugated lipids to be separated. These molecules were introduced into an SLB adjacent to the separations SLB and electrophoresis was employed to move these species through it. The separation of two isomers of Texas Red dye and a green dye, BODIPY, was achieved with high resolution and small band broadening. This procedure could be extended to the purification of peripheral and transmembrane proteins.

---

*Parts of this chapter are reprinted from "Separation of Membrane-Bound Compounds by Solid-Supported Bilayer Electrophoresis" by Daniel, S.; Diaz, A.J.; Martinez, K.M.; Bench, B.J.; Albertorio, F.; Cremer, P.S. 2007. *Journal of the American Chemical Society*, 129, 8072-8073, Copyright [2007] American Chemical Society.

4.2 Introduction

Separation, purification, and detection of biomembrane species such as lipids and transmembrane proteins are difficult tasks. The processing conditions are often harsh, which can result in alteration of native structures or complete loss of material.[125,126] Furthermore, it is difficult to detect subtle post-translational changes in these molecules that occur on the cell surface.[127-129] The procedures often require one to dissolve the membrane in detergent, sonicate, filter through chromatographic columns, and separate into bands using gel electrophoresis. The use of detergents has negative impact on the yields and stability of the proteins and often interferes with biophysical and crystallographic studies. Procedures that circumvent such drawbacks would represent an attractive alternative and could significantly impact transmembrane proteomics.

Herein, we describe a new method to rapidly separate membrane components without exposing the molecules to harsh environments. We employ a solid-supported lipid bilayer (SLB) made of POPC and cholesterol as the separation medium to laterally separate membrane-bound species (Figure 4.1). This procedure is somewhat analogous to gel electrophoresis, except that the SLB replaces the gel. It is well-documented that membrane components can be manipulated in SLBs using electrophoresis, including lipids,[46,48,98,130] vesicles tethered to the bilayer using DNA hybridization,[131,132] and GPI-linked proteins.[47] To conduct separations, however, it is necessary to tune the bilayer chemistry to attenuate the diffusion coefficient of the lipids and, therefore, reduce the diffusive mixing. Cholesterol significantly decreases the lipid diffusion coefficient[133,134] and **i**ncreases the band resolution one can obtain. As will be shown, this analytical-scale

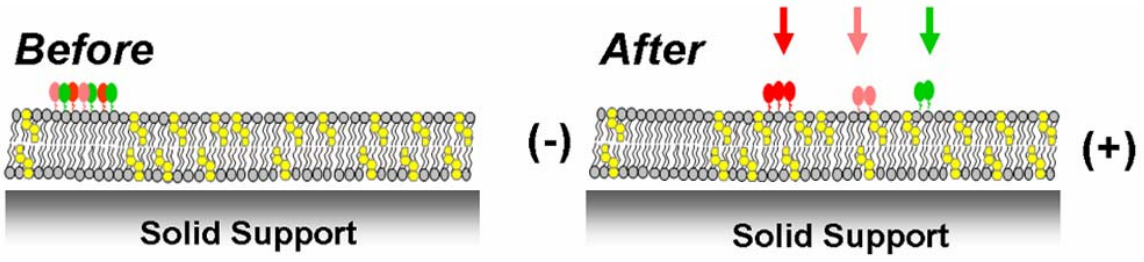

Figure 4.1 Schematic diagram of a solid supported lipid bilayer before and after applying an electric field. Before applying voltage across the supported lipid bilayer a section of analyte membrane is spliced next to the separation bilayer.

separation technique is powerful enough to separate isomers of fluorescently labeled lipids.

4.3 Experimental

Materials

The following lipids were used in these experiments: 1-palmitoyl-2-oleoyl-*sn*glycero- 3-phosphocholine (POPC), 1,2-dilauroyl-sn-glycero-3-phosphocholine (DLPC), and 1,2-dioleoyl-*sn*-glycero-3-phosphocholine (DOPC). These were obtained from Avanti Polar Lipids (Alabaster, AL). Fluorescently labeled lipids used in the separation experiments were: Texas Red 1,2-dihexadecanoyl-*sn*-glycero-3-phosphoethanolamine, triethylammonium salt (Texas Red DHPE) and *N*-(4,4-difluoro-5,7-dimethyl-4-bora-3a,4a-diaza-s-indacene-3-propionyl)-1,2-dihexadecanoyl-sn-glycero-3-phosphoethanolamine, triethylammonium salt (BODIPY DHPE), obtained from Molecular Probes (Eugene, OR). Phosphate buffer saline (PBS) used in the preparation of vesicles was made with 10 mM Na_2HPO_4, 5 mM $NaH_2PO_4^2$, and 150 mM NaCl (pH 7.4). Sodium chloride, sodium phosphate monobasic, and sodium phosphate dibasic were all obtained from Sigma-Aldrich (St. Louis, MO). The pH was adjusted to 7.4 using sodium hydroxide (EMD, Germany). The purified water used in the preparation of all solutions was obtained from a NANOpure Ultra Water System (Barnstead, Dubuque, IA) and had a minimum resistivity of 18 MΩ·cm. Polycarbonate filters (Whatman, Fisher Scientific) with pore diameters of 100 nm and 50 nm were used in the preparation of vesicles. Glass coverslips (VWR) were used as supports for the

bilayers and were boiled in 7X solution (MP Biomedicals, Aurora, OH) that was diluted four fold by volume with purified water. Polydimethylsiloxane (PDMS; Sylgard 184) was obtained from Dow Corning. Platinum electrodes were made from platinum wire with a diameter of 0.25 mm from Alfa Aesar (Ward Hill, MA). Thin layer chromatography (TLC) was carried out using glass-backed TLC plates made of silica gel with pore sizes of 60 Å and a layer thickness of 250 μm (VWR).

Preparation of the Supported Bilayers Used in the Separation Experiments

Small unilamellar vesicles (SUV) were used to form solid-supported lipid bilayers (SLBs) on glass substrates by vesicle fusion.[26,46,113,115,116] The vesicles used to create the separation bilayer were composed of POPC and cholesterol. Vesicles containing the fluorescently labeled lipids were composed of POPC mixed with a suitable mol% of Texas Red DHPE and/or BODIPY DHPE. To make the various vesicle solutions, the appropriate components were first dissolved in chloroform and dehydrated under vacuum for three hours. The dried mixtures were rehydrated in PBS and subjected to ten freeze/thaw cycles by alternating between liquid nitrogen and a 30 ^{o}C water bath. The solution was then extruded several times through a polycarbonate filter to produce vesicles of uniform size. For the first extrusion, a filter with 100 nm diameter pores was used, followed by five passes through a filter with 50 nm diameter pores. The resultant SUVs were sized by dynamic light scattering using a 90Plus Particle Size Analyzer (Brookhaven Instruments Corporation) and were found to be highly uniform at each composition and had an average diameter of 80-90 nm.

Glass coverslips used as supports for the bilayers were cleaned in 7X solution following established procedures.[66] They were then annealed in an oven at 550 ^{o}C for five hours to yield flat surfaces with a typical root mean square roughness (RMS) value of 0.13 nm over a 1 μm^2 area as determined by atomic force microscopy. A drop of vesicle solution (~200 μL) was placed on the clean hydrophilic glass coverslip. The solution was confined to a rectangular area in the center of the glass coverslip by a thin hydrophobic PDMS mold. The mold was made by cross-linking PDMS between two silanized glass microscope slides separated by a thin metal spacer between 200 to 400 μm thick. After cross-linking, a rectangular hole approximately 1 cm^2 was cut out of the center of the elastomeric sheet using a razor blade. The outer edges of the mold were trimmed to fit exactly over the glass coverslip.

The separation bilayer was prepared first. The vesicle solution containing cholesterol was incubated on the glass slide for ten minutes and rinsed with copious amounts of purified water to remove any excess, unfused vesicles from the surface. In the next step, a thin strip of the supported bilayer was completely removed so that vesicles containing the mixture of fluorophores could be fused in that region. We found that the edge of a coverslip wrapped with several ply of Teflon tape was an effective tool to plow out a thin line (80 μm wide) of bilayer material while not causing any damage to the underlying substrate. Immediately following this step, ~ 100-200 μL of vesicle solution containing the dye-labeled lipids were added to the PDMS well. After about five minutes, the well was thoroughly rinsed with DI water. Figure 4.2 shows a schematic representation of the procedure.

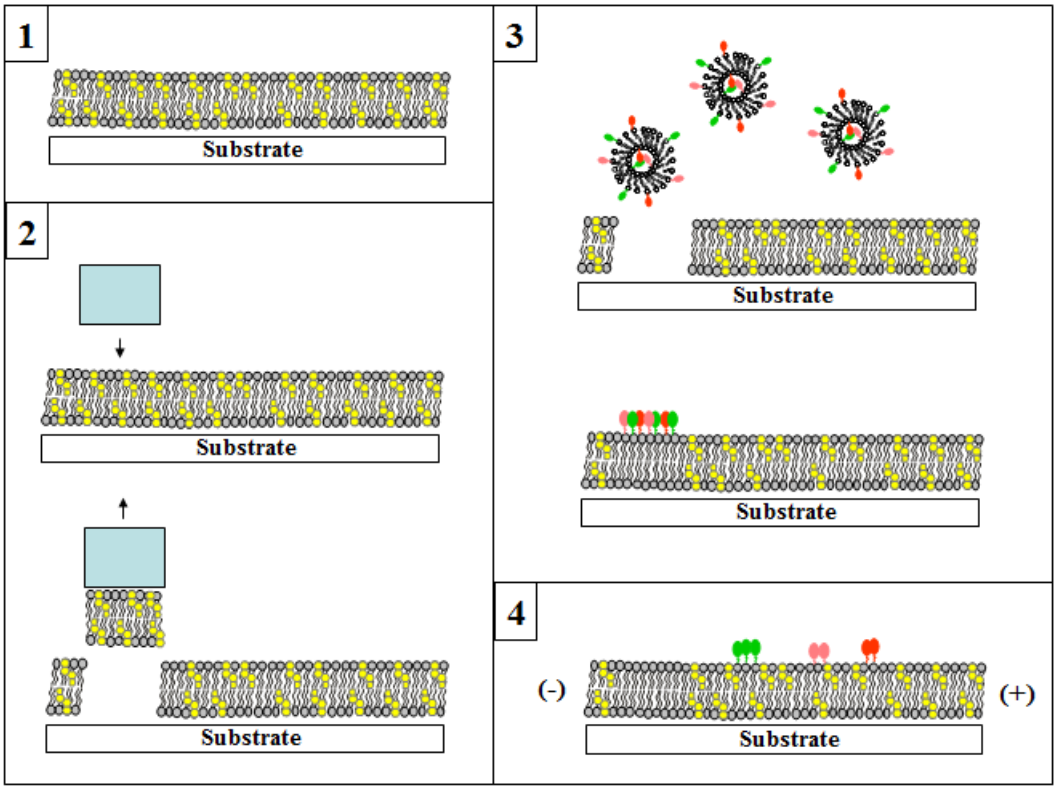

Figure 4.2 Procedure to form bilayer and separate a mixture of dye labeled lipids by electrophoresis. (1) First form a the separation bilayer containing 25 mol% cholesterol (yellow) in POPC lipids (gray) via vesicle fusion. (2) Gently press the edge of a glass coverslip slide coated with Teflon tape into the bilayer and plow out a thin line of the bilayer. (3) Add vesicles containing the mixture of fluorophores to be separated to the bulk aqueous phase above the supported bilayer. These vesicles will fuse in the bare region. (4) Apply a potential laterally across the bilayer and observe the resultant separation of fluorescent lipids, as indicated by the colored arrows corresponding to each kind of lipid.

A 100 V potential was applied laterally across the bilayer by placing a platinum wire electrode on each side of the PDMS well using a standard regulated power supply (Lambda Electronics Corp., Long Island, NY) while monitoring the current through the system with a digital multimeter (Keithly). DI water was used to minimize Joule heating. We maintained currents of only a few microamps or less during all experiments so Joule heating was negligible. Time lapse images were taken of the slide every five minutes to monitor the movement of the fluorescent bands and subsequent separations. A 4X microscope objective was used to maximize the field of view in our set up. Imaging was performed with a Nikon Eclipse TE2000-U equipped with a Sensys CCD camera (Photomatrics, Roper Scientific) working in conjunction with MetaMorph software (Universal Imaging). An illustration of the experimental set up is shown in Figure 4.3.

Preparation of Supported Bilayers with Various Amounts of Cholesterol

The effect of cholesterol on the fluidity of solid supported lipid bilayers was examined using fluorescent recovery after photobleaching (FRAP).[86,96] Bilayers of POPC, DOPC, and DLPC with varying mole percentages of cholesterol and 0.1 mol% Texas Red DHPE were studied. Briefly, the phospholipids, cholesterol, and Texas Red DHPE (all in chloroform) were mixed in proper proportions and dried first under a stream of nitrogen gas and then desiccated for three hours. PBS (pH 7.2) was added to each sample for rehydration. Each was then frozen with liquid nitrogen and thawed a total of five times with vortexing in between the freeze-thaw cycles. These vesicles were extruded through a polycarbonate filter (50 nm pore size) a total of seven times.

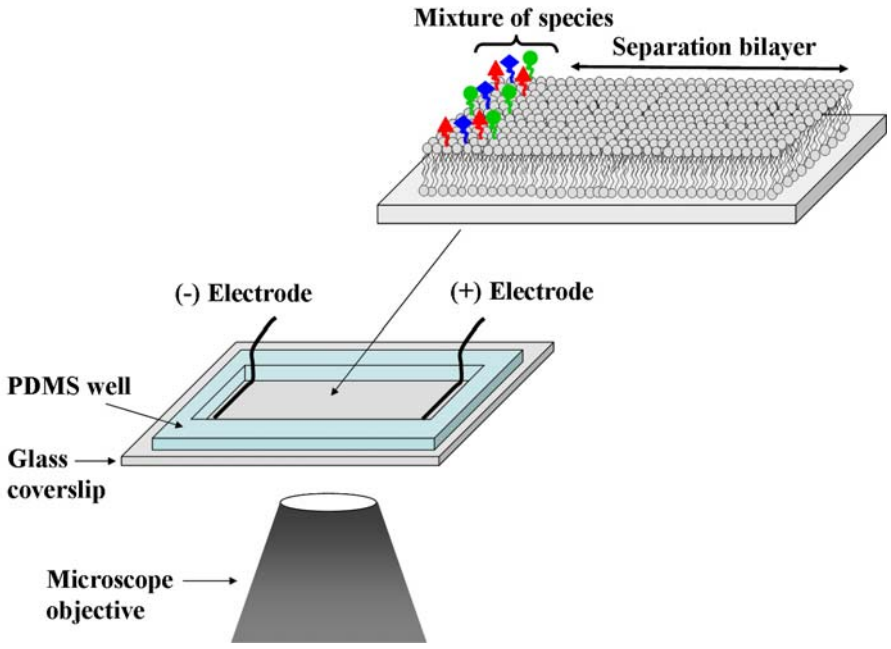

Figure 4.3 Diagram of the experimental set up used in the separation experiments. The bilayer was maintained in an aqueous environment at all times.

The effective diameters of these unilamellar vesicles were determined via light scattering and found to be within the diameter range of 80-110 nm.

Bilayers were then formed from these vesicles by vesicle fusion on previously cleaned and annealed glass, using a PDMS slab with a hole cut in the middle to contain the bilayer and bulk buffer above it. Bilayers formed in this manner appeared to be uniform down to the diffraction limit under all conditions investigated.

Diffusion Measurements

Diffusion coefficients and mobile fractions of Texas Red DHPE were measured by fluorescence recovery after photobleaching (FRAP).[86,96] The dye-labeled lipids were bleached with the 568.2 nm line from a mixed gas Ar^+/Kr^+ laser beam (Stabilite 2018, Spectra Physics). 100 mW of power was directed onto the sample for less than 1 second. The beam, which was sent through a 10X objective, had a full-width at half-maximum of ~17 μm at the sample plane. The recovery of the photobleached spot was followed with the same microscope system described above. The fluorescence intensity of the bleached spot was determined after background subtraction and normalization for each image. The diffusion coefficient of the dye-labeled lipids was determined as follows. First, the fluorescence recovery as a function of time was fit to a single exponential equation, from which we obtained the mobile fraction of the dye-labeled proteins and the half-time of recovery ($t_{1/2}$). The diffusion coefficient, D, was then calculated from the following equation: $D = \frac{w^2}{4t_{1/2}}\gamma$, where w is the full width at half-maximum of the Gaussian profile

of the focused beam and γ is a correction factor (= 1.1) that depends on the bleach time and geometry of the laser beam.

4.4 Results and Discussion

In a first set of experiments, we demonstrate the ability of cholesterol to decrease band broadening during the separation process. We compared the behavior of a band of 1 mol% Texas Red DHPE lipids migrating in a plain POPC bilayer and in a POPC bilayer with 25 mol% cholesterol. To begin an experiment, supported bilayers were formed on a planar glass substrate by the vesicle fusion method. Next, a thin line of bilayer (~80 μm width) was removed using a sharp piece of glass coated with Teflon (see supplemental materials). Vesicles containing POPC and 1 mol% Texas Red DHPE were then introduced into the aqueous phase above the surface. The vesicles fused to the bare portion of the substrate, creating a thin bilayer strip with Texas Red DHPE in it. A 100 V potential (DC) was applied parallel to the plane of the bilayer. Because the fluorophores were negatively charged, they migrated toward the positive electrode. We monitored the lateral movement and band broadening of the Texas Red bands as a function of time using an inverted epifluorescence microscope (Figure 4.4).

The bilayer without cholesterol showed substantial band broadening after 30 minutes of applied voltage (Figure 4.4, left images). By contrast, the band in the bilayer containing 25 mol% cholesterol (Figure 4.4, right images) remained much more compact.

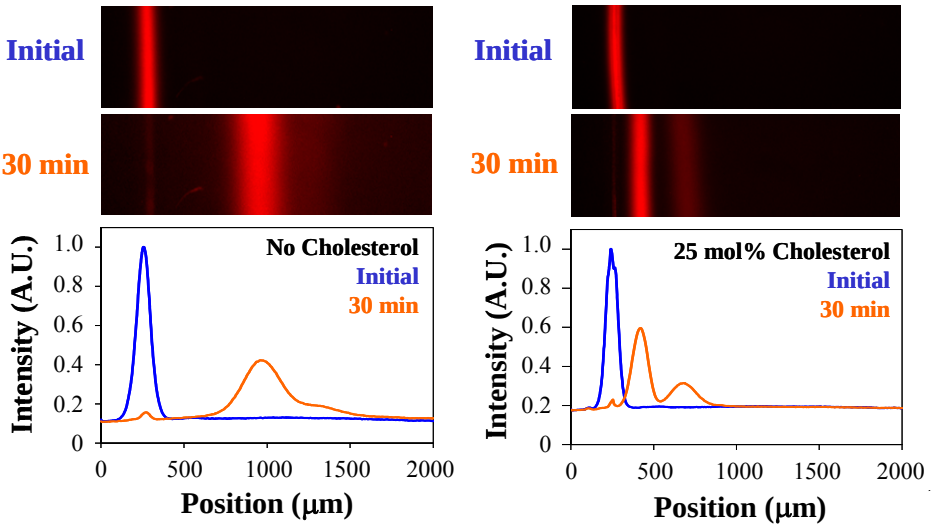

Figure 4.4 Comparison of the band broadening of Texas Red-labeled lipids migrating in either pure POPC (left) or POPC doped with 25 mol% cholesterol (right). The upper two images are epifluorescence micrographs of the systems immediately after formation of the Texas Red-containing strips. The lower two images show band migration after applying 100 V across the sample for 30 minutes. The positive and negative electrodes were located on the right and left sides of the frame, respectively. The faint line to the left in the bottom panels represents a 2% immobile fraction of lipids. The plots below the images show the corresponding linescans initially and after 30 minutes. The linescans have been corrected for vignetting and normalized to the fluorescence level of the initial image to account for photobleaching. The length of the images matches the scale of the x-axis in the plots.

Moreover, this band resolved into two distinct chromatographic features with an area ratio of ~ 70:30.

Mass spectral analysis showed that Texas Red DHPE had a molecular weight of 1381.85 Da and was relatively pure. It is well known, however, that the sample should consist of an isomeric mixture[135] (Figure 4.5, left side). Indeed, phosphatidylethanolamine lipids can conjugate to Texas Red sulfonyl chloride at either the ortho or para positions of the lower aromatic ring. This accounts for the presence of two bands in Figure 4.4 and is illustrated schematically in Figure 4.5 (right side).

Two other possible origins for the band splitting need to be considered. First, a difference in the mobilities of the lipids in the upper and lower leaflets might lead to band separation. Also, it is conceivable that that the separated bands represent species in different microdomains or lipid rafts.[136,137] We ruled out both these possibilities by purifying the Texas DHPE using thin layer chromatography. Several small spots of Texas Red DHPE in chloroform were formed on a TLC plate using a glass pipette. The spotted plate was then placed into a development jar and eluted with ethanol. Figure 4.6 shows the TLC plate after separation of the bands from six individually placed spots. Texas Red labeled phospholipids were recovered from the TLC plate by carefully scraping the separated bands with a razor blade and re-suspending in ethanol to extract the lipids from the silica beads. The mixture was centrifuged at 13,500 RPM (5415, Eppendorf) for 5 minutes and the supernatant was collected. This procedure was repeated (typically 5 times) until no Texas Red phospholipids were detected in the pellet by observing the color. To take away the ethanol, the samples were dried using nitrogen

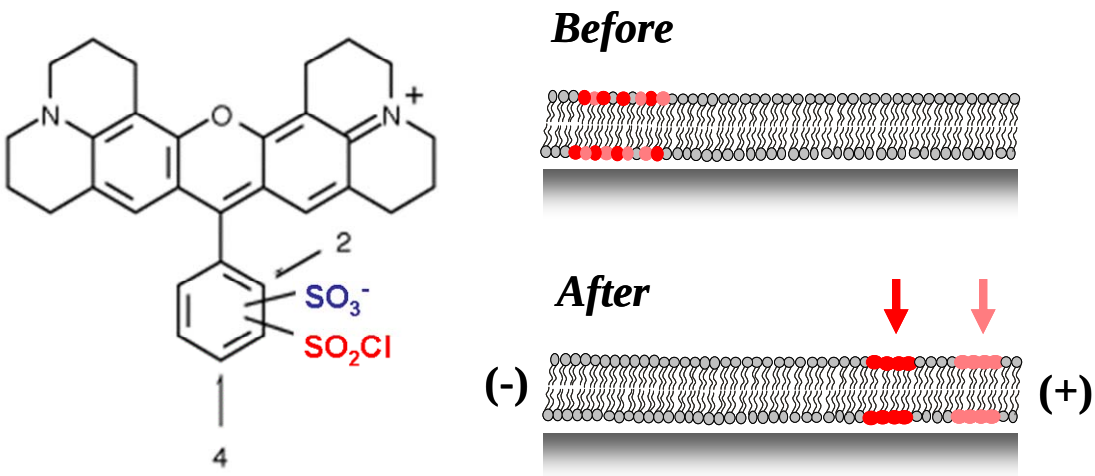

Figure 4.5 **(**Left) Chemical structure of Texas Red sulfonyl chloride.[88] The lower ring contains the reactive sulfonyl chloride group (red), which can reside at either the 2 (ortho) or 4 (para) position. (Right) Illustration of the separation of a mixture of Texas Red DHPE lipid isomers into distinct bands in a supported bilayer

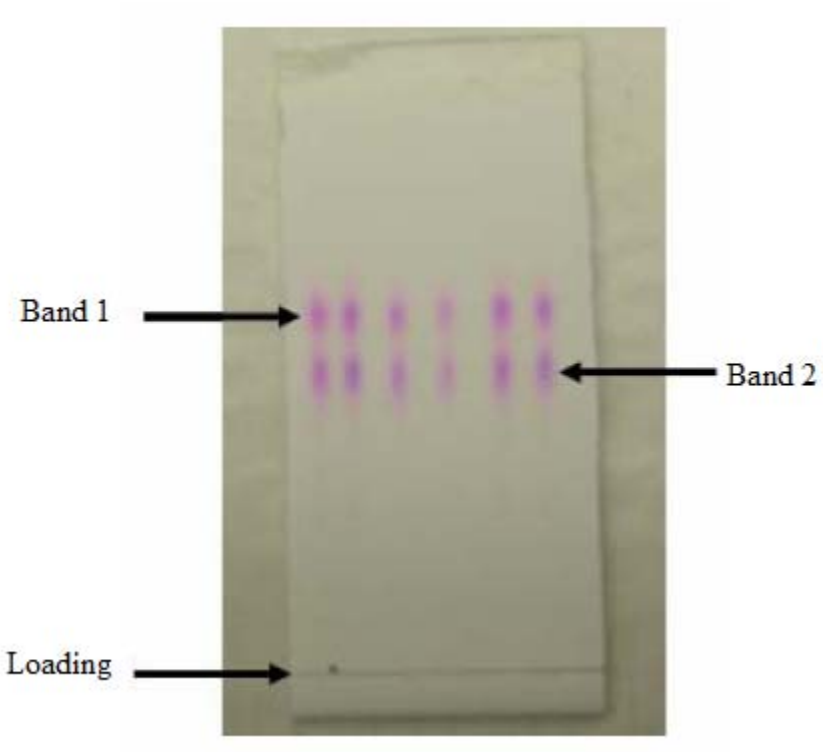

Figure 4.6 Image of a TLC plate after Texas Red DHPE separation. Six individual spots of Texas Red DHPE were placed at the bottom of the plate (horizontal loading line) and eluted with ethanol for approximately 20 minutes.

followed by desiccation under vacuum for 1 hour.

Each pure lipid isomer was separately mixed into POPC vesicles and fused into supported bilayer strips adjacent to a separation matrix consisting of a bilayer made from 75 mol% POPC and 25 mol% cholesterol. As expected, 30 min. of electrophoresis gave rise to only one band in each case (Figure 4.7). As a control, UV-Vis spectroscopy was performed on the isolated compounds as well. These experiments confirmed that the isomers existed in an approximately 70:30 mole ratio.

TLC purification was also carried out on BODIPY DHPE to verify that this compound was pure. We did not detect any band splitting using this method in agreement with the electrophoresis studies.

Matrix assisted laser desorption ionization (MALDI) mass spectroscopy was performed on the isolated fractions of Texas Red DHPE obtained from TLC. The spectrum for each band is shown in Figure 4.8. Comparing the spectra, both fractions have nearly identical masses, indicating that they arise from two different isomers of the same compound. The mass of Texas Red DHPE is 1381.85 g/mol. The compound is a salt and consists of the negatively charged dye-conjugated lipid, 1279.65 g/mol, as well as triethylammonium cations, 102.2 g/mol. The low mass peak in each spectrum corresponding to *m/z* 1302.7 represents the negatively charged dye-conjugated lipid with one sodium ion and one proton. The peak at *m/z* 1324.7 represents the dye-conjugated lipid with two sodium ions. The peak at *m/z* 1340.7 corresponds to the dye-conjugated lipid with one sodium ion and one potassium ion. The peak at *m/z* 1354.7 represents the

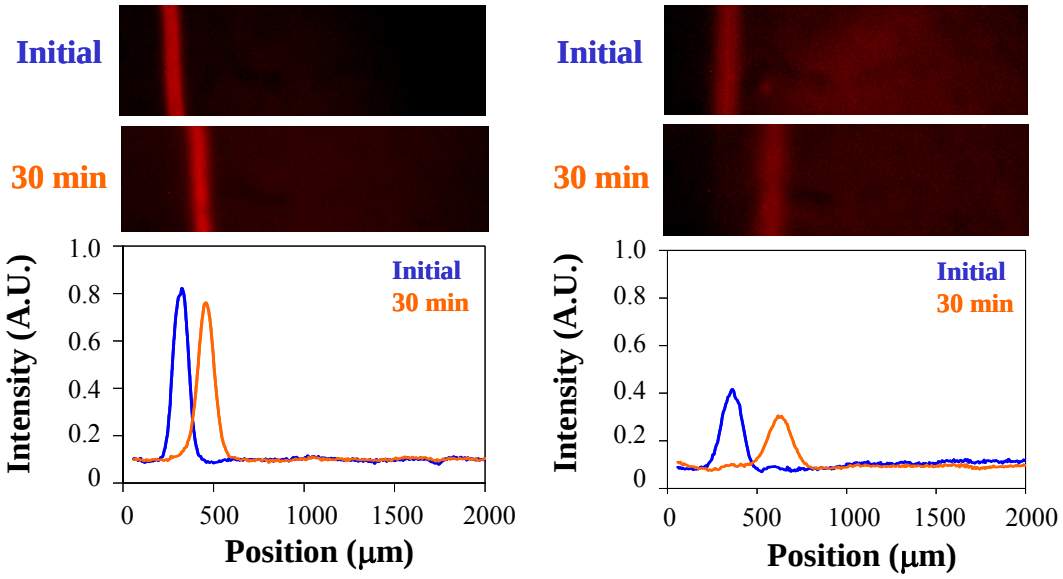

Figure 4.7 Images of Texas Red DHPE migrating through a 75 mol% POPC/ 25 mol% cholesterol bilayer after TLC purification. Left: Texas Red from the large mol. fraction isomer after TLC purification, initially (top) and after 30 min of 100 V applied potential (middle). Right: the corresponding images for the other isomer. The plots below the images show the associated linescans, initially and after 30 minutes, corrected for vignetting.

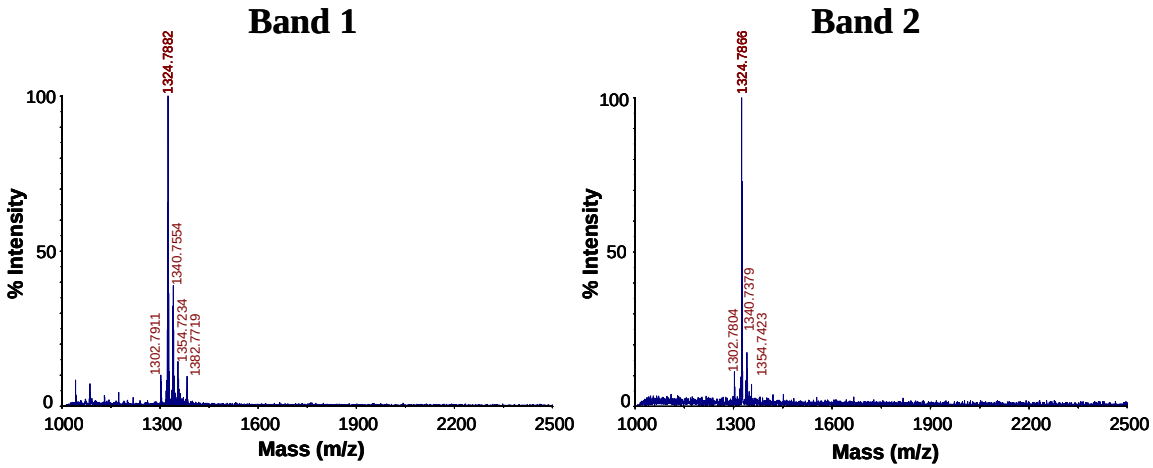

Figure 4.8 Mass spectra of each fraction of the TLC purified Texas Red DHPE isomers.

dye conjugated lipid with two potassium ions. The peak at *m/z* 1382.7 is attributed to the Texas Red salt with an additional proton.

In a final set of experiments, we demonstrated that a more complex mixture can be separated. For this purpose, we fused POPC vesicles containing 1 mol% Texas Red DHPE and 1 mol% BODIPY DHPE into a bilayer strip as performed above. Figure 4.9 (top) shows the three bands that were resolved after 30 min. of electrophoresis at 100 V. As can be seen, the Texas Red lipid bands move more slowly that the single green BODIPY band. The linescan (bottom) shows that the bands are resolved.

Finally, MALDI Mass Spectrometry (MS) Imaging[138] was used to analyze the separated species in the bilayer. Imaging MS provides native state analyte identification (owing to the molecular mass of individual molecules) and does not require the use of a fluorophore or a "tag" for analysis. Matrix assisted laser desorption/ionization time-of-flight mass spectrometry (MALDI-TOF MS) is used to obtain mass spectra at discrete x-y spatial positions. Each pixel or mass spectrum can be individually interrogated for a specific m/z value and assembled to produce an ion image. In that, multiple MS images can be obtained for each single experiment.

To prepare supported lipid bilayer samples for MS, the water must be removed from the system without disrupting the lateral organization of the membrane. Figure 4.10 outlines the procedure used to prepare the lipid bilayers for MS analysis. Firstly, the bulk water solution is removed from the PDMS well and the sample is plunge frozen in liquid nitrogen-cooled ethane. Then, samples are dried under vacuum (millitorr) at 4ºC for about 4 hr. Finally, the sample is adhered to a MALDI plate, and a matrix (20 mg/mL

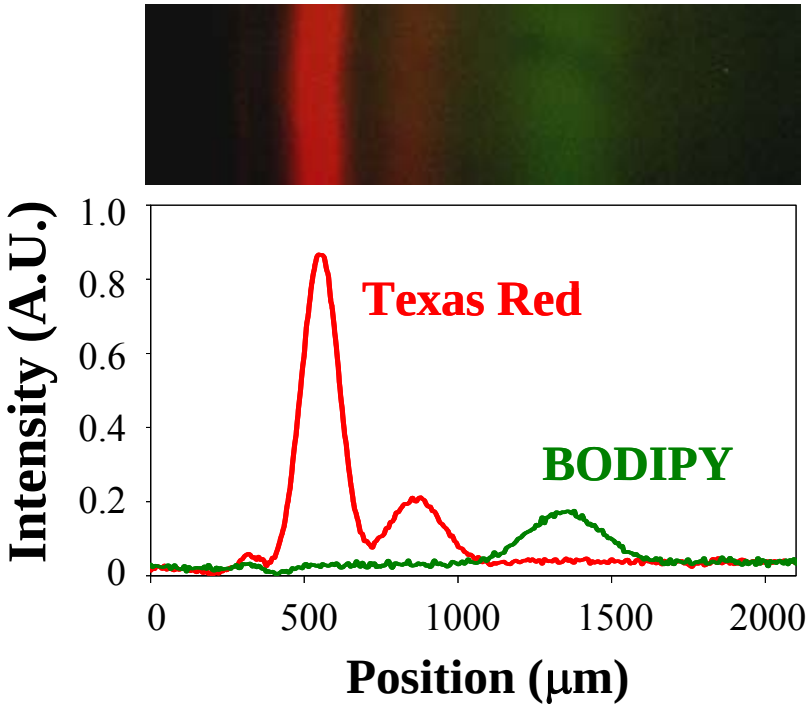

Figure 4.9 (Top) Composite image of the separation of TR DHPE and BODIPY DHPE in a POPC bilayer containing 25 mol% cholesterol after 35 minutes of applying a 100 V potential. (Bottom) corresponding linescan of the image, corrected for vignetting. The small peak at ~300 μm represents an approximately 2% immobile fraction of total dye-labeled molecules. The areas of the large and small peaks of Texas Red are ~ 75% to 25%, which is slightly different than the areas in Figure 1 and probably represents a small amount of batch-to-batch variability in the dye formulation of the manufacturer.

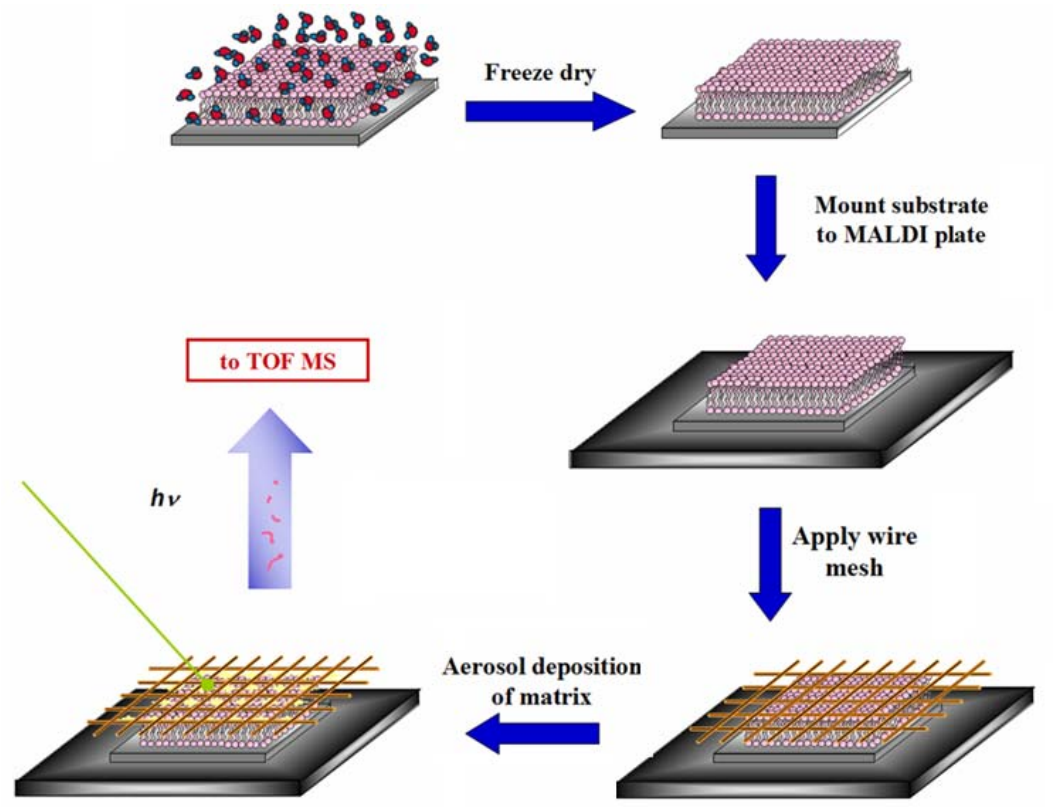

Figure 4.10 Schematic diagram of the sample preparation protocol used for MS analysis.

α-cyano 4-hydroxycinamic acid in 80 % acetone and 20% methanol) is aerosol deposited onto the sample. After being introduced into the mass spectrometer, the sample is interrogated in 60μm increments to produce the resulting images in Figure 4.11. In particular, the two separated TR-DHPE lipid (m/z 1324.6) bands are detected at different locations in the ion image, agreeing well with fluorescent images. Each mass spectrum represents the average of 500 laser shots and the laser spots size is ~ 60 μm x 60 μm. The ability to use a lipid bilayer as a separation medium followed by MS imaging might have an impact on the analysis of cell membranes. In that, it may be possible to monitor biological processes such as the formation and chemical composition of lipid rafts without the need for molecular tags.

All MS experiments were performed on a 4800 TOF TOF Mass Analyzer (Applied Biosystems, Framingham, MA) equipped with a Nd:YAG laser (355 nm). Imaging was acquired using 4000 Imaging Series software and data was worked up using Bio-Map (www.maldi-msi.org).

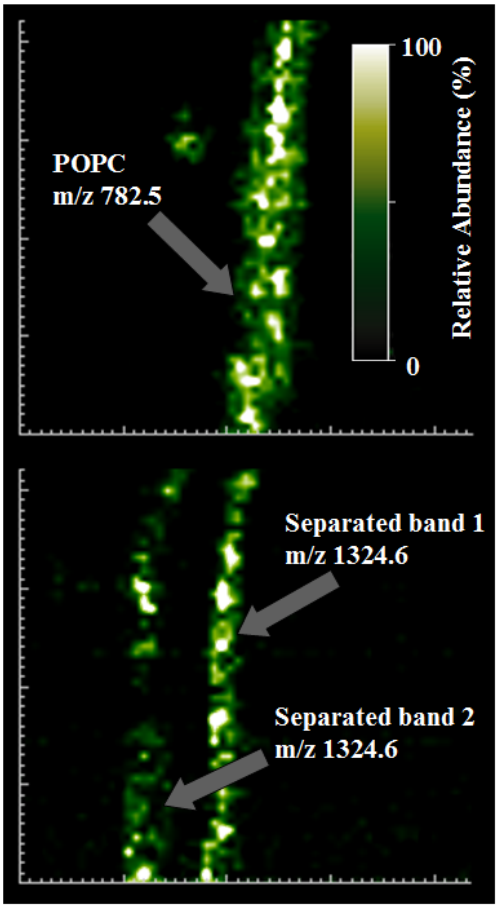

Figure 4.11 Mass spectrometry images of the separated species in a lipid bilayer. (Top) Ion image of m/z 782 which corresponds to the other lipid (POPC) in the original fused vesicles (should only move due to diffusion). (Bottom) The two TR-DHPE isomers (both at m/z 1324.6) are separated from each other and imaged using MS. Data taken by Ms. Stacy Sherrod in Dr. Russell Laboratory (Texas A&M University).

4.5 Summary and Conclusions

We have developed a simple on-chip device that can detect membrane proteins and lipids and even subtle differences in isoform within the native environment of a lipid bilayer. The method was powerful enough to completely resolve two isomers of Texas Red DHPE from each other. Moreover, these isomers could be separated from a BODIPY-conjugated lipid as well. This method could be extended to the purification and separation of membrane proteins by incorporating an appropriate polymer cushion[70] into our supported bilayer system to ensure mobility of the transmembrane species. Protein bands could be detected by Western blotting with appropriate protein-specific antibodies or the bilayers could be imaged via mass spectrometry for label-free detection.[139] Such an advance might even have impact in the analysis of whole cell membranes. In fact, cell membranes could be analyzed to follow protein expression or post-translational modifications.

CHAPTER V

SEPARATION OF PERIPHERAL PROTEINS BY SOLID-SUPPORTED BILAYER ELECTROPHORESIS

5.1 Synopsis

In Chapter IV, a method was developed for the purification of membrane-bound species within a supported lipid bilayer platform. Herein, the electric field generated by an applied potential has been used to separate streptavidin proteins bound to a supported phospholipid bilayer. By geometry, streptavidin proteins can bind either monovalently or bivalently via lipid-conjugated biotin moieties present within the membrane. The separation of doubly bound proteins from singly bound proteins was achieved with high resolution. We showed that we can control the fraction of protein which is singly and doubly bound by varying the concentration of ligand moieties within the supported membrane. This study demonstrates that first, bilayer electrophoresis can be used to separate membrane associated proteins, and second, and that the technique is sensitive to elucidating the valency state of the ligand-receptor pair.

5.2 Introduction

Elucidating the profile of membrane proteins on live cells is vital for developing new therapeutic agents and potential drugs candidates. Investigating these proteins has proven to be difficult, mostly due to their hydrophobic nature and low abundance. Conventional methods for membrane protein purification are cumbersome and time

consuming. Protein yields are extremely low and they can easily denature and lose their function during the purification procedure.

We have created a method to separate membrane bound species in a solid-supported lipid bilayer platform.[140] Membrane-bound species that can potentially be separated include conjugated lipids with various functionalities (such as fluorescent dyes), colloidal particles, and vesicles, ligands for specific binding reactions, and peripheral and transmembrane proteins. This technique is to some extent similar to gel electrophoresis, except here the separation matrix is now a solid-supported bilayer.

As a first step towards purifying transmembrane proteins, we investigated the separation of streptavidin in a supported bilayer system. We showed that we could electrophoretically move fluorescently labeled streptavidin proteins bound to a phospholopid bilayer via lipid-conjugated biotin moieties to form discrete bands. Streptavidin is a 52.8 kD tetrameric protein produced by *Streptomyces avidinii*.[141-143] There are two binding pockets on each side of a single streptavidin protein (Figure 5.1) and, hence, it can bind either monovalently or bivalently to a supported lipid bilayer doped with biotin-conjugated lipids.

Herein, we show separation of streptavidin proteins bound to a supported phospholipid bilayer. The separation of doubly bound proteins from singly bound proteins was achieved with high resolution. Also, we found that the fraction of protein which is singly and doubly bound can be varied by adjusting the concentration of ligand moieties in the membrane. This electrophoretic platform allows for the direct observation of the different valency states of ligand-receptors pairs at the membrane

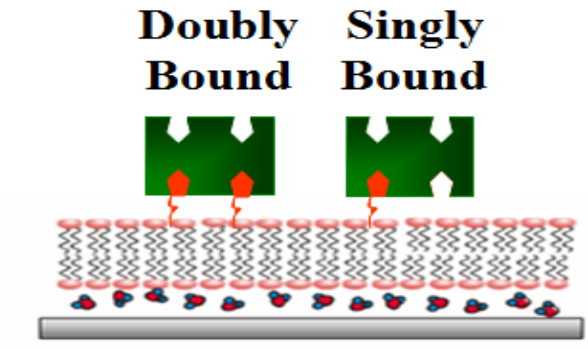

Figure 5.1 Schematic representation of streptavidin bound to a supported lipid bilayer. Streptavidin has two binding pockets on each side of the protein. It can bind either monovalently or bivalently to biotin-conjugated lipids within the lipid membrane.

interface. This technique could be extended to study other multivalent ligand-receptor interactions, such as the interaction between the pentameric cholera toxin B subunit and the membrane ligand, ganglioside GM_1.[144,145] Numerous biological processes, such as cell signaling[146] and cell-pathogen interactions[147,148] are linked with multivalent interactions. Understanding the nature of multivalency is crucial for the development of more accurate therapeutic agents that can interfere with pathological interactions.

5.3 Experimental

Materials

1-palmitoyl-2-oleoyl-*sn*-glycero- 3-phosphocholine (POPC) was the major component of all lipid bilayers. POCP was mixed with various amounts of 1,2-dipalmitoyl-*sn*-glycero-3-phosphoethanolamine-*N*-(Cap Biotinyl) (Sodium Salt) lipids, which served as the ligand for protein binding. All the lipids were obtained from Avanti Polar Lipids (Alabaster, AL). Streptavidin was conjugated with Texas Red dye prepared by and obtained from Molecular Probes (Eugene, OR). The reported degree of labeling was 2.1 dyes/streptavidin. The molecular weight of streptavidin is 53,000 Da (Molecular Probes, Product Information). Phosphate buffer saline (PBS) used in the preparation of vesicles was made with 10 mM Na_2HPO_4, 5 mM $NaH_2PO_4^2$, and 150 mM NaCl (pH 7.4). Sodium chloride, sodium phosphate monobasic, and sodium phosphate dibasic were all obtained from Sigma-Aldrich (St. Louis, MO). The pH was adjusted to 7.4 using sodium hydroxide (EMD, Germany). The purified water used in the preparation of all solutions was obtained from a NANOpure Ultra Water System (Barnstead, Dubuque, IA) and had

a minimum resistivity of 18 MΩ·cm. Polycarbonate filters (Whatman, Fisher Scientific) with pore diameters of 100 nm and 50 nm were used in the preparation of vesicles. Glass coverslips (VWR) were used as supports for the bilayers and were cleaned with 7X solution (MP Biomedicals, Aurora, OH). Polydimethylsiloxane (PDMS; Sylgard 184) was obtained from Dow Corning.

Solid Supported Lipid Bilayer Preparation

Small unilamellar vesicles (SUVs) were used to form solid-supported lipid bilayers on glass substrates by vesicle fusion.[26,46,92,115] Vesicles were composed of POPC with different mol% of biotinylated lipids. The appropriate composition of lipids were dissolved and mixed in chloroform, then dehydrated under vacuum for approximately 4 hours. The dried mixture was rehydrated in PBS buffer and subjected to ten freeze/thaw cycles by alternating between liquid nitrogen and a 30 °C water bath. The solution was then extruded several times through a polycarbonate filter to produce vesicles of uniform size. For the first extrusion, a filter with 100 nm diameter pores was used, followed by five passes through a filter with 50 nm diameter pores. The resultant SUVs were sized by dynamic light scattering using a 90Plus Particle Size Analyzer (Brookhaven Instruments Corporation) and were found to be highly uniform at each composition and had an average diameter of 80-90 nm.

Glass coverslips used as supports for the bilayers were cleaned in 7X solution following established procedures.[66] They were then annealed in an oven at 550 °C for five hours to yield flat surfaces with a typical root mean square (RMS) value of 0.13 nm

over a 1μm^2 are as determined by AFM. A 100 mL drop of vesicle solution was placed on the clean hydrophilic glass coverslip. The solution was confined to a circular area in the center of the glass coverslip by a thin hydrophobic PDMS mold. The mold was made by crosslinking PDMS between two silanized glass microscope slides separated by a thin metal spacer between 200 to 400 mm thick. After crosslinking, a circular hole approximately 1 cm in diameter was punctured through the elastomeric sheet using a hole punch. The outer edges of the mold were trimmed to fit exactly over the glass coverslip.

Protein Solution Preparation

Solutions of streptavidin were prepared in PBS buffer, pH 7.4, at a concentration of 0.5 μM. Prior to use, each solution was centrifuged at 13,500 RPM for 20 minutes (5415D, Eppendorf) to remove any large protein aggregates from the bulk solution.

Mobility Measurements

Diffusion coefficients and mobile fractions of streptavidin were measured by FRAP.[86] The dye-labeled proteins were bleached with the 568.2 nm line form a mixed gas $Ar^{+}/Kr^{=}$ laser beam (Stabilite 2018, Spectra Physics). 100 mW of power was directed onto the sample for approximately one second. The beam, which was sent through a 10X objective, had a full-width at half maximum of ~ 13 μm at the sample plane. The recovery of the photobleached spot was followed as a function of time using a time-lapse imaging under a fluorescence microscope (Nikon Eclipse TE2000-U) equipped with a

Sensys CCD camera (Photomatrics, Roper Scientific) and employing MetaMorph software (Universal Imaging). The fluorescence intensity of the bleached spot was determined after background subtraction and normalization for each image. The diffusion coefficient of the dye-labeled proteins was determined using standard procedures.[86] Briefly, the fluorescence recovery as a function of time was fit to a single exponential equation, from which we obtained the mobile fraction of the dye-labeled proteins and the half-time recovery ($t_{1/2}$). The diffusion coefficient, D, was then calculated from the following equation: $D = (w^2/ 4t_{1/2}) \gamma_D$, where w is the full width at half maximum of the Gaussian profile of the focused beam and γ_D is a correction factor that depends on the bleach time and geometry of the laser beam.

Bilayer Electrophoresis of Streptavidin

Figure 5.2 shows a schematic representation of the procedure. First, the separation bilayer was prepared first. The vesicle solution containing POPC and 25 mol% cholesterol was incubated on the glass slide for ten minutes and rinsed with copious amounts of deionized water to remove any excess, unfused vesicles from the surface. In the next step, a thin strip of the supported bilayer was completely removed with a coverslip wrapped with several ply of Teflon tape. A thin line (80 μm wide) of bilayer material was removed without causing any damage to the underlying substrate. Immediately following this step, ~ 100-200 μL of vesicle solution containing the biotinylated lipids were added to the PDMS well. After about five minutes, the well was thoroughly rinsed to remove unfused vesicles. Then, the bilayer was incubated with the

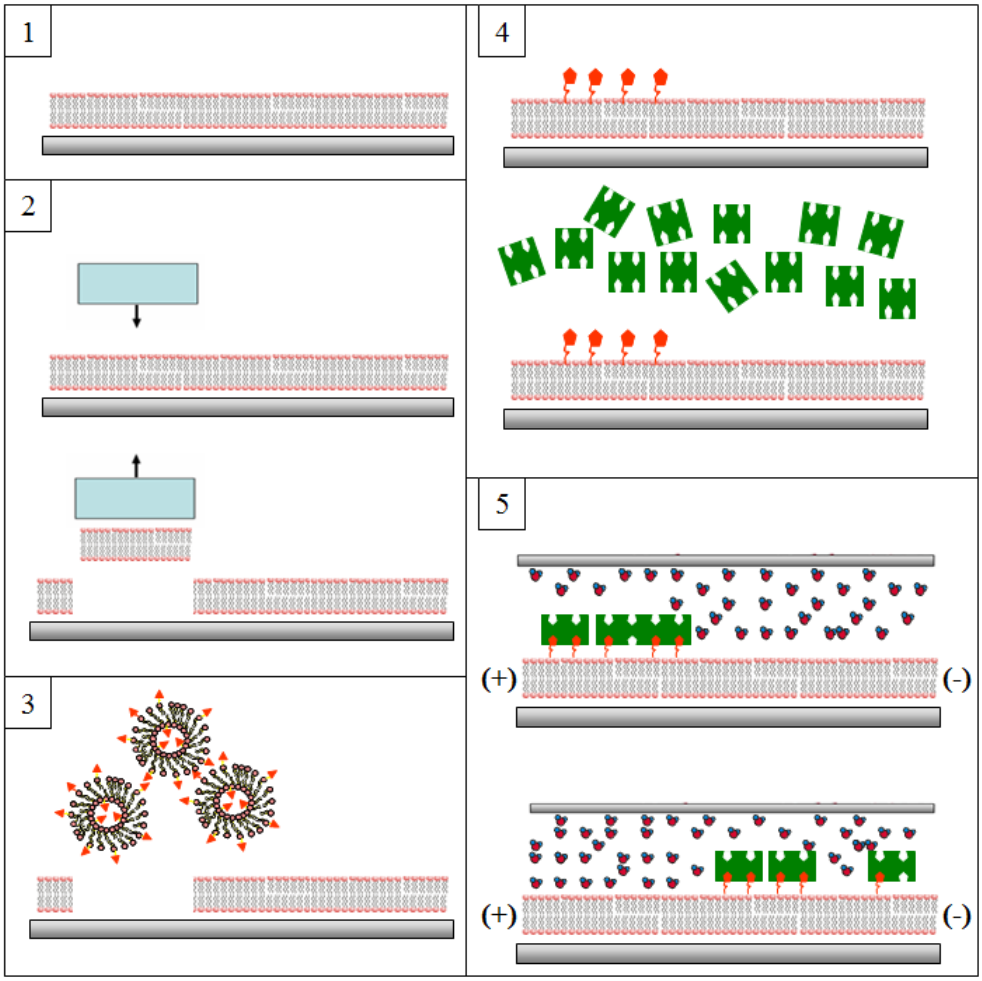

Figure 5.2 Procedure to form bilayer and separate streptavidin proteins by electrophoresis.

streptavidin solution for 30 minutes, followed again by vigorous rinsing with buffer to remove unbound protein. The sample was then assembled, under buffer, into a sandwich with another coverslip and mounted in the electrophoresis device. The electrophoretic device (Figure 5.3), made of Teflon, consisted of two platinum wire electrodes placed in solution-filled wells. The coverslip sandwich (inset; Figure 5.3B) was arranged to form a bridge between the two electrode wells. The electrical link was achieved all the way through the solution in the coverslip sandwich.

Finally, a 250 V potential was applied laterally across the bilayer by placing a platinum wire electrode on each side of the PDMS well using a standard regulated power supply (Lambda Electronics Corp., Long Island, NY) while monitoring the current through the system with a digital multimeter (Keithly). Time lapse images were taken every five minutes to monitor the movement of the protein bands and subsequent separations. A 4X microscope objective was used to maximize the field of view in our set up. Imaging was performed with a Nikon Eclipse TE2000-U equipped with a Sensys CCD camera (Photomatrics, Roper Scientific) working in conjunction with MetaMorph software (Universal Imaging).

As the potential is applied across the membrane, the negatively charged streptavidin proteins will move toward the cathode by electroosmosis (Figure 5.4). Electroosmosis is the bulk motion of liquid over a stationary, charged surface in response to an applied electric field.[149] In our separation platform, the motion arises from the flow of mobile counter ions (Na^+) that are present in excess near the negatively

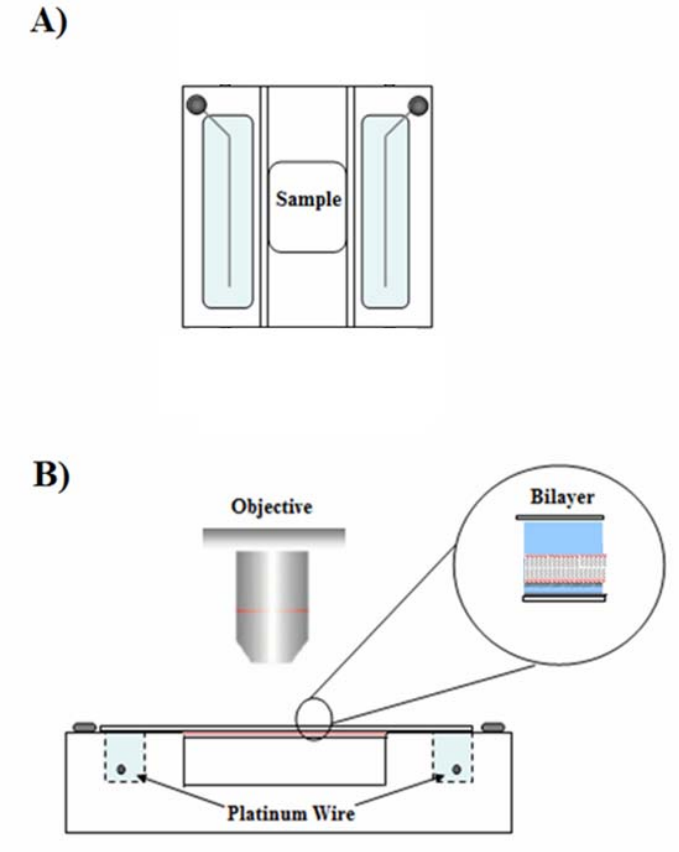

Figure 5.3 (A) Top view of the supported bilayer electrophoretic device. The body device is made of Teflon. (B) Side view of the device showing the platinum wire electrodes on each side. The inset depicts a cross-section of the coverslip sandwich, illustrating the supported membrane (not drawn at scale). The water on top of the bilayer is approximately 50 μm.

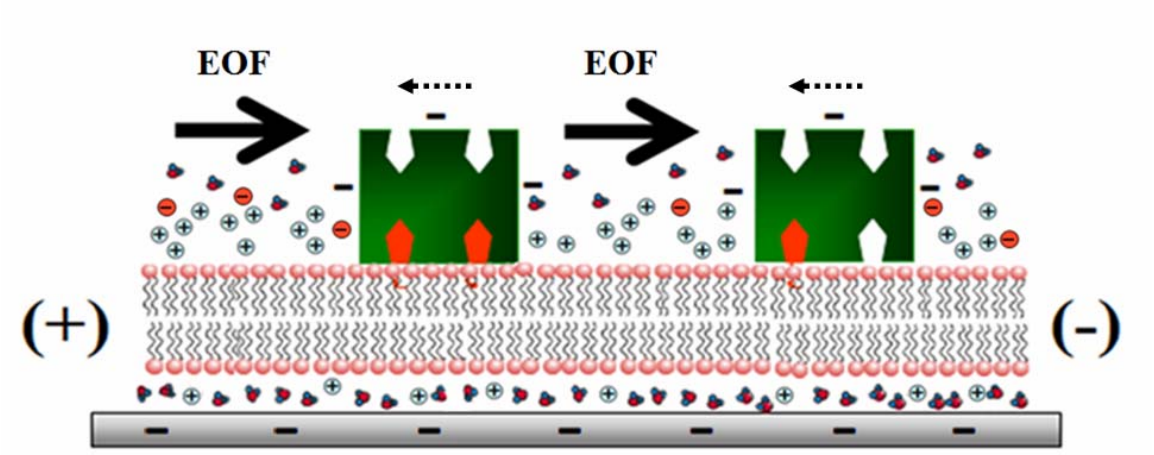

Figure 5.4 Schematic representation of the movement of peripheral proteins by supported lipid bilayer electrophoresis. Negatively charge proteins, such as streptavidin, will move toward the positive electrode after a potential is applied across the lipid bilayer, moving in the direction of the dash arrow above them. The black solid arrows indicate the direction of the Electro-osmotic Flow (EOF).

charged glass substrate. The major components of these membranes, POPC, is neutral and thus is expected to be unaffected by the field.

5.4. Results and Discussion

Diffusion Measurements

Solid supported phospholipid bilayers containing various amount of biotinylated lipids were formed on glass supports to characterize the effect of increasing ligand density on two-dimensional protein diffusion. Under each set of conditions, 0.5 μM streptavidin was added above the interface and incubated for 20 minutes before being washed out. This concentration is sufficiently high to saturate the binding sites at this time scale.[150] Moreover, the fluorescence measurements showed no evidence for protein desorption during the course of the FRAP measurements. This is to be expected because of the extremely low k_{off} rate for avidin and streptavidin for bioin ligands.[150] Figure 5.5 shows a representative FRAP curve for streptavidin bound to 2 mol% biotin in the bilayer. The data were fit to a single exponential curve, from which the half-time of recovery ($t_{1/2}$) could be determined and used to calculate the diffusion coefficients (see *Experimental*). The diffusion coefficient and mobile fraction for streptavidin were (0.95 x 10^{-8}) cm^2/sec and 0.90, respectively.

Electrophoresis

As mentioned above, there are two binding pockets on each side of a single streptavidin protein (Figure 5.1) and, hence, it can bind either monovalently or bivalently

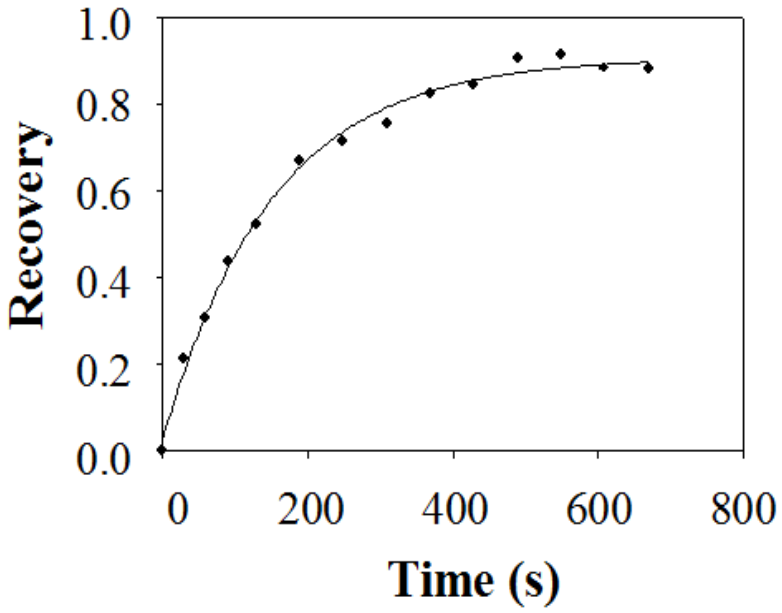

Figure 5.5. Fluorescence recovery as a function of time for streptavidin in POPC bilayers containing 2 mol % biotin. The diffusion coefficient, D, is (0.95 x 10^{-8}) cm^2/sec with a mobile fraction of 0.90.

to a supported lipid bilayer doped with biotin-conjugated lipids within the membrane. The biotin/streptavidin binding pair represents one of the strongest ligand-receptor interactions know in biological systems (K_D = 10^{-15} M).[150,151] In fact, the apparent K_D value at substrate surfaces is in the low picomolar range, while values in the femtomolar range have been found in bulk solution. Moreover, K_{off}, for this system is far longer than the 30 to 60 minutes timeframe over which an electrophoretic separation is typically performed. Therefore, one should expect to find two bands when separating the bound form of this protein from an analyte region containing both forms of the molecule into a separation matrix (Figure 5.6A).

In the first set of experiments, supported bilayers composed of POPC and 25 mol % cholesterol were used as a separation matrix. A thin line of bilayer was removed as described in the experimental section. Vesicles containing POPC and 3 mol% biotinylated lipids were then introduced and fused to the exposed section of the substrate, creating a thin bilayer strip with biotinylated lipids in it. Then, the bilayer was incubated with the streptavidin solution (0.25 μM) for 30 minutes. After rinsing with buffer to remove unbound protein, a 250 V potential was applied parallel to the plane of the bilayer. The lateral movement as a function of time was followed using an inverted epifluorescence microscope. Figure 5.6B shows a fluorescence image of the two bands that were resolved after 20 minutes of electrophoresis at 250 V. The linescan associated with the fluorescence image shows that the bands are completely resolved. We determined that the observed velocity scales linearly with the applied potential (Figure 5.7).

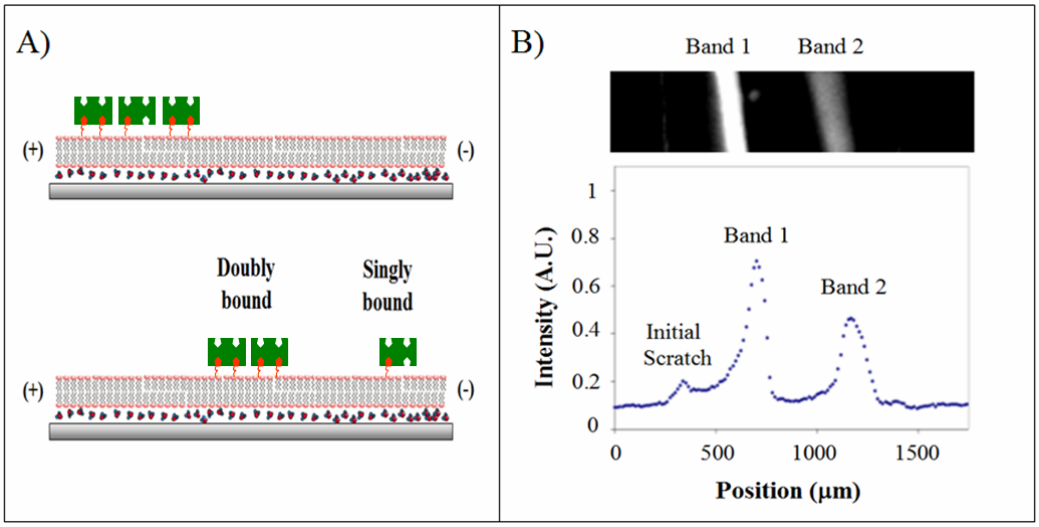

Figure 5.6 (A) Schematic representation of the separation of streptavidin singly bound from doubly bound to POPC bilayers containing 3 mol % biotinylated conjugated lipids. (B) (Top) Epifluorescence image of separated dye-labeled streptavidin after 20 minutes of applied potential across the bilayer. This image was taken with a 4X air objective using a mercury arc lamp with exposure time of 200 ms. (Bottom) A line scan across the epifluorescence image shows that the bound protein has separated into two distinct bands; Band 1 (doubly bound) and Band 2 (singly bound).

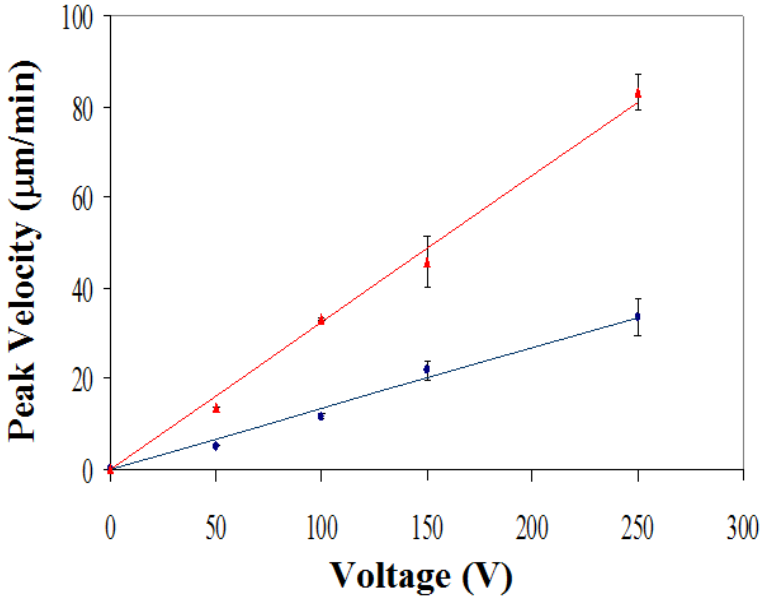

Figure 5.7 A plot of peak velocity vs. applied voltage for streptavidin bands moving through 75 mol% POPC and 25 mol% cholesterol. The straight lines are least square fits to the data.

One of the drawbacks of working at high voltage is the generation of heat. Joule heating will increase in our system as V^2/R.[152] Joule heating can affect separation by increasing thermal dispersion or possibly damage proteins that are temperature sensitive.[152] The temperature generated in our electrophoretic system (Figure 5.3) was monitored in control experiments by utilizing poly(*N*-isopropylacrylamide) (PNIPAM). PNIPAM is a thermoresponsive polymer which aggregates and falls out of solution, making the solution cloudy, above its lower critical solution temperature (LCST).[153-155] 10 mg/mL PNIPAM (M.W. 1.78 x 10^4 g/mol) solutions were prepared in 10 mM PBS buffer in the presence of 500 mM NaCl. For this set of conditions, PNIPAM shows a LCTS of approximately 25 °C. The PNIPAM solution was placed between two pieces of glass and the sample was mounted in the electrophoretic device. An electric field was applied across the samples for over than two hours at 250 V. No visible changes were detected. The solution stays clear during this period of time. For higher voltages a cooling system can be designed and added directly beneath the sample on which the electrophoresis experiment takes place.

Diffusion Measurements of the Separated Species

Previous studies[156,157] have shown that membrane-bound proteins, which are attached to the bilayer only by association with the lipid head group, have diffusion coefficients similar to a phospholipid molecule in the dilute limit. As mentioned above, streptavidin molecules could be associated either to one or two biotin moieties within in a supported lipid bilayer. Previous studies[156,158] have shown that the diffusion constant of

proteins attached to two biotin moieties is reduced by a factor of two compared to an individual lipid's value. The factor of two reduction arises because two lipids now need to be dragged together through the bilayer, while the viscous drag of the associated protein in the adjacent aqueous solution is practically negligible.[156] By Einstein's relation the diffusion coefficient of a lipid is: $D_{lipid} \sim kT/f_{lipid}$ where k is the Boltzmann constant, T is the absolute temperature and f_{lipid} is the friction coefficient of the lipid bilayer. When to lipids are linked together, becoming a dimer, the total friction coefficient becomes the sum of the of the friction factors of each lipid, $f_{dimer} = 2\ f_{lipid}$. The diffusion coefficient of proteins linked to two lipid molecules is then given by: $D_{dimer} \sim kT/f_{dimer} = D_{lipid}/2$.

FRAP experiments were performed on each one of the bands to determine the diffusion coefficients for the two species. Figure 5.9 shows fluorescence recovery curve for the two separated bands. As expected the diffusion coefficient of fluorescently labeled proteins within Band 2 was roughly a factor of 2 higher than labeled proteins present in Band 1 (Figure 5.8).

Effect of Biotin Concentration on Protein Separation

In a second set of experiments, we attempt to study the effect of decreasing the concentration of biotinylated lipids on the electrophoresis of bound streptavidin. For these experiments, the procedure is the same as outline above, except in this case, vesicles containing POPC and 2.5 mol% biotinylated lipids were used. Then, the bilayer

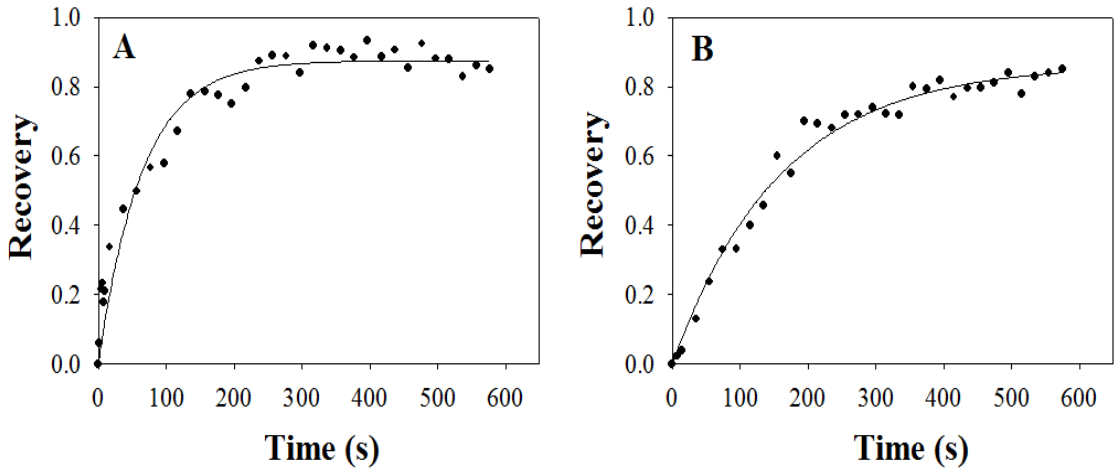

Figure 5.8 Fluorescence recovery as a function of time for streptavidin singly-bound (A) and streptavidin doubly-bound (B) in POPC bilayers containing 3 mol % biotinylated conjugated lipids. The diffusion coefficient, D, of streptavidin singly bound to the bilayer is 1.12 x 10^{-8} cm^2/sec with a mobile fraction of 0.87; for streptavidin doubly bound, D = 0.53 x 10^{-8} cm^2/sec with a mobile fraction of 0.81.

was incubated with the streptavidin (0.25 μM) solution for 30 minutes. After rinsing the sample with 5 mM PBS buffer to remove unbound protein the sample was mounted in the electrophoretic device, as described in the experimental section. The lateral diffusion of the proteins as a function of time was followed using an inverted epifluorescence microscope. Figure 5.9 shows an epifluorescence image of the separated dye-labeled streptavidin after 20 minutes of applied potential across the bilayer. As we can observe, similar level of fluorescence intensity were obtained for both band. FRAP experiments were performed on each one of the bands to determine the diffusion coefficients for the two species. Once again, the diffusion coefficient of fluorescently labeled proteins within Band 2 was a factor of 2 higher than the labeled proteins present Band 1. The diffusion coefficient, D, of streptavidin within Band 2 is 1.17×10^{-8} cm^2/sec with a mobile fraction of 0.85; for streptavidin present in Band 1, $D = 0.65 \times 10^{-8}$ cm^2/sec with a mobile fraction of 0.83.

In the next experiments, the mol % of biotin within the supported membrane was decreased to 0.5 mol %. By decreasing the mol percent of biotinylated lipids within the supported membrane while maintaining the same concentration of streptavidin we expected to have only the proteins attached to the membrane via one biotin moiety. We

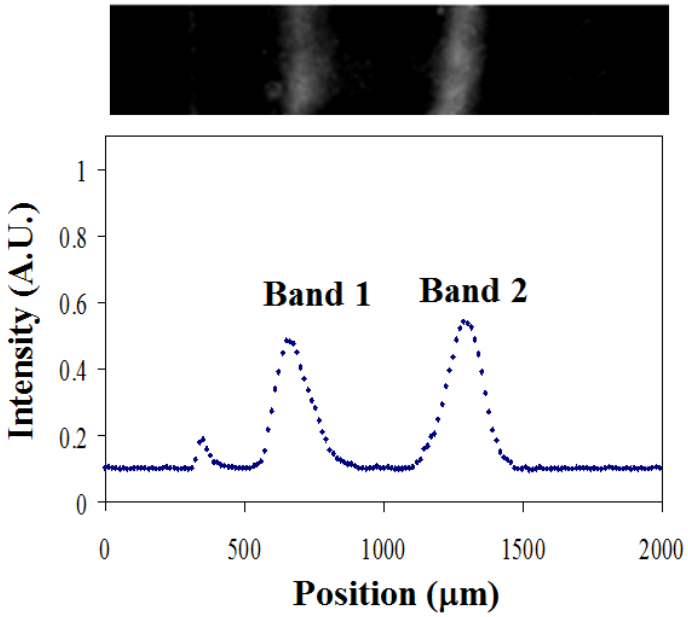

Figure 5.9 Epifluorescence image of the separation of streptavidin singly bound from doubly bound to POPC bilayers containing 2.5 mol % biotinylated conjugated lipids after 20 minutes of applied potential. This image was taken with a 4X air objective with exposure time of 200 ms. (Bottom) A line scan across the epifluorescence image shows that the protein bands are separated and detectable by fluorescence.

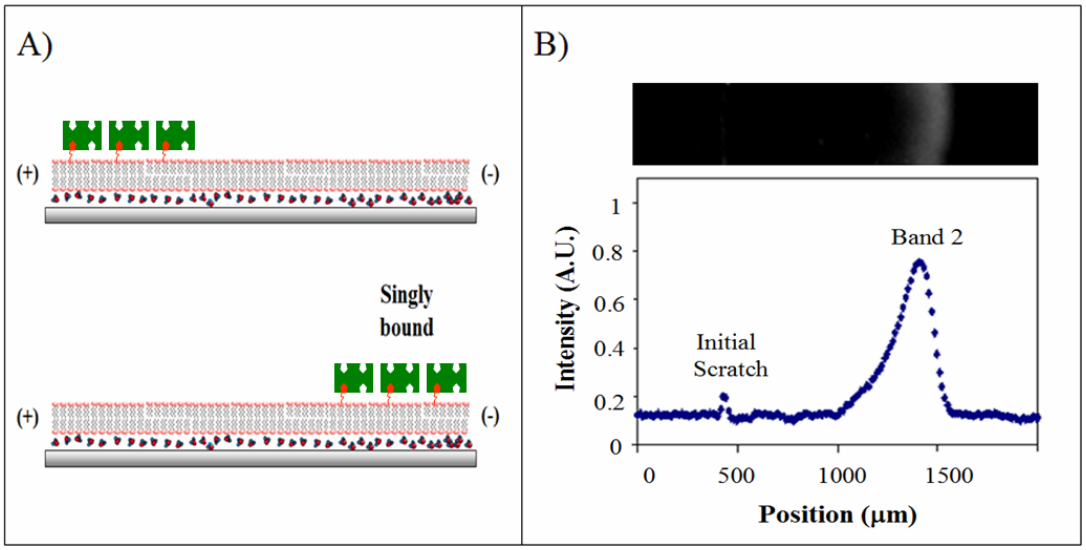

Figure 5.10 (A) Schematic representation of the electrophoresis of streptavidin singly bound to POPC bilayers containing 0.5 mol % biotinylated conjugated lipids. (B) (Top) Epifluorescence image of dye-labeled streptavidin after 20 minutes of applied potential across the bilayer. This image was taken with a 4X air objective using a mercury arc lamp with exposure time of 200 ms. (Bottom) Line scan across the fluorescence micrograph after 20 minutes of applied potential.

found the presence of only one band after a 250 V potential was applied parallel to the plane of the lipid membrane for 20 minutes, as described in Figure 5.10. The linescan associated with the fluorescence image shows that only one band is present and that its migration distance is similar to Band 2 (Figure 5.10B). FRAP experiments shows a diffusion coefficient for streptavidin of 1.12×10^{-8} cm^2/sec with a mobile fraction of 0.84.

In the last set of experiments, the mole percent of biotinylated lipid within the membrane was fixed 3 mol %, but the concentration of the streptavidin solution was decreased from 0.25 μM to 0.05 μM. Under this set of conditions, we expected to have a high population of proteins doubly bound to the membrane. We found the presence of only one band after a 250 V potential was applied parallel to the plane of the lipid membrane for 20 minutes, as described in Figure 5.11. The linescan associated with the fluorescence image shows that only band is present and that its migration distance is similar of Band 1 (Figure 5.11B). FRAP experiments shows a diffusion coefficient for streptavidin of 0.57×10^{-8} cm^2/sec with a mobile fraction of 0.82.

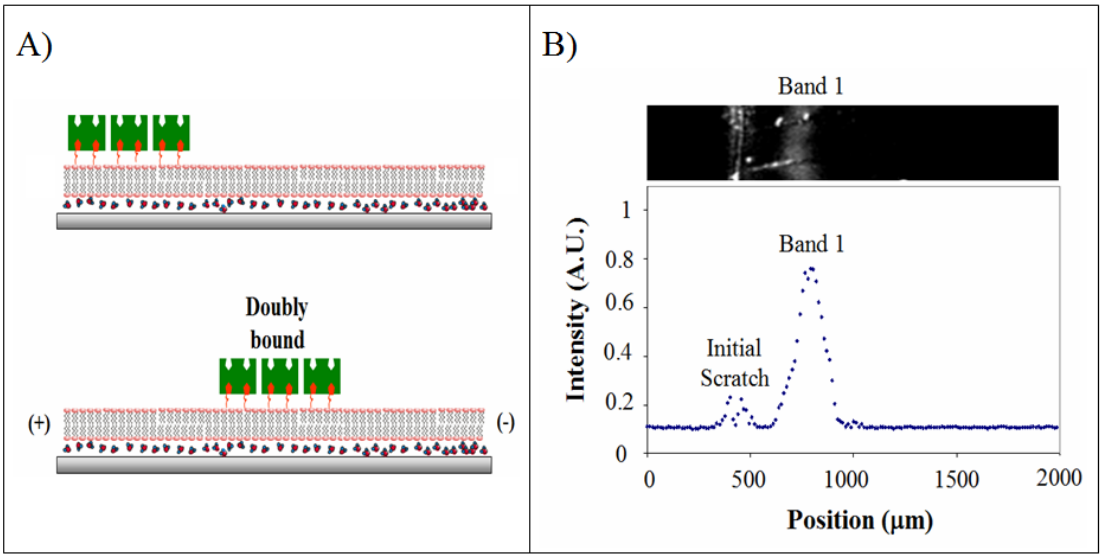

Figure 5.11 (A) Schematic representation of the electrophoresis of streptavidin doubly bound to POPC bilayers containing 3 mol % biotinylated conjugated lipids. (B) (Top) Epifluorescence image of dye-labeled streptavidin after 20 minutes of applied potential across the bilayer. This image was taken with a 4X air objective using a mercury arc lamp with exposure time of 200 ms. (Bottom) Line scan across the fluorescence micrograph after 20 minutes of applied potential.

5.5 Summary and Conclusions

In this chapter, an electrophoretic platform was developed for the separation of peripheral proteins. We showed separation of streptavidin proteins bound to a supported phospholipid bilayer. The separation of doubly bound proteins from singly bound proteins was achieved with high resolution. As clearly illustrated, the fraction of protein which is singly and doubly bound can be controlled by adjusting the percent of ligand moieties in the membrane. This bilayer electrophoresis platform offers several advantages; it can be used to separate membrane associated proteins and is sensitive enough to get a better understanding of the valency state of the ligand-receptor pair. Furthermore, this novel electrophoresis technique can be used to study the 2D crystallization of proteins and it can be coupled to non-label techniques, such as Mass Spectrometry, for proteomics applications.

CHAPTER VI

BIOPRESERVATION OF SUPPORTED PHOSPHOLIPID BILAYERS

6.1 Synopsis

The work presented in this chapter focuses on the study of supported lipid bilayer stability during exposure to air. The two-dimensional fluidity allows for individual components to rearrange as they would in real cell membranes and is key for mimicking biochemical reactions that occur on the cell surface, such as protein-protein interactions and pathogen attack. One drawback of this biological platforms its inability to remain stable upon exposure to air and withstand the harsh mechanical and chemical stress associated with real-world sensor applications. Recently, our group found that the addition of trehalose to planar supported membranes, preserve bilayer integrity and functionality upon exposure to dry conditions.[159] Herein, we demonstrate the practical application of such technology towards the development of robust sensor platforms. Supported lipid bilayer (SLB) samples dried in the presence of trehalose were packed and shipped to two different destinations in order to determine how the SLB system will react to conditions outside of the laboratory. FRAP measurements showed that the lipid bilayers were still mobile with high mobile fraction. This methodology demonstrates the above mentioned application and moreover can be coupled to the electrophoresis technique. Species of interest can be separated in the membrane and then dried in the presence of trehalose for further analytical studies.

6.2 Introduction

Supported phospholipid bilayers have proven to be useful mimics of the cell membrane. They preserve the lateral fluidity of the lipid molecules which is a fundamental property of native membranes. Lateral fluidity makes these platforms ideal for creating biosensors because they can readily mimic the same two-dimensional rearrangements that take place on cell surfaces during ligand-receptor recognition events. The forces that hold the bilayer at the solid/aqueous interface of a glass substrate involve electrostatic, van der Waals, hydrophobic, and steric interactions. A major problem is that the lipid bilayer is not stable in dry conditions. The thin layer delaminates from the interface if the film is exposed to the air/water interface.[41,56,113,160-162]

Efforts to preserve the stability of supported bilayers upon exposure to air include but are not limited to the use of closed-packed protein layer linked to the lipid bilayer,[161] the incorporation of lipopolymers within the supported lipid membrane,[113] and the addition of Trehalose.[159] Recently, Albertorio and coworkers compared the efficacy of six disaccharide and glucose molecules for the preservation of supported lipid bilayer upon exposure to air.[159] The results showed that α,α-trehalose was the most effective in preserving the integrity of SLBs upon exposure to air (Figure 6.1).

Herein, we tested if samples treated with α,α-trehalose are able to survive traveling conditions. Samples were prepared in the Department of Chemistry-Texas A&M University and then shipped to Washington, DC and the Unites Kingdom. FRAP

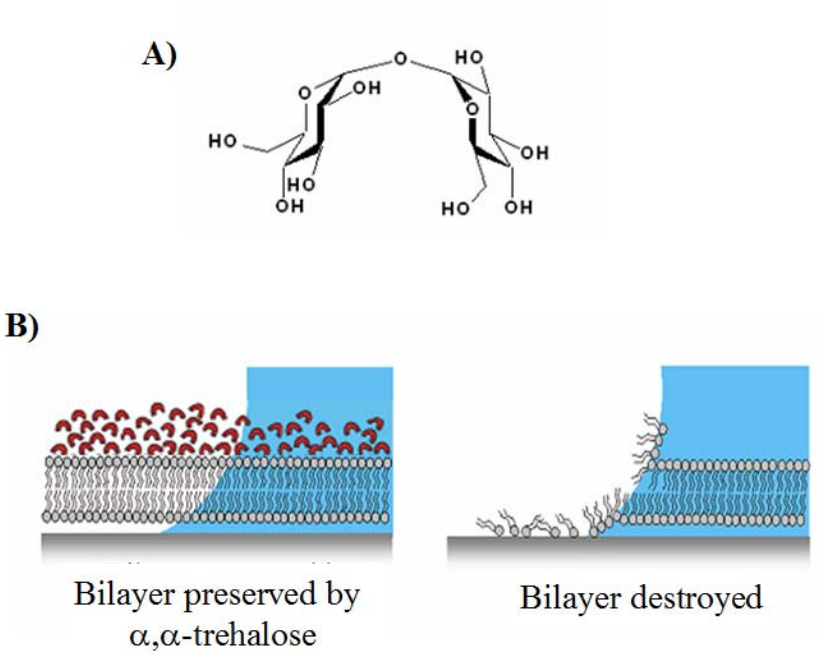

Figure 6.1 A) Chemical structure of α,α-trehalose. B) Dehydration of supported phospholipid bilayers in the presence (right) and in the absence (left) of α,α-trehalose.

measurements show identical diffusion constants and mobile fractions of dye-conjugated lipid as before drying and shipping.

6.3 Experimental

Materials

1-Palmitoyl-2-Oleoyl-*sn*-Glycero-3-Phosphocholine (POPC) was purchased from Avanti Polar Lipids (Alabaster, AL). *N*-(Texas Red sulfonyl)-1,2-dihexadecanoyl-sn-glycero-3- phosphoethanolamine (Texas Red DHPE) were obtained from Molecular Probes (Eugene, OR). α,α-Trehalose (99.5% was purchased from Fluka BioChemika (Buchs, CH). Purified water acquired from a NANOpure Ultrapure Water System (Barnstead, Dubuque, IA), had a minimum resistivity of 18.2 MΩ·cm, and was used in the preparation of all buffer solutions. Phosphate buffer saline (PBS) was prepared using 10.0 mM sodium phosphate with the addition of 150 mM NaCl (Sigma-Aldrich).The pH was adjusted to 7.4 by the addition of NaOH (EM Science). Solutions of α,α-Trehalose were prepared in deionized water at 20% w/w. Poly(dimethylsiloxane) (PDMS) was used to fabricate PDMS wells devices.[66] The polymer and crosslinker were purchased from Dow Corning (Sylgard Silicone Elastomer-184, Krayden Inc.). Glass microscope (VWR International) were cleaned and annealed according to established procedures.[66]

Preparation of Small Unilamellar Vesicles and Bilayer Formation

Small unilamellar vesicles (SUVs)[163] were prepared with POPC and 0.1 mol % Texas Red DHPE as a fluorescent probe. Solutions with proper amount of each lipid

constituent were mixed in chloroform. A stream of dry nitrogen was used to evaporate the chloroform and the dried lipids were desiccated under vacuum for at least 4 hours. After evaporation of the solvent, the lipids were reconstituted in PBS buffer to a final concentration of 2.5 mg/ml and subjected to 10 freeze-thaw cycles. The solution was then extruded five times through a polycarbonate filter (VWR International) with a pore size of 50 nm to produce vesicles of uniform size. Small unilamellar vesicles prepared by this method were approximately 90 nm in diameter as determined by dynamic light scattering using a 90Plus Particle Size Analyzer from Brookhaven Instrument Corp.

Fluorescence Recovery after Photobleaching (FRAP)

FRAP[86] measurements were performed using 2.5 W mixed gas argon/krypton ion laser (Stabilite 2018, Spectra Physics). Samples were irradiated at 568.2 nm for periods of ~1 second at 100 mW.A 13 μm full width at half-maximum bleach spot was made by focusing the light laser onto the bilayer through the 10x objective. The fluorescence recovery was measured using MetaMorph Software (Universal Imaging). The fluorescence intensity of a bleached spot was determined as a function of time after background subtraction and intensity normalization. The data was fit to single exponential equation. From these curves, mobile fraction of the dye-label lipids and the half-time of recovery, $t_{1/2}$, were determined according to established procedures.[86] The diffusion constant, *D*, could be acquired by employing the following equation:

$$D = (w^2 / 4t_{1/2})\, \gamma_D$$

where *w* is the full width at half-maximum of the Gaussian profile of the focused beam and γ_D is a correction factor that depends on the bleach time and the geometry of the laser beam.[86] The value of γ_D was 1.1.

Dehydration and Rehydration of Supported Phospholipid Bilayers

Freshly formed bilayers were initially examined by fluorescence microscopy and analyzed by FRAP before the introduction of the sugar. After, FRAP measurements were made, the buffer solution above the bilayer was exchanged for the sugar solution and allowed to incubated for 1 hour. Trehalose solution was prepared in PBS buffer where the amount of sugar in solution is given as a weight percent (w/w %). FRAP measurements were performed again to check the quality of the phospholipid bilayer in the presence of the sugar solution. To dehydrate the bilayer, the bulk solution was removed from the PDMS well with a pipette and the platform was placed on top of the oven for approximately 30 minutes. The dried bilayer was again observed under a fluorescence microscope to inspect for any damage or delamination. Samples were then shipped to Washington, D.C. and the United Kingdom. After the samples were back in Texas theses were rehydrate with deionized water and analyzed by FRAP.

Sample Shipment

Samples treated with α,α-trehalose were labeled and packed inside small plastic boxes. The samples were shipped to Washington D.C. and to the United Kingdom. The idea is that during shipment, the supported membranes will be exposed to the non-sterile

conditions outside the laboratory setting and prove the applicability of the aforementioned technology.

6.4 Results and Discussion

In an initial set of experiments, supported phospholipid bilayers in PBS containing 99.9 mol % POPC and 0.1 mol % Texas Red DHPE were formed by vesicle fusion. FRAP experiments showed that the bilayers were 2D-dimensional fluid with diffusion constants of $4.6 \pm (0.3) \times 10^{-8}$ cm^2/sec. The sample recovered approximately 97% of its initial fluorescence at $t = \infty$. Then the aqueous solution was exchanged for the trehalose solution (20 w/w %) and incubated for 1 hour. It should be noted that a 20 w/w % solution of trehalose corresponds to a concentration of 0.6 M. FRAP experiments were repeated after the introduction of 20 w/w % trehalose and similar results were obtained. Then the samples were dried and analyzed by fluorescence microscopy. Figure 6.2 shows fluorescence micrographs of the supported bilayer before and after drying from 20 w/w% trehalose solution. The sample showed uniform fluorescence and no evidence for delamination. To test sample stability, the samples were properly labeled, packed, and shipped to Washington, D.C. using standard post office services. Samples shipped to Washington D.C. returned 20 days later. The samples were rehydrated and tested again to check if the bilayers were still functional. FRAP measurements demonstrated that the bilayer were still highly mobile. The inset image in Figure 6.3 shows a fluorescence micrograph of the bilayer right after photobleaching and again 300 sec later. The FRAP curve (Figure 6.3) refers to the

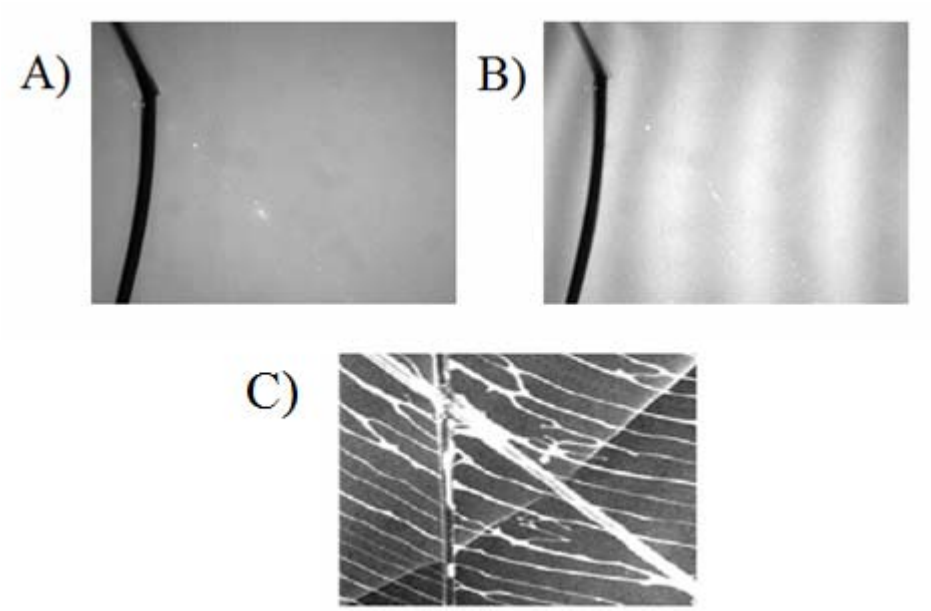

Figure 6.2 Images of supported POPC lipid membranes doped with 1 mol% Texas Red DHPE before drying (A), after drying (B) from 20 w/w % solutions of trehalose, after drying (C) in the absence of trehalose.

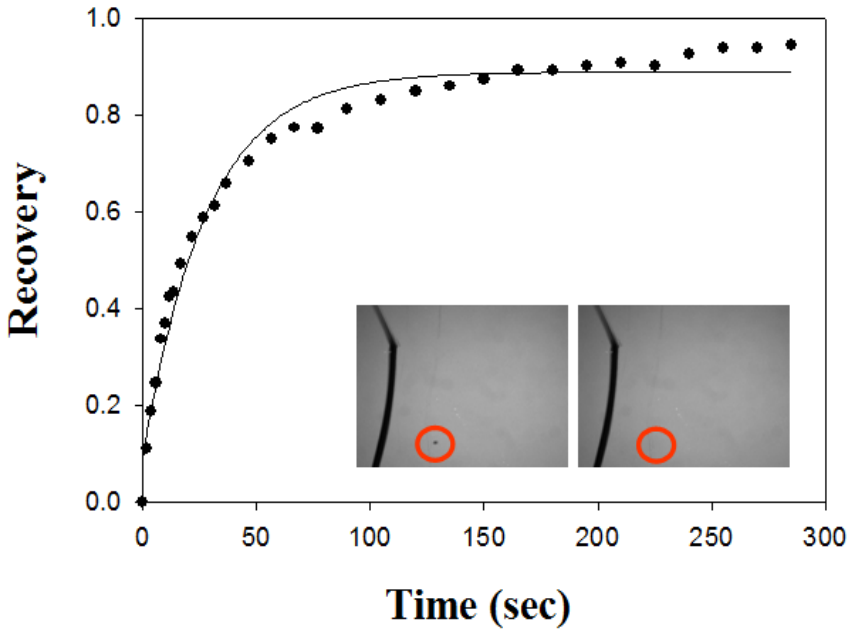

Figure 6.3 Fluorescence recovery after photobleaching curve for a supported bilayer shipped to Washington, D.C. and analyzed 20 days later. Insets: fluorescence micrographs of the bilayer showing the laser bleach spot both before and after recovery (red circles).

fluorescence intensity in the bleached spot as a function of time. As can be seen, relatively complete recovery was observed with a diffusion constant of $4.5 \pm (0.3) \times 10^{-8}$ cm^2/sec. Moreover, the sample recovered over 90% of its initial fluorescence.

A second group of samples were prepared following the procedure explained above. These groups of samples were also prepared using vesicles composed of 99.9 mol % POPC and 0.1 mol % Texas Red DHPE. After drying the samples in the presence of 20 w/w% α,α-trehalose, the samples were properly labeled, packed, and shipped over sea to the United Kingdom. Figure 6.4 shows fluorescence micrographs of the supported bilayer before (A) and after drying (B) from 20 w/w% trehalose solution. These images were taken before shipping the samples to the United Kingdom. Figure 6.4 also shows the fluorescence micrographs of the supported bilayer right after arrived (C) from the United Kingdom and after rinsed and rehydrated (D) with deonized water. Samples shipped to the United Kingdom returned 15 days later and there were tested in our laboratory. All the samples tested shows similar behaviors. The inset image in Figure 6.4 shows a fluorescence micrograph of the bilayer right after photobleaching and again 300 sec later. The FRAP curve (Figure 6.5) shows relatively complete recovery of the fluorescence with a diffusion constant of $4.5 \pm (0.5) \times 10^{-8}$ cm^2/sec. Moreover, the sample recovered approximately 92% of its initial fluorescence.

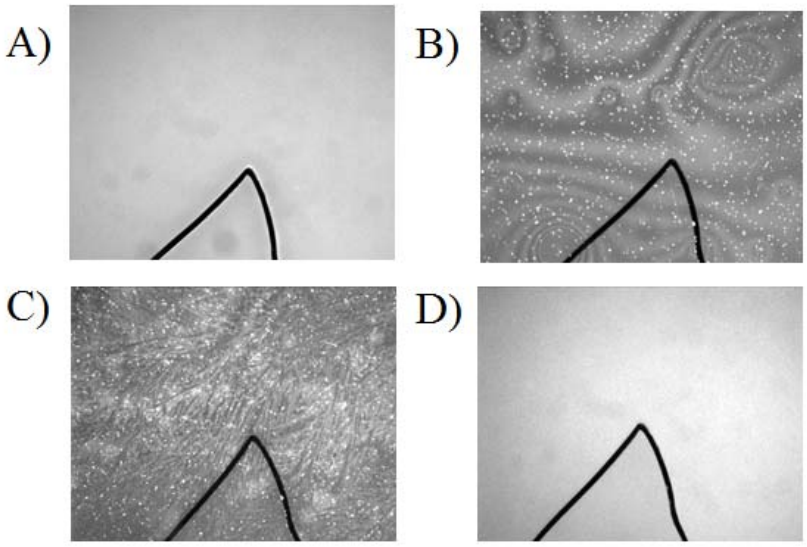

Figure 6.4 Images of supported POPC lipid membranes before drying (A), after drying (B) from 20 w/w % solutions of trehalose, after returned (C) from the United Kingdom, and after rehydrated (D) with deionized water.

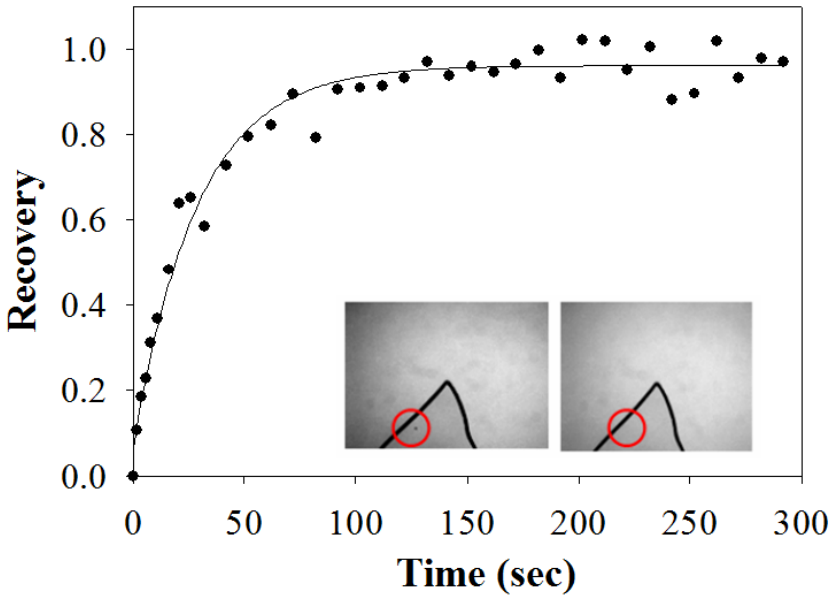

Figure 6.5 Fluorescence recovery after photobleaching curve for a supported bilayer shipped to the United Kingdom and analyzed 15 days later. Insets: fluorescence micrographs of the bilayer showing the laser bleach spot both before and after recovery (red circles).

6.5 Summary and Conclusions

In this study we showed that supported bilayers dried in the presence of α,α-trehalose are able to survive robust conditions. Samples dried in the presence of trehalose were packed and shipped to two different destinations, Washington, D.C. and the United Kingdom. After several days of transport and exposure to non-sterile environment and stress that occur during shipment, FRAP measurements showed that the lipid bilayers were still mobile with high mobile fraction. This open the doors towards creating working biosensors that could be dried in the presence of saccharides, shipped, and then later rehydrated in order to return to their original state. Also, the addition of the sugar does not alter the bilayer structure. This drying procedure could be coupled to the electrophoresis technique. Species of interest can be separated in the membrane and then dried in the presence of trehalose for further analytical studies. This could open the area for studying protein crystal structure and sequence analysis of candidate proteins via mass spectrometry where samples need to exist under dry conditions.

CHAPTER VII

CONCLUSIONS

The main goal of the research presented in this dissertation was to develop a new biological platform for use in making biophysical studies of membrane proteins and protein chromatography. As clearly stated in the introduction section, membrane proteins play a crucial role in many cellular processes by providing vital communication between the cell and its surroundings. The normal functions of this class of protein are fundamental to our health, and many damaged proteins have been associated to serious human diseases. Today membrane proteins are targets for the majority of drugs currently developed by the pharmaceutical industry. Thus, developing new tools for obtaining structural information could greatly improve the efficiency of drug discovery.

The first goal of this project was to develop a solid supported lipid bilayer (SLB) that mimics the cell membrane/cytoskeletal network, in which biophysical studies of integral transmembrane protein can be done. SLB have been extensively used as model systems to study numerous cell membrane processes, but one well-know drawback of the system has been the successful incorporation of an integral transmembrane protein. Transmembrane protein mobility has been hindered by denaturation of these species on the underlying inorganic support. The thin layer of water that separates the bilayer from the substrate (~ 1 nm) does not offer an adequate space between the membrane and the substrate. To solve this problem, I designed a “double cushion” bilayer system. This new platform, as discussed in Chapter III, consisted of a first cushion layer formed by

uniformly adsorbing BSA onto a planar glass supports and a second layer formed when lipid vesicles containing polymer-conjugated lipids are fused on top of this first layer. In this double cushion system, the distance between the BSA layer and the lower leaflet of the bilayer can be manipulated by varying the density and size of the lipopolymer incorporated into the lipid bilayer. Diffusion constants in the order 10^{-8} cm^2/sec with mobile fractions up to 75 % were obtained for a model transmembrane protein. This represents a significant improvement over other platforms fabricated directly on glass or using single cushion strategies.

The second goal of this dissertation project was to develop a new biological platform for the purification of membrane associated species, such as lipids conjugated with fluorescent markers and peripheral proteins, in their native environment. As discussed in Chapter IV and V, this method consisted of a solid supported bilayer platform doped with cholesterol. Cholesterol was used to control the physical properties of the bilayer. In Chapter IV, we achieved with high resolution and small band broadening, the separation of two isomers of Texas Red dye and a green dye, BODIPY. Our technique was sensitive enough to resolve into two distinct bands isomers of Texas Red-DHPE. The separation of isomers is not simple since the difference between the two compounds in only structural. Isomers of the same compound have the same charge and molecular weight. In our supported platform, the separation of isomers was possible because they presumably interact differently with the lipid bilayer due to their structures. This difference in interaction most likely lead to different migration speeds. In Chapter IV, this electrophoretic platform was modified to be able to move and separated

peripheral proteins. We showed that we could electrophoretically move fluorescently labeled streptavidin proteins bound to a bilayer via a biotinylated lipids present within the supported membrane. The separation of doubly bound proteins from singly bound proteins was achieved with high resolution. For the first time, this platform allows for the direct observation of the different valency states of ligand-receptors pairs.

The next goal is to extend this electrophoretic technique for the separation of transmembrane proteins. Prior to achieving this objective, it is important to modify the composition of the bilayer to accommodate transmembrane species. I have already accomplished this goal (Chapter III) and shown that the proper bilayer composition can maintain transmembrane fluidity. Combining the double cushion bilayer platform with the electrophoretic technique outlined in Chapter IV, we should be able to extend this method to separate transmembrane proteins within their native environment as shown in Figure 7.1.

7.1 Electrophoretic Separation in Microfluidic Devices

One of the advantages of our electrophoretic platform is the possibility of combining this technique with microfluidics for the separation and analysis of membrane species on a single chip. Initial experiments in this area were performed using a simple microfludic device. Figure 7.2 illustrates a schematic diagram of the microfluidic device. The device consists of two channels; channel A (200 μm) and channel B (100 μm). To apply a voltage across channel B two platinum electrodes were placed into holes in the PDMS of the microfluidic device.

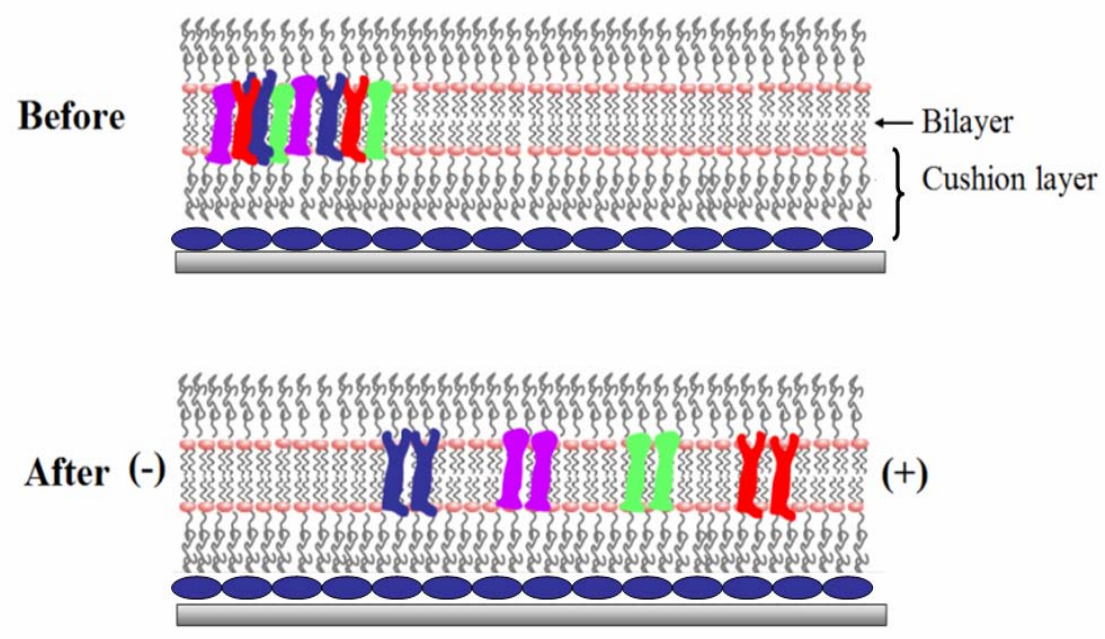

Figure 7.1 Strategy to separate transmembrane proteins using double cushion to prevent immobilization.

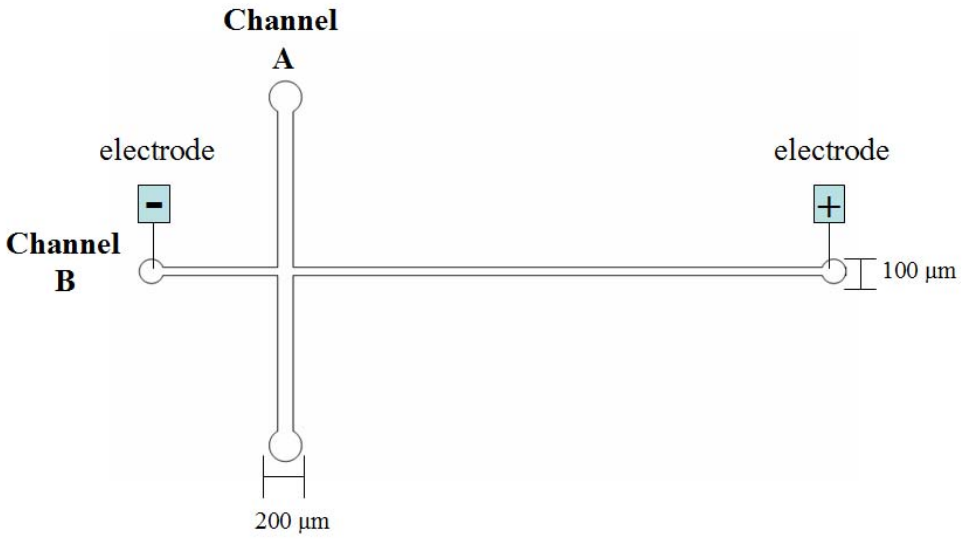

Figure 7.2 Schematic representation of a T-form microfluidic device used for the electrophoresis experiment. The device consists of two channels connected together in T-form.

In a first set of experiments, we demonstrated the ability to electrophoretically move Texas Red labeled lipids inside the microfluidic device. First, the two channels were filled with DI water. Then a vesicle solution containing POPC and of 1 mol % Texas Red DHPE was flowed across Channel A. The vesicles fused to this area, creating a supported bilayer with Texas Red DHPE in it. After rinsing to remove unfused vesicles, the separation bilayer was formed in Channel B by flowing vesicles composed of 100 mol % POPC across Channel B. Figure 7.3A shows a cartoon representation and epifluorescence micrograph of the system. A 100 V potential (DC) was applied parallel to the plane of the membrane formed inside Channel B (Figure 7.3 B). Because Texas Red DHPE lipids are negatively charged, they will migrate toward the positive electrode. We monitored the lateral movement of the Texas Red lipids as a function of time using an inverted microscope. Figure 7.3B shows an epifluorescence micrograph of the system after applying a 100 V across the channel for 30 minutes. As shown, we were able to move, by electrophoresis, Texas Red DHPE lipids inside a microfluidic channel.

One of our Laboratory future goals is to design a microfluidic platform whereby we separate and analyze multiple proteins at the same time using a single microfluidic device. This high trough-put platform can be easily coupled to other techniques such as mass spectrometry for proteomics applications. A design of a possible device is illustrated in Figure 7.4. Figure 7.5 shows a 3D-cartoon of the separation experiment. The experiment consists of four steps. First, vesicles containing the analyte are introduced through the left side channel. Then vesicles containing the desired composition to form the separation bilayer are introduced into the rest of the device.

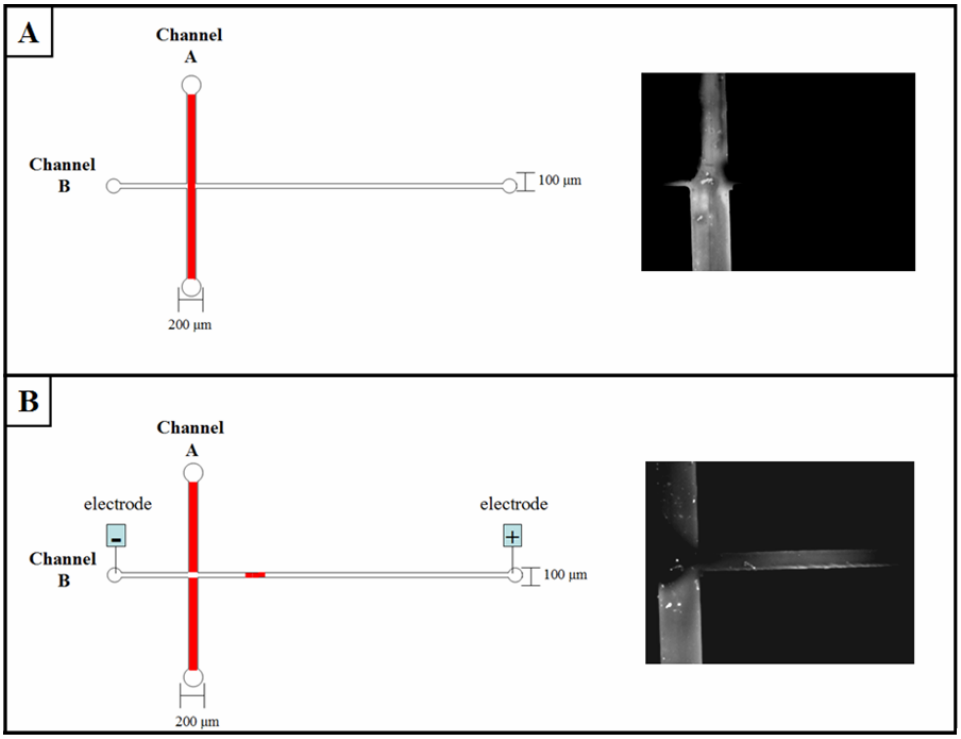

Figure 7.3 Texas Red- DHPE labeled lipids migrating in pure POPC bilayer. A) Cartoon representation and epifluorescence micrograph of the system before applying a potential across the bilayer. B) Cartoon representation and epifluorescence micrograph of the system after applying 100 V across the bilayer for approximately 30 minutes.

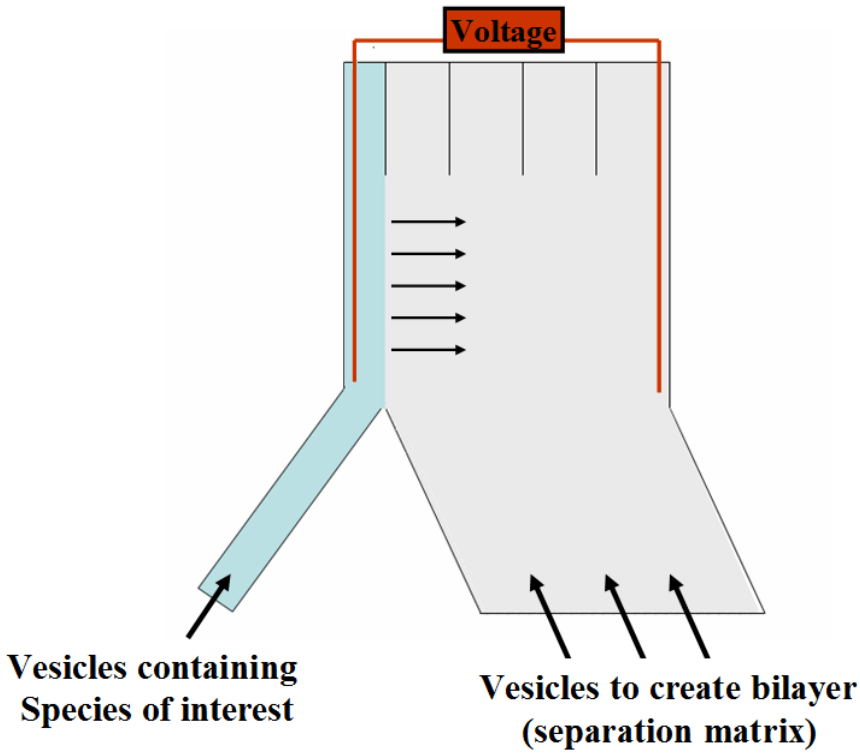

Figure 7.4 Schematic diagram of a microfluidic device for proteomic applications.

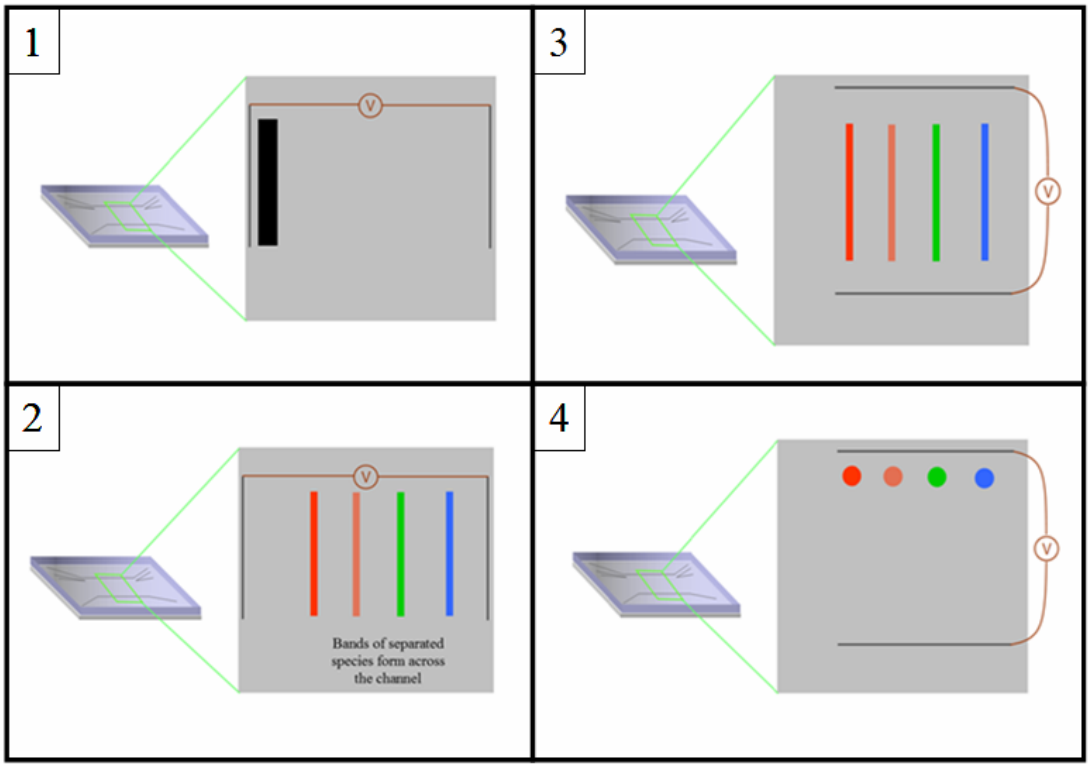

Figure 7.5 Schematic illustration of an electrophoresis experiment inside a microfluidic device. (1-2) Species are separated in the x-direction first. (3-4) Then the voltage is changed to the y-direction to collect the samples.

A voltage can be applied across the bilayer to separate the species in the x-direction. Then, the direction of the voltage can be changed to collect the species into spots as shown in Figure 7.5.

7.2 Catalysis on a Chip-Biosensor Device

Another exciting application is the possibility of using our electrophoretic platform as a medical diagnostic device for the early detection of human disease. Certain enzymatic reactions can lead to the formation of 'biomarkers' which can indicate the onset of a particular disease. For example, the increased hydrolysis of a particular ganglioside is to related to Alzheimer.[164] Thus an interesting system that we could study is the hydrolysis of gangliosides, such as GM_1, by the enzyme β-galactosidase. β-galactosidase is a hydrolase enzyme that is responsible for the hydrolysis of β-galactosides into monosaccharides.[165] Some of the substrates for this enzyme include but are not limited to ganglioside GM_1, lactosylceramides, and some glycoproteins. GM_1 are membrane lipids in which the polar head group is a complex oligosaccharide containing a sialic acid and other monosaccharide residues (Figure 7.6).

Figure 7.7 shows a schematic representation of the proposed experiment. We have previously showed that we can prepare solid supported lipid bilayers by the fusion of POPC vesicles containing GM_1.[145] GM_1 bears a net charge of negative 1.[166] Under an electric field we expect GM_1 to migrate toward the positive electrode (Figure 7.7A). The GM_1 lipid exhibits a specific mobility which can be calculated from the velocity profile,

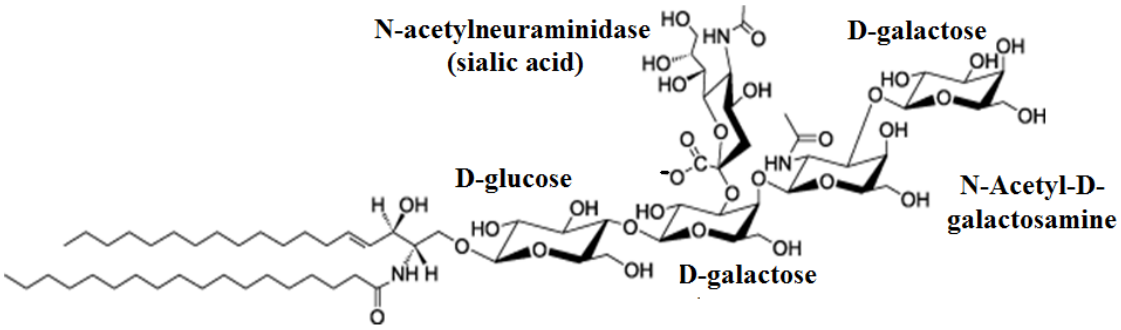

Figure 7.6 Chemical structure of ganglioside GM_1.[167]

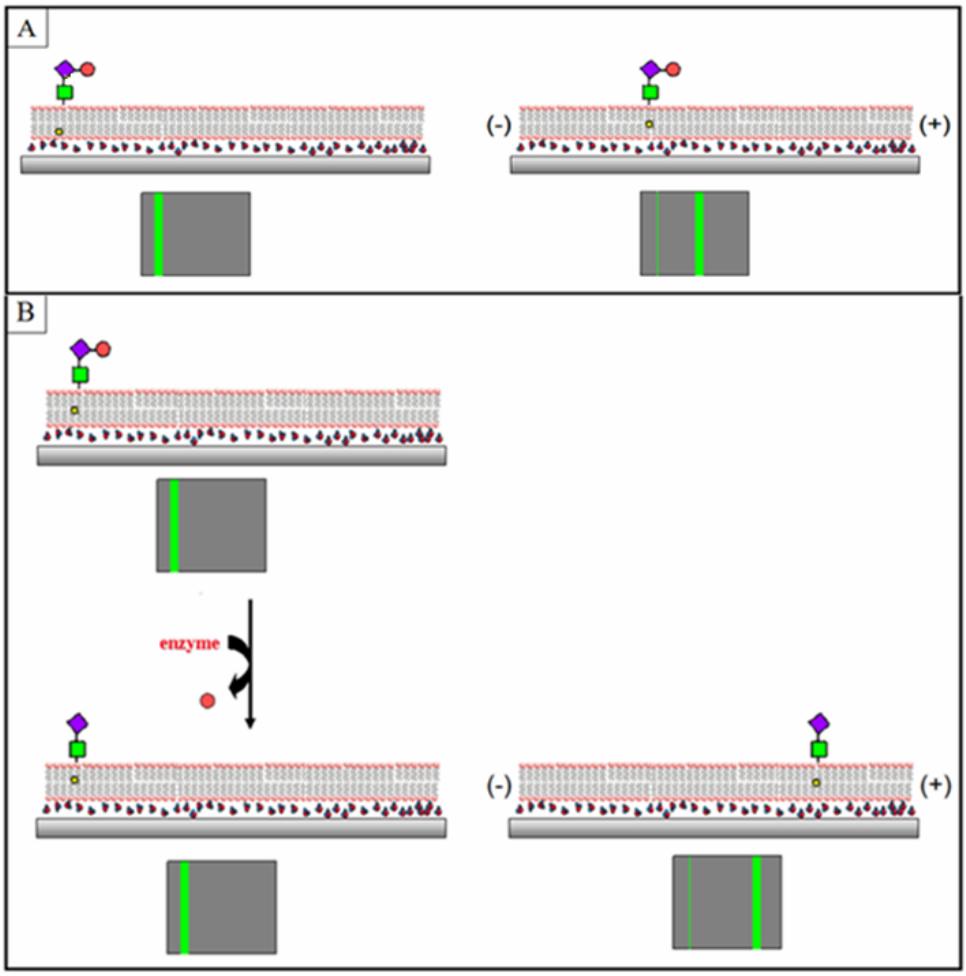

Figure 7.7 Catalysis on a chip. (A) Before adding the enzyme, the species of interest travel a distance equal to x. (B) After the reaction of the enzyme with the species of interest (e.g. hydrolysis) the species travel a distance y different from distance x.

which depends on the applied potential. Addition of β-galactosidase causes the hydrolysis of GM_1, releasing a D-galactose moiety. After applying a potential across the supported membrane we expect the ganglioside to exhibit a different electrophoretic mobility (Figure 7.7B). By measuring the change in the electrophoretic mobility, one can determine important parameters, such as the stoichiometry of the reaction and the enzyme efficiency.

In conclusion, this dissertation project further supports the importance of solid supported phospholipid bilayers as cell biomembrane mimics. This biological platform can be coupled within microfluidics devices and with numerous analytical techniques, such as fluorescence microscopy, mass spectrometry, and atomic force microscopy. This opens the door to the development of novel proteomics methodologies that will elucidate a variety of biological processes.

The double cushion system developed here mimics the cell membrane/cytoskeletal network. This new system presents a new biological platform in where biophysical study of transmembrane proteins, such as ion transport, protein-protein interactions, and binding, can be studied. Furthermore, this novel biological platform can be coupled to our electrophoresis technique for the purification and study of transmembrane species. The separated species can be characterized with non-label techniques, such as mass spectrometry, for proteomics applications. Finally, a biosensor device can be designed for the early detection of human diseases.

REFERENCES

(1) Fischer, F.; Wolters, D.; Rogner, M.; Poetsch, A. *Molecular & Cellular Proteomics* **2006**, *5*, 444-453.

(2) Kyogoku, Y.; Fujiyoshi, Y.; Shimada, I.; Nakamura, H.; Tsukihara, T.; Akutsu, H.; Odahara, T.; Okada, T.; Nomura, N. *Acc. Chem. Res.* **2003**, *36*, 199-206.

(3) Drews, J. *Science* **2000**, *287*, 1960-1964.

(4) Stoeckenius, W.; Engelman, D. M. *J. Cell Biol.* **1969**, *42*, 613-646.

(5) Voet, D.; Voet, J. G. *Biochemistry*, 2nd ed.; John Wiley & Sons: New York, *1995.*

(6) Singer, S. J.; Nicolson, G. L. *Science* **1972**, *175*, 720-731.

(7) Geigel, G., 2008, http://sun.menloschool.org/~cweaver/cells/c/cell_membrane/.

(8) Boesze-Battaglia, K.; Schimmel, R. J. *J. Exp. Biol.* **1997**, *200*, 2927–2936.

(9) Wallin, E.; von Heijne, G. *Protein Sci.* **1998**, *7*, 1029-1038.

(10) Nelson, D. L.; Cox, M. M. *Principles of Biochemistry*; 4th ed.; W.H. Freeman and Company: New York, 2005.

(11) Alberts, B. B.; D. Lewis, J.; Raff, M.; Roberts, K.; Watson, J. pp. 446-506, In *Molecular Biology of the Cell*,. Garland Publishing, New York, 1994.

(12) Branton, D. *Proc. Natl. Acad. Sci.* **1966**, *55*, 1048-1056.

(13) Palczewski, K. *Annu. Rev. Biochem.* **2006**, *75*, 743-767.

(14) Palczewski, K.; Kumasaka, T.; Hori, T.; Behnke, C.; Motoshima, H.; Fox, B.; Trong, I.; Teller, D.; Okada, T.; Stenkamp, R.; Yamamoto, M.; Miyano, M. *Science* **2000**, *289*, 739-745.

(15) Filipek S; Teller DC; Palczewski K; R., S. *Annu. Rev. Biophys. Biomol. Struct.* **2003**, *32*, 375–397.

(16) Filmore, D. *Mod. Drug Discovery* **2004**, 7, 24-28.

(17) Teller, D.; Okada, T.; Behnke, C.; Palczewski, K.; Stenkamp, R. *Biochemistry* **2001**, *40*, 7761-7772.

(18) Lundstrom, K.; Wagner, R.; Reinhart, C.; Desmyter, A.; Cherouati, N.; Magnin, T.; Zeder-Lutz, G.; Courtot, M.; Prual, C.; Andre, N.; Hassaine, G.; Michel, H.; Cambillau, C.; Pattus, F. *J. Struct. Funct. Genomics* **2006**, *7*, 77-91.

(19) Hubner, C. A.; Jentsch, T. J. *Human Molecular Genetics* **2002**, *11*, 2435-2445.

(20) Doyle, D. A.; Cabral, J. M.; Pfuetzner, R. A.; Kuo, A. L.; Gulbis, J. M.; Cohen, S. L.; Chait, B. T.; MacKinnon, R. *Science* **1998**, *280*, 69-77.

(21) Agre, P.; Sasaki, S.; Chrispeels, M. J. *Am. J. Physiol.* **1993**, *265*, F461.

(22) Agre, P.; Kozono, D. *FEBS Lett.* **2003**, *555*, 72-78.

(23) Singh, S.; Malik, B. K.; Sharma, D. K. *Bioinformation* **2006**, *1*, 314-320.

(24) Lundstrom, K. *Mol. Biotech.* **2006**, *34*, 205-212.

(25) Görg, A.; Weiss, W.; Dunn, M. *Proteomics* **2004**, *4*, 3665–3685.

(26) Brian, A. A.; McConnell, H. M. *Proc. Natl. Acad. Sci. U.S.A.* **1984**, *81*, 6159-6163.

(27) Tamm, L. K.; Mcconnell, H. M. *Biophys. J.* **1985**, *47*, 105-113.

(28) McConnell, H. M.; Watts, T. H.; Weis, R. M.; Brian, A. A. *Biochim. Biophys. Acta* **1986**, *864*, 95-106.

(29) Kalb, E.; Frey, S.; Tamm, L. K. *Biochim. Biophys. Acta* **1992**, *1103*, 307-316.

(30) Hubbard, J. B.; Silin, V.; Plant, A. L. *Biophys. Chem.* **1998**, *75*, 163-176.

(31) Tamm, L. K.; Shao, Z. pp.169-185 In *Biomembrane Structure;* IOS Press: Amsterdam, 1998.

(32) Koenig, B. W.; Gawrisch, K.; Krueger, S.; Orts, W.; Majkrzak, C. F.; Berk, N.; Silverton, J. V. *Biophys. J.* **1996**, *70*, 229.

(33) Thompson, N. L.; Pearce, K. H.; Hsieh, H. V. *Eur. Biophys. J. Biophy.* **1993**, *22*, 367-378.

(34) Yang, T.; Baryshnikova, O. K.; Mao, H. B.; Holden, M. A.; Cremer, P. S. *J. Am. Chem. Soc.* **2003**, *125*, 4779-4784.

(35) Thompson, N. L.; Drake, A. W.; Chen, L. X.; VandenBroek, W. *Photochem. Photobiol.* **1997**, *65*, 39-46.

(36) Stelzle, M.; Weissmuller, G.; Sackmann, E. *J. Phys. Chem.* **1993**, *97*, 2974-2981.

(37) Cornell, B. A.; BraachMaksvytis, V. L. B.; King, L. G.; Osman, P. D. J.; Raguse, B.; Wieczorek, L.; Pace, R. J. *Nature* **1997**, *387*, 580-583.

(38) van Oudenaarden, A.; Boxer, S. G. *Science* **1999**, *285*, 1046-1048.

(39) Johnson, J. M.; Ha, T.; Chu, S.; Boxer, S. G. *Biophys. J.* **2002**, *83*, 3371-3379.

(40) Kim, J.; Kim, G.; Cremer, P. S. *Langmuir* **2001**, *17*, 7255-7260.

(41) Cremer, P. S.; Boxer, S. G. *J. Phys. Chem. B* **1999**, *103*, 2554-2559.

(42) Bayerl, T. M.; Bloom, M. *Biophys. J.* **1990**, *58*, 357-362.

(43) Johnson, S. J.; Bayerl, T. M.; Mcdermott, D. C.; Adam, G. W.; Rennie, A. R.; Thomas, R. K.; Sackmann, E. *Biophys. J.* **1991**, *59*, 289-294.

(44) Williams, L. M.; Evans, S. D.; Flynn, T. M.; Marsh, A.; Knowles, P. F.; Bushby, R. J.; Boden, N. *Langmuir* **1997**, *13*, 751-757.

(45) Koenig, B. W.; Kruger, S.; Orts, W. J.; Majkrzak, C. F.; Berk, N. F.; Silverton, J. V.; Gawrisch, K. *Langmuir* **1996**, *12*, 1343-1350.

(46) Cremer, P. S.; Groves, J. T.; Kung, L. A.; Boxer, S. G. *Langmuir* **1999**, *15*, 3893-3896.

(47) Groves, J. T.; Wulfing, C.; Boxer, S. G. *Biophys. J.* **1996**, *71*, 2716-2723.

(48) Groves, J. T.; Boxer, S. G. *Biophys. J.* **1995**, *69*, 1972-1975.

(49) Cremer, P. S.; Groves, J. T.; Ulman, N.; Boxer, S. G. *Biophys. J.* **1998**, *74*, A311-A311.

(50) Graneli, A.; Rydstrom, J.; Kasemo, B.; Hook, F. *Langmuir* **2003**, *19*, 842-850.

(51) Groves, J. T.; Ulman, N.; Boxer, S. G. *Science* **1997**, *272*, 651-653.

(52) Kam, L.; Boxer, S. G. *J. Am. Chem. Soc.* **2000**, *122*, 12901-12902.

(53) Plant, A. L. *Langmuir* **1999**, *15*, 5128-5135.

(54) Wagner, M. L.; Tamm, L. K. *Biophys. J.* **2000**, *79*, 1400-1414.

(55) Sackmann, E.; Tanaka, M. *Trends Biotechnol.* **2000**, *18*, 58-64.

(56) Conboy, J. C.; Liu, S.; O'Brien, D. F.; Saavedra, S. S. *Biomacromolecules* **2003**, *4*, 841-849.

(57) Rossetti, F. F.; Textor, M.; Reviakine, I. *Langmuir* **2006**, *22*, 3467-3473.

(58) Zasadzinski, J. A.; Helm, C. A.; Longo, M. L.; Weisenhorn, A. L.; Gould, S. A. C.; Hansma, P. K. *Biophys. J.* **1991**, *59*, 755-760.

(59) Egawa, H.; Furusawa, K. *Langmuir* **1999**, *15*, 1660–1666.

(60) Spinke, J.; Yang, J.; Wolf, H.; Liley, M.; Ringsdorf, H.; Knoll, W. *Biophys. J.* **1992**, *63*, 1667-1671.

(61) Fang, Y.; Cheley, S.; Bayley, H.; Yang, J. *Biochemistry* **1997**, *36*, 9518-9522.

(62) Merino, S.; Domenech, O.; Vinas, M.; Montero, M. T.; Hernandez-Borrell, J. *Langmuir* **2005**, *21*, 4642-4647.

(63) Schonherr, H.; Johnson, J. M.; Lenz, P.; Frank, C. W.; Boxer, S. G. *Langmuir* **2004**, *20*, 11600-11606.

(64) Merino, S.; Domenech, O.; Montero, M. T.; Hernandez-Borrell, J. *Biosens. Bioelectron.* **2005**, *20*, 1843-1846.

(65) Yuan, C. B.; Johnston, L. J. *Biophys. J.* **2001**, *81*, 1059-1069.

(66) Yang, T. L.; Jung, S. Y.; Mao, H. B.; Cremer, P. S. *Anal. Chem.* **2001**, *73*, 165-169.

(67) Shaw, J. E.; Slade, A.; Yip, C. M. *J. Am. Chem. Soc.* **2003**, *125*, 11838-11839.

(68) Kuziemko, G. M.; Stroh, M.; Stevens, R. C. *Biochemistry* **1996**, *35*, 6375-6384.

(69) Terrettaz, S.; Stora, T.; Duschl, C.; Vogel, H. *Langmuir* **1993**, *9*, 1361-1369.

(70) Tanaka, M.; Sackmann, E. *Nature* **2005**, *437*, 656-663.

(71) Sackmann, E. *Science* **1996**, *271*, 43-48.

(72) Castellana, E. T.; Cremer, P. S. *Surface Science Reports* **2006**, *61*, 429-444.

(73) Zhang, L. Q.; Longo, M. L.; Stroeve, P. *Langmuir* **2000**, *16*, 5093-5099.

(74) Majewski, J.; Wong, J. Y.; Park, C. K.; Seitz, M.; Israelachvili, J. N.; Smith, G. S. *Biophys. J.* **1998**, *75*, 2363-2367.

(75) Ma, C.; Srinivasan, M. P.; Waring, A. J.; Lehrer, R. I.; Longo, M. L.; Stroeve, P. *Colloids. Surf. B* **2003**, *28*, 319-329.

(76) Kugler, R.; Knoll, W. *Bioelectrochemistry* **2002**, *56*, 175-178.

(77) Hillebrandt, H.; Wiegand, G.; Tanaka, M.; Sackmann, E. *Langmuir* **1999**, *15*, 8451-8459.

(78) Elender, G.; Kuhner, E.; Sackmann, E. *Biosens. Bioelectron.* **1996**, *11*, 565-577

(79) Shen, W. W.; Boxer, S. G.; Knoll, W.; Frank, C. W.; *Biomacromolecules* **2001**, *2*, 70-79.

(80) Beyer, D.; Elender, G.; Knoll, W.; Kuhner, M.; Maus, S.; Ringsdorf, H.; Sackmann, E. *Angew. Chem.Int. Edn* **1996**, *35*, 1682-1685.

(81) Hausch, M.; Zentel, R.; Knoll, W. *Macromol. Chem. Phys.* **1999**, *200*, 174-179.

(82) Seitz, M.; Ter-Ovanesyan, E.; Hausch, M.; Park, C. K.; Zasadzinski, J. A.; Zentel, R.; Israelachvili, J. N. *Langmuir* **2000**, *16*, 6067-6070.

(83) Seitz, M.; Wong, J. Y.; Park, C. K.; Alcantar, N. A.; Israelachvili, J.; Films, T. S. *Thin Solid Films* **1998**, *329*, 767-771.

(84) Weng, K. C.; Stalgren, J. J. R.; Duval, D. J.; Risbud, S. H.; Frank, C. W. *Langmuir* **2004**, *20*, 7232-7239.

(85) Davis, R. W.; Flores, A.; Barrick, T. A.; Cox, J. M.; Brozik, S. M.; Lopez, G. P.; Brozik, J. A. *Langmuir* **2007**, *23*, 3864 -3872.

(86) Axelrod, D.; Koppel, D. E.; Schlessinger, J.; Elson, E.; Webb, W. W. *Biophys. J.* **1976**, *16*, 1055-1069.

(87) Daniel, S.; Diaz, A. J.; Martinez, K. M.; Bench, B. J.; Albertorio, F.; Cremer, P. S. *J. Am. Chem. Soc.* **2007**, *129*, 8072-8073.

(88) Haugland, R. P., p.70, In *The Handbook*; 10th ed.; Invitrogen Corp., California, 2005.

(89) Mammen, M.; Choi, S.-K.; Whitesides, G. M. *Angew. Chem. Int. Ed.* **1998**, *37*, 2754-2794.

(90) Bowden, N.; Brittain, S.; Evans, A. G.; Hutchinson, J. W.; Whitesides, G. M. *Nature* **1998**, 146-149.

(91) Xia, Y.; Whitesides, G. M. *Annu. Rev. Mater. Sci.* **1998**, *28*, 153-184.

(92) Mao, H. B.; Holden, M. A.; You, M.; Cremer, P. S. *Anal. Chem.* **2002**, *74*, 5071-5075.

(93) Holden, M. A.; Kumar, S.; Castellana, E. T.; Beskok, A.; Cremer, P. S. *Sens. Actuators, B* **2003**, 199-207.

(94) Holden, M. A.; Kumar, S.; Beskok, A.; Cremer, P. S. *J. Micromech. Microeng.* **2003**, *13*, 412-418.

(95) Holden, M. A., Studies in biological surface science: microfluidics, photopatterning and artificial bilayers, Ph.D. Dissertation, Texas A&M University, 2004.

(96) Jacobson, K.; Derzko, Z.; Wu, E. S.; Hou, Y.; Poste, G. *J. Supramol. Str.* **1976**, *5*, 565-576.

(97) Lopez, A.; Dupou, L.; Altibelli, A.; Trotard, J.; Tocanne, J. F. *Biophys. J.* **1999**, *53*, 963-970.

(98) van Oudenaarden, A.; Boxer, S. G. *Science* **1999**, *285*, 1046-1048.

(99) Goennenwein, S.; Tanaka, M.; Hu, B.; Moroder, L.; Sackmann, E. *Biophys. J.* **2003**, *85*, 646-655.

(100) Baumgart, T.; Offenhausser, A. *Langmuir* **2003**, *19*, 1730-1737.

(101) Lang, H.; Duschl, C.; Vogel, H. *Langmuir* **1994**, *10*, 197-210.

(102) Purrucker, O.; Fortig, A.; Jordan, R.; Tanaka, M. *Chem. Phys. Chem.* **2004**, *5*, 327-335.

(103) Naumann, C. A.; Frank, C. W.; Prucker, O.; Lehmann, T.; Ruehe, J.; Knoll, W.; J., B. *Biophys. J.* **2000**, *78*, 273a-273a.

(104) Tanaka, M. *Mrs Bull.* **2006**, *31*, 513-520.

(105) Wiegand, G.; Jaworek, T.; Wegner, G.; Sackmann, E. *J. Colloid Interface Sci.* **1997**, *196*, 299-312.

(106) Wagner, M. L.; Tamm, L. K. *Biophys. J.* **2001**, *81*, 266-275.

(107) Smith, E. A.; Coym, J. W.; Cowell, S. M.; Tokimoto, T.; Hruby, V. J.; Yamamura, H. I.; Wirth, M. J. *Langmuir* **2005**, *21*, 9644-9650.

(108) Berendes, R.; Voges, D.; Demange, P.; Huber, R.; Burger, A. *Science* **1993**, *262*, 427-430.

(109) Seaton, B. A. pp. 15-29, In *Annexins: Molecular Structure to Cellular Function*; Landes Co., Austin, TX, 1996.

(110) Isas, J. M.; Cartailler, J. P.; Sokolov, Y.; Patel, D. R.; Langen, R.; Luecke, H.; Hall, J. E.; Haigler, H. T. *Biochemistry* **2000**, *39*, 3015-3022.

(111) Langen, R.; Isas, J. M.; Hubbell, W. L.; Haigler, H. T. *Proc. Natl. Acad. Sci. U.S.A.* **1998**, *95*, 14060-14065.

(112) Binder, H.; Kohler, G.; Arnold, K.; Zschornig, O. *Chem. Phys. Chem.* **2000**, *2*, 4615-4623.

(113) Albertorio, F.; Diaz, A. J.; Yang, T. L.; Chapa, V. A.; Kataoka, S.; Castellana, E. T.; Cremer, P. S. *Langmuir* **2005**, *21*, 7476-7482.

(114) Nollert, P.; Kiefer, H.; Jahnig, F. *Biophys. J.* **1995**, *69*, 1447-1455.

(115) Groves, J. T.; Ulman, N.; Cremer, P. S.; Boxer, S. G. *Langmuir* **1998**, *14*, 3347-3350.

(116) Mao, H. B.; Yang, T. L.; Cremer, P. S. *Anal. Chem.* **2002**, *74*, 379-385.

(117) Albertorio, F.; Daniel, S.; Cremer, P. S. *J. Am. Chem. Soc.* **2006**, *128*, 7168-7169.

(118) Cezanne, L.; Lopez, A.; Loste, F.; Parnaud, G.; Saurel, O.; Demange, P.; Tocanne, J. F. *Biochemistry* **1999**, *38*, 2779-2786.

(119) Saurel, O.; Cezanne, L.; Milon, A.; Tocanne, J. F.; Demange, P. *Biochemistry* **1998**, *37*, 1403-1410.

(120) Richter, R. P.; Him, J. L. K.; Tessier, B.; Tessier, C.; Brisson, A. R. *Biophys. J.* **2005**, *89*, 3372-3385.

(121) Marsh, D.; Bartucci, R.; Sportelli, L. *BBA-Biomembranes* **2003**, *1615*, 33-59.

(122) Kunding, A.; Stamou, D. *J. Am. Chem. Soc.* **2006**, *128*, 11328-11329.

(123) Munro, J. C.; Frank, C. W. *Langmuir* **2004**, *20*, 3339-3349.

(124) Sweryda-Krawiec, B.; Devaraj, H.; Jacob, G.; Hickman, J. J. *Langmuir* **2004**, *20*, 2054-2056.

(125) Zheng, H.; Zhao, J.; Sheng, W.; Xie, X.-Q. *Biopolymers* **2006**, *83*, 46-61.

(126) Lundstrom, K. *Cell. Mol. Life Sci.* **2006**, *63*, 2597-2607.

(127) Zhu, H.; Bilgin, M.; Bangham, R.; Hall, D.; Casamayor, A.; Bertone, P.; Lan, N.; Jansen, R.; Bidlingmaier, S.; Houfek, T.; Mitchell, T.; Miller, P.; Dean, R. A.; Gerstein, M.; Snyder, M. *Science* **2001**, *293*, 2101-2105.

(128) Cristea, I. M.; Gaskell, S. J.; Whetton, A. D. *Blood* **2004**, *103*, 3624-3634.

(129) Phizicky, E.; Bastiaens, P. I. H.; Zhu, H.; Snyder, M.; Fields, S. *Nature* **2003**, *422*, 208-215.

(130) Groves, J. T.; Boxer, S. G.; McConnel, H. M. *Proc. Natl. Acad. Sci.* **1997**, *94*, 13390-13395.

(131) Yoshina-Ishii, C.; Boxer, S. G. *J. Am. Chem. Soc.* **2003**, *125*, 3696-3697.

(132) Yoshina-Ishii, C.; Boxer, S. G. *Langmuir* **2006**, *22*, 2384-2391.

(133) Filippov, A.; Oradd, G.; Lindblom, G. *Biophys. J.* **2003**, *84*, 3079-3086.

(134) Filippov, A.; Oradd, G.; Lindblom, G. *Langmuir* **2003**, *19*, 6397-6400.

(135) Titus, J. A.; Haugland, R.; Sharrow, S. O.; Segal, D. M. *J. Immunol. Methods* **1982**, *50*, 193-204.

(136) Dietrich, C.; Bagatolli, L. A.; Volovyk, Z. N.; Thompson, N. L.; Levi, M.; Jacobson, K.; Gratton, E. *Biophys. J.* **2001**, *80*, 1417-1428.

(137) Simons, K.; Vaz, W. L. C. *Annu. Rev. Biophys. Biomol. Struct.* **2004**, *33*, 269-295.

(138) Caprioli, R. M.; Farmer, T. B.; Gile, J. *Anal. Chem.* **1997**, *69*, 4751–4760

(139) Kraft, M. L.; Weber, P. K.; Longo, M. L.; Hutcheon, I. D.; Boxer, S. G. *Science* **2006**, *313*, 1948-1951.

(140) Daniel, S.; Diaz, A. J.; Martinez, K. M.; Bench, B. J.; Albertorio, F.; Cremer, P. *J. Am. Chem. Soc.* **2007**, *129*, 8072-8073.

(141) Sano, T.; Vajda, S.; Cantor, C. R. *J. Chromatogr. B* **1998**, *715*, 85-91.

(142) Chaiet, L.; Miller, T. W.; Tausing, F.; Wolf, F. J. *Antimicrob. Agents Chemother.* **1963**, *3*, 28-32.

(143) Chaiet, L.; Wolf, F. J. *Arch. Biochem. Biophys.* **1964**, *106*, 1-5.

(144) Keizer, J. *Acc. Chem. Res.* **1985**, *18*, 235-241.

(145) Shi, J. J.; Yang, T. L.; Kataoka, S.; Zhang, Y. J.; Diaz, A. J.; Cremer, P. S. *J. Am. Chem. Soc.* **2007**, *129*, 5954-5961.

(146) Heldin, C. H. *Cell* **1995**, *80*, 213-223.

(147) Kiessling, L. L.; Pohl, N. L. *Chem. Biol.* **1996**, *3*, 71-77.

(148) Mammen, M.; Choi, S. K.; Whitesides, G. M. *Angew. Chem. Int. Ed.* **1998**, *37*, 2755-2794.

(149) Hunter, R. J. *Zeta Potential in Colloid Science*; Academic Press: London, 1981.

(150) Chilkoti, A.; Stayton, P. S. *J. Am. Chem. Soc.* **1995**, *117*, 10622-10628.

(151) Green, N. M. *Biochem. J.* **1963**, *89*, 585-&.

(152) Jost, W. *Diffusion in Solids, Liquids, Gases*; Academic Press, Inc., Publishers: New York, 1952.

(153) Zhang, Y. J.; Furyk, S.; Bergbreiter, D. E.; Cremer, P. S. *J. Am. Chem. Soc.* **2005**, *127*, 14505-14510.

(154) Zhang, Y.; Furyk, S.; Sagle, L. B.; Cho, Y.; Bergbreiter, D. E.; Cremer, P. S. *J. Phys. Chem. C* **2007**, *111*, 8916-8924.

(155) Furyk, S.; Zhang, Y. J.; Ortiz-Acosta, D.; Cremer, P. S.; Bergbreiter, D. E. *J. Polymer Sci. Polymer Chem.* **2006**, *44*, 1492-1501.

(156) Tamm, L. *Biochemistry* **1998**, *27*, 1450-1457.

(157) Smith, L. M.; Parce, J. W.; Smith, B. A.; Mcconnell, H. M. *Proc. Natl. Acad. Sci.* **1979**, *76*, 4177-4179.

(158) Subramaniam, S.; Seul, M.; Mcconnell, H. M. *Proc. Natl. Acad. Sci.* **1986**, *83*, 1169-1173.

(159) Albertorio, F.; Chapa, V. A.; Chen, X.; Diaz, A. J.; Cremer, P. S. *J. Am. Chem. Soc.* **2007**, *129*, 10567-10574.

(160) Morigaki, K.; Kiyosue, K.; Taguchi, T. *Langmuir* **2004**, *20*, 7729-7735.

(161) Holden, M. A.; Jung, S. Y.; Yang, T. L.; Castellana, E. T.; Cremer, P. S. *J. Am. Chem. Soc.* **2004**, *126*, 6512-6513.

(162) Morigaki, K.; Schonherr, H.; Frank, C. W.; Knoll, W. *Langmuir* **2003**, *19*, 6994-7002.

(163) Barenholz, Y.; Gibbes, D.; Litman, B. J.; Goll, J.; Thompson, T. E.; Carlson, F. D. *Biochemistry* **1977**, *16*, 2806-2810.

(164) Pitto, M.; Raimondo, F.; Zoia, C.; Brighina, L.; Ferrarese, C.; Masserini, M. *Neurobiol. Aging* **2005**, *26*, 833-838.

(165) Matthews, B. W. *C R Biol.* **2005**, *328*, 549-556.

(166) Mcdaniel, R. V.; Mclaughlin, A.; Winiski, A. P.; Eisenberg, M.; Mclaughlin, S. *Biochemistry* **1984**, *23*, 4618-4624.

(167) Avanti Polar Lipids, 2008, www.avantilipids.com.

VITA

Name: Arnaldo Joel Diaz Vazquez

Address: Department of Chemistry, 3255 TAMU, College Station, TX 77843

E-mail: adiaz@mail.chem.tamu.edu

Education: B.S., Chemistry, University of Puerto Rico - Rio Piedras, Puerto Rico, 2002